Doctoral Dissertation

Contributions to Channel Modelling and Performance Estimation of HAPS-based Communication Systems regarding IEEE Std 802.16™

Author

ISRAEL ROMUALDO PALMA LÁZGARE

Electronics Engineer

Adviser

PROF. DR. ING. JOSÉ ANTONIO DELGADO PENÍN

Doctorate Program in Signal Theory & Communications
Departament de Teoria del Senyal i Comunicacions (TSC)
Universitat Politècnica de Catalunya (UPC) BarcelonaTech

A SUBMISSION IN PARTIAL FULFILMENT OF THE REQUIREMENTS
FOR THE DEGREE OF DOCTOR OF PHILOSOPHY (Ph.D.)

May 2011

In memory of the formation of a bit of a better mind

in the midst of a deeper science.)

Resumen

Las nuevas y futuras redes de telecomunicación son/serán de banda ancha (broadband). Las infraestructuras de radio comunicaciones terrestres y espaciales actuales podrán complementarse con nuevas redes inalámbricas que hacen/harán uso de la tecnología aeronáutica. Nuestra propuesta de estudio/contribución hace referencia a las radio comunicaciones basadas en estaciones radioeléctricas a bordo de una Plataforma estratosférica denominada por la ITU-R con el nombre de HAPS (High Altitude Platform Station). Estas nuevas redes han sido propuestas como alternativa tecnológica dentro del marco de la ITU para proporcionar diversos servicios de comunicaciones de bandas ancha/estrecha y establecer una tecnología complementaria de las redes de radio comunicaciones terrestres y/o satelitales.

Hoy en día, debido a la posibilidad de embarcar una carga útil para Telecomunicaciones en una aeronave o en un globo aerostático (HAPS), se pueden llevar a cabo radio comunicaciones para proveer conexiones troncales en tierra y accesos de banda ancha para terminales terrestres bien fijos o móviles. Lo anterior implica una planificación radioeléctrica compleja. Por tanto, el análisis de las coberturas radioeléctricas en exteriores e interiores pasa a ser cuestión importante en el diseño de nuevos sistemas radioeléctricos.

En esta Tesis doctoral, la contribución tiene que ver con la aplicación del HAPS para las comunicaciones de banda ancha terrestres y fijas. El HAPS aquí se “hipotizó” como una plataforma cuasi-estática y a una altura sobre la tierra en la denominada capa estratosférica. El estudio/contribución hizo uso de una aproximación vía simulaciones para predecir una cobertura exterior-interior bajo un modelo computacional simple/eficiente y, consideró un radioenlace de bajada entre una “estación base a gran altura” y un terminal terrestre localizado en un área urbana y bien situado en el interior o exterior de un edificio.

El modelo global de radiocomunicación de banda ancha estuvo constituido por tres partes: transmisor, canal y receptor. Las partes transmisora y receptora se basaron en las especificaciones del IEEE Std 802.16™-2009, y la parte correspondiente al canal fue objeto de un análisis que tuvo en cuenta la estación HAPS y las partes terrestres (exterior más interior).

En este trabajo se tuvieron en cuenta las recomendaciones de la ITU-R sobre las bandas reconocidas para estas redes basadas en HAPS. Se consideró la posibilidad de funcionamiento alrededor de 2 GHz (exactamente 1820 MHz) ya que, esta banda está reconocida como alternativa para redes de HAPS que pueden dar servicios comprendidos en lo que se conoce como IMT-2000 e IMT-Advanced. Lo anterior implicó la necesidad de considerar técnicas de transmisiones robustas y fiables como pueden ser las recomendadas por el estándar IEEE 802.16™-2004/2009, es decir, las especificaciones de la capa física WirelessMAN-OFDM.

A la vista de la banda de frecuencia de trabajo propuesta, el modelo de canal para zona urbana hizo uso de una caracterización geométrica basada en las teorías de rayos y de la difracción. Por otra parte, junto con las estructuras urbanas se consideraron estructuras de interiores (tipo oficinas) y, además, se tuvo en cuenta modelos empíricos procedentes del análisis de radiocomunicaciones satelitales/terrestres. Con relación a este último aspecto, la aproximación del canal HAPS utilizó mayoritariamente los registros de datos derivados de los ensayos de un sistema satélite terrestre-móvil (LMSS - land mobile satellite system). La hipótesis de con-

siderar las características de un sistema LMSS se tomó por el hecho de considerar los HAPS con ángulos de llegada semejantes y, teniendo en consideración las caracterizaciones a corto y largo plazos temporales.

En el modelado de canal se planteó el uso de una caracterización mediante varios estados (situaciones físicas asociadas a la transmisión/recepción de las señales). El caso analizado aquí consideró dos estados. Uno de ellos contempló situaciones del entorno de transmisión definidos por un camino de enlace directo del transmisor con el receptor y, el otro estado de canal tiene en cuenta las condiciones de sombra. Dichos estados son dependientes del ángulo de elevación y también están asociados al análisis de trazado de rayos. Dentro del entorno de propagación, se puede considerar que una porción representativa de la energía total de la señal se recibe por el camino de una onda directa o difractada, y que la potencia restante de la señal viene a través de una onda especular. A estas ondas (rayos) se les sumarían los rayos dispersos y aleatorios que constituyen la onda difusa.

En el caso de transmisión/recepción en interiores se hizo la hipótesis de no tener un repetidor o estación en el exterior (posicionado en un tejado/ático) con lo que el HAPS establece los oportunos apoyos de cobertura. En este caso, sobre las variaciones de la señal transmitida deberán tenerse en cuenta, además: la penetración en el edificio, material de construcción, ángulo de incidencia, altura del piso, posición del terminal dentro de la habitación, y desvanecimientos del interior. Aquí se asumió que estas radio comunicaciones en interiores llegan a presentar diferentes tipos de trayecto para llegar al receptor: LOS obscurecido, no LOS (NLOS), y NLOS excesivo.

La evaluación del posible funcionamiento del sistema HAPS-estación de tierra fija (con interiores incluida) se llevó a cabo mediante la construcción de un experimento estadístico que se ejecutó usando una simulación intensiva del diagrama de bloques representativa del sistema completo: HAPS-Canal-Estación receptora en tierra. Las hipótesis de construcción del sistema consideraron varias alternativas de técnicas de transmisión digital codificada COFDM recogidas en el estándar IEEE 802.16™; diversos tipos de canal útiles para zonas urbanas y, las posibilidades de recepción en exteriores y/o interiores. Los resultados del experimento, teniendo en cuenta estas hipótesis y otras colaterales, se presentan en términos de BER versus E_b/N_0, obteniéndose unas conclusiones importantes en este tipo de sistemas para redes de acceso basadas en HAPS.

Abstract

New and future telecommunication networks are and will be broadband (Broadband). The existing terrestrial and space radio communication infrastructures might be supplemented by new wireless networks that make and will make use of aeronautics-technology. Our study/contribution is referring to the radio communications based on radio stations aboard a stratospheric platform called by ITU-R with the name of HAPS (High Altitude Platform Station). These new networks have been proposed as an alternative technology within the ITU framework to provide various narrow/broadband communication services and establish a complementary technology for radio communication networks at terrestrial and satellite levels.

Today, because of the possibility of having a payload for Telecommunications in an aircraft or a balloon (HAPS), it can be carried out radio communications to provide backbone connections on ground and to access to broadband points for fixed ground terminals, either fixed or mobile. The latest implies a complex radio network planning. Therefore, the analysis of radio coverage at outdoors and indoors become an important issue on the design of new radio systems.

In this doctoral thesis, the contribution is related to the implementation of HAPS for terrestrial fixed broadband communications. Herein, the HAPS is hypothesised as a quasi-static platform with height above ground at the so-called stratospheric layer. The proposed contribution is fulfilled by the approach via simulations to predict the outdoor-indoor coverage with a simple efficient computational model and, considers the downlink "high altitude base station"-to-terrestrial terminal located into an urban environment situated at indoors or outdoors of a building.

The global broadband radio communication model is consisting of three parts: transmitter, channel, and receiver. The transmitter and receiver parts are based on the specifications of the IEEE Std 802.16™-2009, and the part corresponding the channel is subjected to the analysis that took into account the HAPS and the terrestrial parts (outdoors plus indoors).

This work is assessing the ITU-R recommendations at the bands recognised for the HAPS-based networks. It is contemplated the possibility of operating around 2 GHz (1820 MHz, specifically) because this band is recognised as an alternative for HAPS networks that can provide IMT-2000 and IMT-Advanced services. Such tasks are implying the need of considering techniques for robust and reliable transmissions such as those recommended at the IEEE Std 802.16™-2004/2009, i.e., the WirelessMAN-OFDM physical layer specifications.

Working at the proposed frequency band, the channel model for the urban area is using a geometric characterisation based on ray-theory and diffraction. On the other hand, along with the urban structures are considered the indoor structures (office-type) and are taking into consideration empirical models from satellite based radiocommunication studies. Regarding the last-mentioned fact, the HAPS channel approach is using mostly data records of tests from the land mobile satellite system (LMSS). The hypothesis of considering the characteristics of an LMSS is because of having the HAPS with similar angles of arrival and the characterisations of the short- and long-terms.

For the channel modelling is proposed the use of a characterisation by means of several states (physical situations associated with the transmitted/received signals), the state-oriented channel modelling. The case discussed here is considering two states. One of the channel state is contemplating the environmental transmission situation defined by a direct path between the transmitter and receiver, and the other channel state is regarding the conditions of shadowing. These states are dependent on the elevation angle and are also related to the ray-tracing analysis. Within the propagation environment, it is considered that a representative portion of the total energy of the signal is received by a direct or diffracted wave, and the remaining power of the signal is coming by a specular wave. To such waves (rays) are added the scattered and random rays that constitute the diffuse wave.

At the case of indoor transmission/reception the hypothesis of not having a repeater or station outside (positioned on a roof/attic) is regarded, so that the HAPS is establishing the pertinent support coverage. At this interior radio transmission situation, the variations of the transmitted signal are also considering the following matters: the building penetration, construction material, angle of incidence, floor height, position of the terminal in the room, and indoor fading. Herein, it was assumed that these indoor radiocommunications are tending to present different type of paths to reach the receiver: obscured LOS, no LOS (NLOS), and hard NLOS.

The evaluation of the feasible performance for the HAPS-to-ground terminal is accomplished by means of building a statistical procedure, which is executed using thorough simulation of the block diagram representative of our complete system: HAPS-channel modelling-ground receiver. The considered hypotheses for this system are contemplating several alternatives of digital coded transmission techniques COFDM from the IEEE Std 802.16™; different types of profitable channels covering the urban zone, and the possibilities of radio reception in outdoors and indoors. The plotting outcomes of the experiment, under the conditions of such hypotheses and other collateral events, are presented in terms of BER vs. E_b/N_0 for significant conclusions at these kind of systems for access networks based on HAPS.

Acknowledgments

I express this memoir with all the appreciation to the support of my kind friends and beyond.

First of all, special thanks to the financial support from CONACyT (National Financial Resource in Mexico for Science and Technology) having made possible this research in an overseas country for the concerns of growing in science.

A remarkable gratefulness to those who helped to carry out and were part of this work: IST Project Capanina (FP6 IST-2003-506745), and the Spanish Government Project TEC2004-0136-E. I appreciate all technical discussions received and experienced as essential feedback when it came on the time as being member of COST297-High Altitude Platforms for Communications and Other Services (HAPCOS) (European Action ended by 2009).

Thank you to all noble colleagues and honourable professors from UPC-TSC Department (and neighbourhood area) and from Centre for Wireless Communications (University of Oulu) who each one has expressed through my doctoral time their outstanding professional qualities together with respectable principles; in addition, thanks to the TSC personnel who have contributed to the correct advising through my doctorate program in edition and instrumental/technical support.

The international people I have been meeting during my stay in Spain have given me his/her kind friendship, and to whom I present a full gratefulness for such big fortune given to my life. My hope for a long friendship with all of them. Special thanks to Gerardo Medina and Katriina Rantala for incentivising my last stage of this work.

My gratitude to my family who has been an important pillar of unconditional support through this time of work despite of our long distance of separation.

Many thanks to Prof. Fernando Pérez Fontán whose dedication to my formation with suggestions belonging to his personal distinguished lectures have provided me with the 'take off' of my research with fruitful ideas and encouragement for a better work.

And definitively, my outstanding recognition to Prof. José A. Delgado Penín who gave me the grateful opportunity for initiating the guidance to my doctorate; such undertaken challenge has conformed for a no replacement time at my professional growth. Thank you so much professor for the consolidation to the direction of my doctorate lifetime where I led for the appropriate study and offer the *ad rem* development on the HAPS research, among others. Thank you for all comprehension and patience.

Deeply thanks to each one.

Barcelona, May 2011

Israel R. Palma Lázgare

Table of Contents

List of Figures

List of Tables

Notation

The following symbols are expressed by their specific interpretations throughout this dissertation. The reader should note that this notation is not exhaustive.

A_1	level power of the direct signal
A_2	level power of the specular reflected signal
α	elevation angle
BW	channel bandwidth
$BW_{coherence}$	coherence bandwidth
$\delta(\cdot)$	impulse function
c	speed of light
d_{HAPS}	radio link distance from HAPS to terminal on ground
d_{srp}	distance from HAPS to the reflection body for the specular reflection path
Δr_{srp}	distance from the reflection body to the receiver
$\Delta\tau_{srp}$	physical space delay of the reflection path from the reflection body to receiver
η	spectral efficiency at the multicarrier system
f	frequency
$f(\cdot)$	probability density function
$f_{D,max}$	maximum Doppler shift
$h_{building}$	the difference between the building and the terrestrial terminal height
h_{mbh}	mean building height
$h_{terminal}$	terrestrial terminal height
$h_{threshold}$	threshold height relative to the point of the direct ray height
$h(t,\tau)$	multipath fading channel (channel impulse response)
λ	carrier wavelength
L	total mean propagation loss
L_{BL}	building loss
L_{BPL}	building entry loss
$L_{I,GI}$	additional external wall loss due to incidence angles away from the normal incidence to the wall

$L_{l,Nl}$	path loss through the external wall at normal incidence
$L_{l,VW}$	loss in the internal walls along the floor
L_{Indoor}	indoor propagation loss step
$L_{Outdoor}$	outdoor propagation loss step
$L_{srp,FSL}$	attenuation for the specular reflection path
$L'_{l,Gl}$	average parameter of Ll,Gl
MP	average multipath power describing the diffuse component of the signal
N_{echoes}	number of echoes conforming the discrete PDP
$N_{l,VW}$	number of penetrated walls
N_{RB}	number of reflections caused by the occurred rooftop diffraction from the opposed building at the back of the interested building
ν	Doppler frequency shift
Φ	azimuth angle
Φ_G	grazing incidence with respect to the external wall
$\rho_{building}$	shadowing probability term according to the building height
$PL_{D,Terrestrial}$	attenuation due to outdoor-indoor diffraction situation at LOS link
PL_{EPLMRB}	excess propagation loss due to multiple reflections from the buildings' walls along the street and surrounding the terminal
PL_{HAPS}	channel propagation model standing for HAPS-to-ground cascade-stage (HAPS-process)
$PL_{HAPS,FSL}$	free space path loss (power transmission ratio)
PL_{LOS}	total transmission loss for the LOS link situation
$PL_{shadowing}$	total transmission loss for the shadowed link situation
$PL_{S,Terrestrial}$	attenuation due to outdoor-indoor diffraction situation at shadowing link
$PL_{Terrestrial}$	channel propagation model standing for effects surrounding the terrestrial terminal relative to its neighbouring scattering (terrestrial process)
$PL_{Terrestrial,DD}$	excess loss due to diffraction situation at LOS link
$PL_{Terrestrial,DS}$	excess loss due to diffraction situation at shadowing link
$PL_{Terrestrial,foliage}$	loss due to greenery areas
$PL_{Terrestrial,RSL}$	excess loss due to diffraction from rooftop down to the street-level terminal
R_b	achievable peak data rate
R_c	channel coding rate
$R_{FZ,LOS}$	Fresnel zone radius
r_{HAPS}	HAPS altitude

R_{HAPS}	radius of the HAPS area coverage
Sp	linear decay rate slope (multipath power decay profile)
t	time
$T_{coherence}$	coherence time
τ	time-delay spread
τ_A	arrival delay from HAPS to terminal for the direct path
τ_B	arrival delay from HAPS to reflector object for the specular reflected path
t_{loss}	transmission loss inside the building per meter (or gradient loss due to furniture and other indoor issues)
T_s	OFDM symbol duration
τ_{srp}	differential arrival delay from HAPS to terminal for the specular reflection path
x_{BB}	width between the supposed buildings at both sides of the street.
x_{indoor}	the width of building for the indoor terminal localisation, with $x_{indoorR}$ at right and $x_{indoorL}$ distance at left (gap from the indoor terminal to the wall-signal entrance)
x_{TB1}	horizontal distance between terminal and the diffraction edge (shadow)

Acronyms & Initialisms

3G	Third-Generation
4G	Fourth-Generation
AWGN	Additive White Gaussian Noise
BER	Bit Error Rate
BS	Base Station
BWA	Broadband Wireless Access
CC	Convolutional Code
CIR	Channel Impulse Response
COFDM	Coded OFDM
CP	Cyclic Prefix
CTF	Channel Transfer Function
DFT	Discrete Fourier Transform
DL	Downlink
DLR	Deutschen Zentrums Für Luft- und Raumfahrt
E_b/N_0	Energy per bit to Noise power spectral density ratio
ESA	European Space Agency
ETRI	Electronics and Telecommunications Research Institute
FBWA	Fixed Broadband Wireless Access
FEC	Forward Error Correction
FFT	Fast Fourier Transform
FSL	Free Space Loss
GEO	Geostationary Earth Orbit
GI	Guard Interval
HAA	High Altitude Airship
HALE	High Altitude Long Endurance
HAPS	High Altitude Platform Station
HAVE	High Altitude Very long Endurance
HNLOS	Hard Non-Line-of-Sight
IBI	Interblock Interference

IDFT	Inverse Discrete Fourier Transform
IEEE	Institute of Electrical and Electronics Engineers
IMT-2000	International Mobile Telecommunications - 2000
IMT-Advanced	International Mobile Telecommunications - Advanced
IP	Internet Protocol
ISI	Intersymbol Interference
ITU	International Telecommunication Union
ITU-R	ITU Radiocommunication Sector
KARI	Korean Aerospace Research Institute
LAN	Local Access Network
LMSS	Land Mobile Satellite System
LOS	Line-of-Sight
LTA	Lighter-than-air
MSDL	Multiple Screen Diffraction Loss
NASA	National Aeronautics and Space Administration
NG	Next-Generation
NLOS	Non Line-of-Sight
OBP	On-Board Processing
OFDM	Orthogonal Frequency Division Multiplexing
OLOS	Obscured Line-of-Sight
PDP	Power Delay Profile
PHY	Physical Layer
PMP	Point-to-Multipoint
PSD	Power Spectral Density
QAM	Quadrature Amplitude Modulation
QLOS	Quasi-Line-of-Sight
QPSK	Quadrature Phase-Shift Keying
RAC	Rural Area Coverage
RF	Radio Frequency
RMS	Root Mean Square
RS	Reed-Solomon
RSL	Rooftop Scattering Loss
Rx	Receiver
SAC	Suburban Area Coverage

SC	Single Carrier
SNR	Signal-to-Noise Ratio
SPF	Stratospheric PlatForm
SPS	Stratospheric Platform System
TDL	Tapped-Delay-Line
Tx	Transmitter
UAC	Urban Area Coverage
UAS	Unmanned Aircraft System
UAV	Unmanned Aerial Vehicles
UMTS	Universal Mobile Telecommunications System
WiMAX	Worldwide Interoperability of Microwave Access
WRC	World Radiocommunication Conference
WSSUS	Wide Sense Stationary Uncorrelated Scattering

1

Introduction

1.1. Liaison of next generation broadband wireless access technologies to HAPS prospects

Today, essential features towards the convergence of wireless networks are mainly described by the compatibility of technologies within IMT-2000 and fixed networks (Ohmori *et al.*, 2000), (Stuckman & Zimmermann, 2007), (ITU-R M.1457, 2001-2007). As we are going aside to a next generation wireless system, our contribution is expressed by the profile of the High Altitude Platform Station (HAPS), which we pursue to exploit for broadband wireless communications with specific interests on serving to stationary terrestrial terminals located at urban outdoors-indoors. Initial steps towards the research about HAPS are already taken in Europe at operative frequency bands below 10 GHz (ITU-Q/2, 1998), (ITU-R 39.8, 1999), (ITU-R M.1456, 2000), (Aubineau *et al.*, 2010), or higher (Morisaki, 2005).

Channel assignment and resource allocation schemes are being required to develop into an operational HAPS scenario becoming the representation of an issue of paramount importance for any communication system, and essentially different from either a terrestrial or a satellite cellular scenario. Hence, strategies are being developed for both packet-based communications and connection-oriented traffic.

HAPS network may hold a star network configuration, where a service is given between the HAPS and the main worldwide node. The HAP payload can project multiple punctual beams in the ground and give a circular radio electric covering that can be subdivided in

three areas to guarantee a service of broadband to the users along the whole HAPS footprint. The covered areas can be (1) Urban Area, extended between 36 and 43 Km from the nadir point (a point exactly below the platform) with heights of 21 and 25 Km respectively; (2) Sub-urban Area, covering an area (with elevation angle values between 15º and 30º) of 76/91 Km radius; (3) And, the Rural Area, which is the largest surface for covering and is considered for elevation angles between 15º and 5º.

ITU has proposed that footprints of a radius more than 150 km can be served from a HAPS. For remote areas where there is no substantial terrestrial infrastructure, satellites can be used as backhaul. Regarding broadband applications, the cellular architecture with frequency reuse and cell disposition of a few kilometres diameter can provide high spectral efficiency, and hence network capacity. Although a BWA network architecture is likely to have chiefly fixed users, some handoff may occur due to the antenna beam and plausible platform motions, depending so far by the HAP stabilisation techniques.

A possible system comprised by optical links can be employed to connect neighbouring HAPS and HAPS with a satellite. The use of Dense Wavelength Division Multiplex (DWDM) technology was proposed for the optical links. Inter-platform links will not suffer outages due to rain/clouds, as they will be used well above cloud height. Also, the adaptation of FLEX-TEC, a state-of-the-art fine pointing and tracking technology developed for optical communications in space was proposed (Karapantazis & Pavlidou, 2005).

Shifting to a new spotlight, the HAPS scheme has to be adapted to multimedia traffic and take into account the system topology and choice of modulation/coding scheme. The most appropriate medium access control (MAC) and network protocols must be selected as a starting point.

1.2. Motivation and Contribution

With the introduction of multimedia and broadband services, the demands in outdoor and indoor coverage are becoming essential and a compulsory to be determined from system performance records. Nowadays, complex or novel technology implementations or applications many times are not affordable and one can turn to less expensive simulation-based tools. Also, according to the novel technology use and high-speed transmission realisation, outdoor and indoor coverage are being important for demands of cost-efficient

implementation, and improvements in outdoor-to-indoor areas are required at radio network planning.

In addition, a normative complex radio-interface usage is expected to add up the essential spectrum efficiency and robust transmission requirements.

Our contribution (proposal) can establish an approach to predict outdoor-to-indoor coverage with an efficient low-computational model at the frequency band of 1.820 GHz. The outdoor and indoor communications coverage prediction has been carried out by means of the high altitude platform (HAP). Accordingly, the HAP station (HAPS) can be a complement to the existent terrestrial and satellite based communication systems, and as such system the HAPS-based wireless communication payload is of concern delivering high capacity services in outdoors and indoors environment.

The simulated system's performance suit in this document deals with the stratospheric broadband channel modelling and can show overcoming the propagation effect predictions for the required communications payload, where the accounted attenuation losses and delay spread have conformed for the adequate fading mitigation technique used. Hence, the examined channel modelling is considered under the adaptive-to-environment transceiver, which is following the IEEE Std 802.16™-2009 assumptions for a potential regulation at ITU —the PHY-layer from the standard specifications are adequate to add up an efficient and robust transmission.

The built-up model and building office-type indoor structure are essential and can be determined with the exploratory records from satellite-based empirical models. On that account, the support from the land mobile satellite system (LMSS) features can support our model with the adoptions of experiencing similar angle of arrivals and mid- and short-term characterisations for HAPS. The presumptions for the downlink modelling occur between HAPS (a quasi-static stratospheric airship) and fixed terminals situated in building indoors and street-level outdoors inside an urban area. Such assumed environmental situation for coverage is described by a first channel state where the line-of-sight (LOS) path exists, and a second state is modelling the statistical fading of the received signal at shadowing conditions. The latter state-oriented statistical-physical channel model was derived from geometrical urban issues represented with diffraction and reflection ray theory.

Consequently, the channel model process is described by a sequence of outdoor- and indoor-cascaded blocks. At the outdoor stage, the conforming blocks of (stratospheric) HAP and terrestrial processes are considered using the satellite term-based LMSS empirical mod-

els. The propagation model at the office-type indoor stage is based on the former outdoor fading and the key variables of building penetration, building material, position inside the room, floor height, and indoor fading.

The overall system performance approach is achieved from simulations of BER vs. E_b/N_0 plotting, and the approximation prompts in a feasible robust HAPS-based broadband communications.

1.3. Scope

Our work is related with a HAPS-based system, in which we effectuate an evaluation approach via intensive simulations to forecast the outdoor-indoor communications coverage and performance at L band. The HAPS-based channel modelling and its *habitat* are determined into a pragmatic approach from the satellite-based systems, and their trial data have been used throughout our hypotheses. The latest allows the direct supposition to the application of the IEEE 802.16™ HAPS-based communication system evaluated by simulation tools, which is aiming to be compared for a feasible broadband system and be competent to complement the existent wireless systems and demands. The robust consistency of our system's performance results can provide confidence with an employed modelling being accurate and putting the potential of being utilised at predictions for the HAPS-communication payload.

1.4. Thesis Outline

The actual work is organised in five chapters plus three appendices, and all are summarised as following:

- Chapter 2 is presenting the relevant state-of-art of the HAPS-based system for wireless communications use, and issues for the communication design and evaluation are described.
- Chapter 3 is containing the contribution of the stratospheric channel modelling development. Specifically, the operating urban physical environment where the HAPS-based system is being developed, and its compound (state-oriented channel) are presented in details.

- Chapter 4 is allowing the proof of the contribution work with the optimised HAPS-based system by means of the use of IEEE Std 802.16™ and the accurate expression of the propagation channel plus environment described in the previous chapter. The formality for the performance results of the system is provided by means of simulation use. And, the discussion concerning the system's performance plotting is given.
- Chapter 5 draws the proper conclusions of the presented contribution based on the HAPS system for broadband communications and according to the approximation of the urban area coverage. Moreover, the extension and challenges of the present work are shortly explored.
- Appendix A. A compendious text concerning the utilisation of the IEEE Std 802.16™ technology is presented, and the expectations of implementing such specific standard into the HAPS-based system network scenario are formed.
- Appendix B. The multicarrier technology is of our interest for developing demanded high-data rate systems in the present days, and its evolution within the standard is of our interest, both are explained in short. Pros and cons of the multicarrier achievements for the HAPS-based system channel situation are also expressed.
- Appendix C. The employment of the IEEE Std 802.16™ into the HAPS-based system communication approach is of importance. The main components of the multicarrier implementation are pointed out. Also, the multicarrier-HAPS channel engineering is identified particularly to have the details of this application.

3

The Stratospheric Channel Modelling Development

3.1. The operating physical environment

3.1.1. Urban scenario and built-up considerations

Even though there are a lot of references in wireless channel characterisation dedicated to conventional terrestrial and satellite links, but specific conditions in the stratospheric outdoor-indoor geometry require further investigation for the particular HAPS-based system application. At this position, it is possible to acquire a couple of radio link types between the HAPS-payload and the ground equipment: the gateway and service link. For our case, the service link where communications can occur between HAPS and the terrestrial still terminal in a cellular configuration mode was focused.

Herein, the global system geometry has been looked before its evaluation, so that the difference with respect to other radio system can be clearly established (Karapantazis & Pavlidou, 2004), (Karapantazis & Pavlidou, 2005). The global geometry can have a mere representation in Figure 3.1 for the HAPS-based system involving the Earth's curvature, a fixed positioned at an altitude r_{HAPS} over the point *C*, and a direct-path illuminating the fixed ground terminal with an elevation angle α_{Earth}; point *O* represents the Earth's centre and r_{Earth} is the Earth's radius. Then, from the principle of trigonometry it is expressed

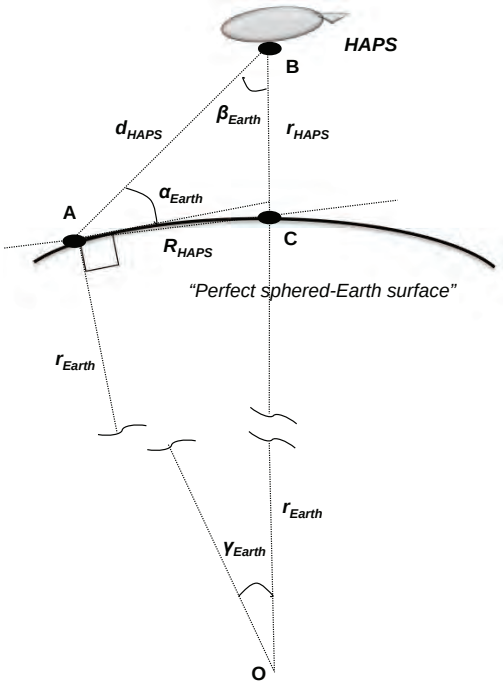

Figure 3.1. Early geometry of the HAPS-based system (not to scale) (Widiawan & Tafazolli, 2007), (Saunders & Evans, 1997), (Czylwik, 1998).

$$\frac{\overline{OA}}{\sin\beta_{Earth}} = \frac{\overline{OB}}{\sin\left(90+\alpha_{Earth}\right)} = \frac{\overline{OB}}{\cos\alpha_{Earth}}, \tag{3.1}$$

and

$$\sin\beta_{Earth} = \frac{r_{Earth}}{r_{Earth}+r_{HAPS}} \cdot \cos\alpha_{Earth}. \tag{3.2}$$

Assuming that the Earth's surface has a perfect-sphered shape, the arc *AC* indicates the radius of HAPS coverage on ground expressed as to the following equation

$$\widehat{AC} = \gamma_{Earth} \cdot r_{Earth}. \tag{3.3}$$

Let us consider the triangle Δ*OAB*, the total internal angle of the triangle is 180° so the angle γ_{Earth} could satisfy the equation

$$\gamma_{Earth} = 90^{\circ} - \alpha_{Earth} - \beta_{Earth}. \tag{3.4}$$

After substitutions, rewriting the radius of the HAPS area coverage

$$R_{HAPS} = r_{Earth} \cdot \left[\cos^{-1}\left(\frac{r_{Earth}}{r_{Earth}+r_{HAPS}} \cdot \cos\alpha_{Earth}\right) - \alpha_{Earth}\right]; \tag{3.5}$$

r_{Earth} = 6378*⅓ was used, instead of the only effective 6378 km Earth's radius, considering the atmospheric refraction that causes the radio wave path bending so compensating the geometry at time of linear propagation.

Regarding the above geometrical analysis, HAPS at 21 km altitude can have the capability to cover an area on the ground up to 406 km (diameter) for 5º of elevation angle (refer to Figure 3.2) among others (Table 3.1).

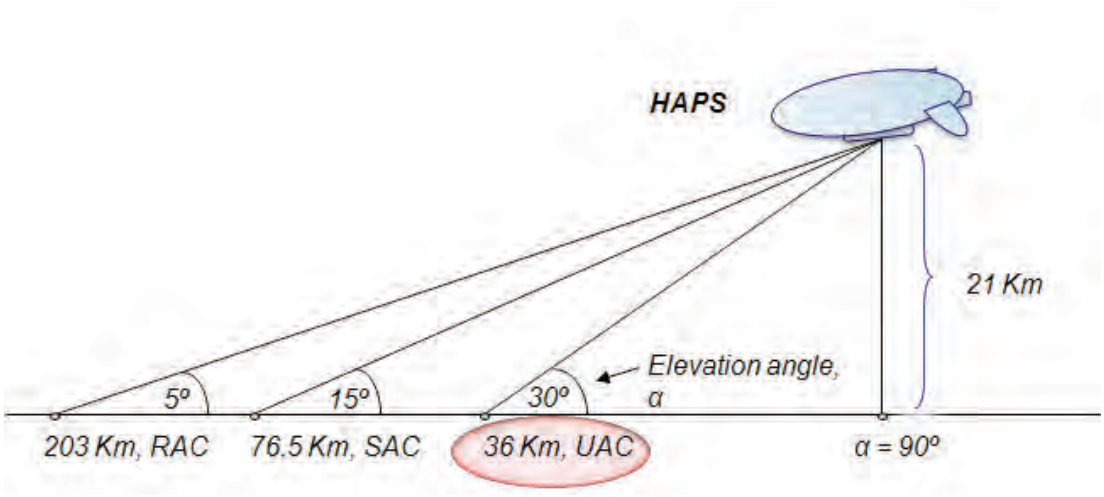

Figure 3.2. The influence of the elevation angle and radio coverage.

TABLE 3.1. FEATURING THE COVERED AREA BY THE HAPS.

Area	Elevation angle, α	Coverage radio [km]	
		h=21 km	h=25 km
Urban	90-30º	0-36	0-43
Semi-urban	30-15º	36-76.5	43-90.5
Rural	15-5º	76.5-203	90.5-234

The terrestrial terminals are described as being inside the urban zone, or urban area coverage (UAC) (ITU-R M.1456, 2000). This work has been dealt specifically with the examination of a communication link approach with the physical characteristics presented in terms of the unobstructed and built-up conditions at a specific elevation angle α, in which land mobile satellite system (LMSS) research deployment and measurements were kindly adopted to our HAPS-based system (Figure 3.3 through Figure 3.7); the rationale behind such proposed selection is remarked in Vázquez-Castro *et al.* (2002) and Vázquez-Castro & Pérez-Fontán

(2002). Propagation from HAPS communications behaves practically in the same manner as for the LMSS case where similar elevation angles can be used, but with a difference being the link length that sets the free space loss reference level. It is also very distinctive that the HAPS channel is compared to the model where no longer only a single distribution (or one single channel state) can describe its behaviour: HAPS and satellite communications were determined by more than two conditions of the radio link (*e.g.*, the link being available when there is LOS or unavailable shadowing/blockage case otherwise). And, as long as the influence of the geometry-statistics of the ground terminal environment approximates the satellite-based channel characterisation which also allows for a practical prediction where measurements were unavailable for HAPS, such terms are incurring in our stratospheric channel modelling (Palma-Lázgare *et al.,* 2010), (Palma-Lázgare & Delgado-Penín, 2010b); specifically, the channel states were assumed in physical terms from unobstructed and built-up shadowed environments at $\alpha = 43^{\circ}$.

Now, for performance optimisation, the HAPS-to-terminal path has been defined into the cascaded stages associated to the outdoors and to the indoors; the free space path, shadowing, multipath, and built-up indoor effects have counted for the major signal fading.

Next, the advantage and application for the two considered statistical and site-specific model categories are emphasised. The assumed physical environment was opened to reflection, scattering and diffraction, thus path loss via base ray tracing was conceived. The case of the ray tracing application has resulted from the strategy to offer path loss formulation by assuming a finite number of reflectors —a reflector was considered as another source of signal apportion and the resultant signal at the receiver was the sum of signals coming from all such sources with different distances and altered antenna fields. On the other hand, statistical/empirical modelling was carried out in order to provide an accurate formulation demanded by complex broadband communications, as well as to give an approach to a low computational but robust channel modelling under urban conditions with appropriate records from the field.

The channel modelling was assumed with a set of rays originated from the same source plus possible reflections from the set of surfaces that are part of such wave front —some possible reflection contributions from ground or building structures can be considered, as well as possible from outdoor trees next to the building. Our stratospheric channel modelling has been based on basic ray tracing algorithm and echo-terminology (Palma-Lazgare *et al.*, 2008), (Palma-Lázgare *et al.*, 2010), the reflection ray from ground has not been considered, and the significant portion of the total signal energy arrived at the terrestrial

receiver by way of a direct wave, plus a remaining power determined by a specular wave, with the many randomly scattered rays that constituted the diffuse wave.

The presumed built-up model in Figure 3.3 has been found useful for a real case approach where the positions of individual buildings were certainly unknown but some estimates of the mean building height and spacing were available. The buildings' allocation at ground, between the HAPS-nadir point and the receiver, were assumed of approximately uniform height and spacing, even if we had a large number of them. The average building height h_{mbh} was supposed between 15 and 35 m with an approximation to the Rayleigh distribution, resulting in a situation where the probability of LOS state would go down if the average building height increases. The inter-building street width was assumed to be equal or slightly wider than a real average street width, and a constant mean inter-building spacing $x_{building}$ (or x_{BB}) has been assumed. Referring to the receiver, it was located in a position where was surrounded by buildings at right and left sides along the street. The receiver was assumed to have at least 1 m in height and was located (outdoors) at some point across the width street, not necessarily at the middle of the two surrounding buildings.

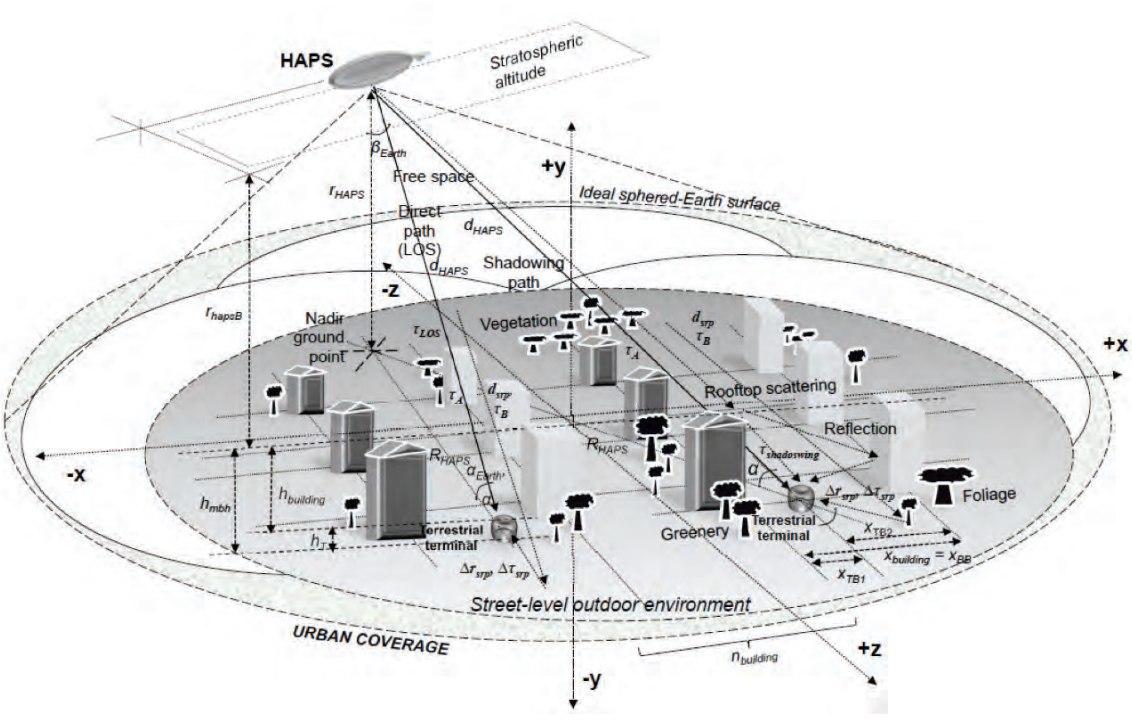

Figure 3.3. HAPS-based network communications for the urban outdoor coverage approach. The path state of the HAPS-based communication system to ground is depending on the local built-up morphology, which is introduced by the situations of direct and shadowing paths.

An additional investigation and comparison can be mentioned with two (micro-cellular) environments into the urban specifications determined by regular and chaflane street corners. These determinations were not accounted for the HAPS-channel modelling, but can be of considerations according to Molina-Garcia-Pardo *et al.* (2004): for LOS conditions delay spread can increase 10 ns in regular corners and 5 ns in chaflane when frequency varies from 450 to 2400 MHz, and for NLOS conditions RMS delay spread can be around 60 ns in both environments; for LOS situations, the coherence bandwidth is bigger in chaflanes than in regular street corners, and growing as frequency increases, however, for NLOS the bandwidth remains steady around 4 MHz under the conditions in Molina-Garcia-Pardo *et al.* (2004). Also, the frequency correlation is shown to be higher in chaflanes than in regular street corners and decreasing when the distance in frequency decreases.

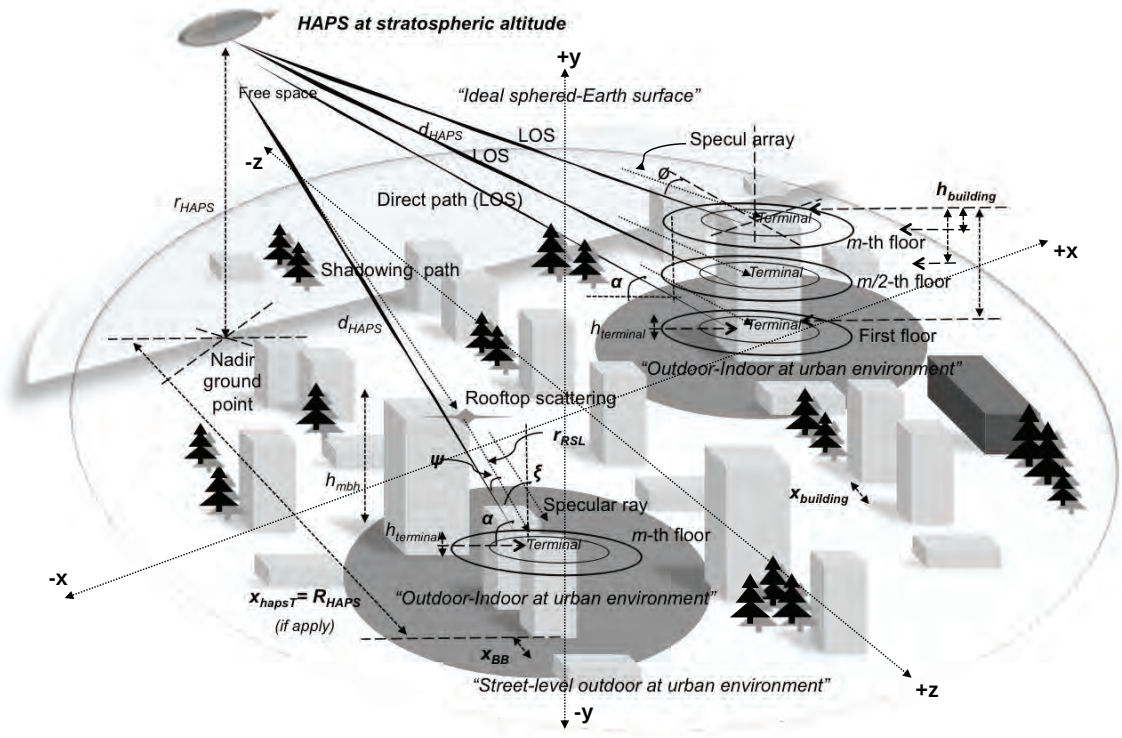

Figure 3.4. HAPS-based network communications for the urban outdoor-indoor coverage.

As long as the IEEE Std 802.16^{TM}-2009 is revised (IEEE 802.16, 2009), the transmission transceiver has been concerned for our fading channel conditions with particularities at indoor coverage. Therefore, the possibility to deploy indoor customer installable end-user terminals is focusing the attention to have cost savings (WiMAX White Paper, 2005). For an

adequate development of the wireless network, a great interest to provide a high coverage quality within buildings using HAPS and acting as a high altitude base station located outdoors were considered; the models dealing with outdoor-to-indoor paths were followed for an adequate development.

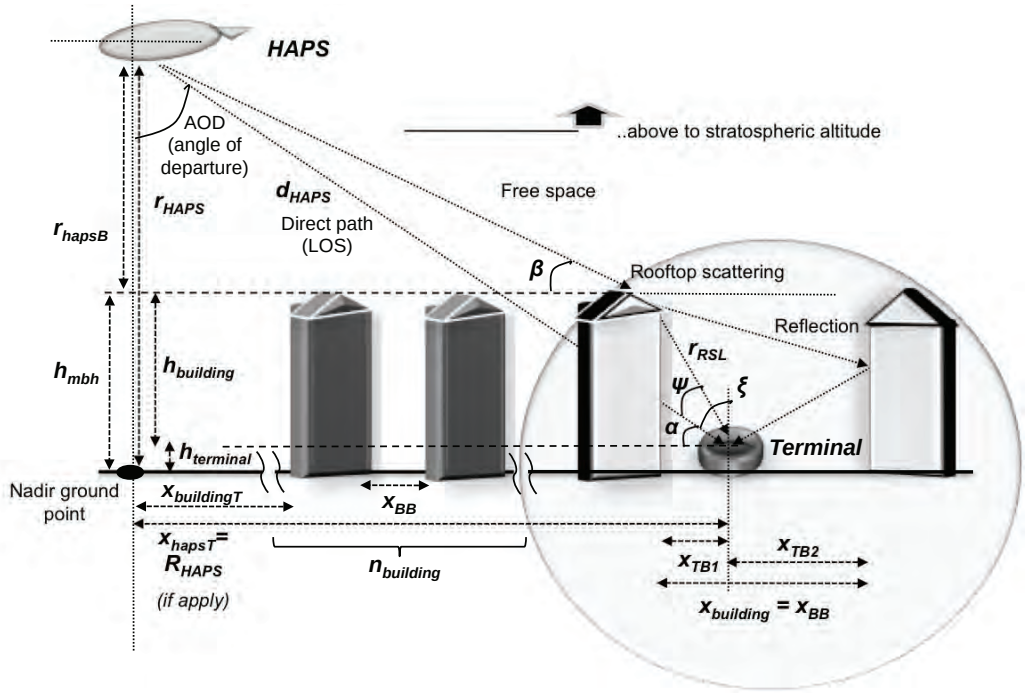

Figure 3.5. Geometrical radio propagation model in the built-up area for downlink HAPS-based communications (not to scale): the idealised building geometry.

The presumed channel modelling at indoors (Figure 3.4) is described by h_{mbh} = 30 m (with height of 5 m at each m-th floor, m = 6) with a distributed Rayleigh assumption (Fernández *et al.*, 2007) resulting in a situation where the probability of direct-path (or quasi-direct-path in this indoor case) is minor if the average building height increases suitably. The indoor still receiver was located in an office-type environment and in a position stood at any possible floor inside the building.

In order to establish the indoor loss, practical assumptions were required and referenced to Pérez-Fontán *et al.* (2008), (Kürner & Meier, 2002), Vogel & Torrence (1993), Oestges & Paulraj (2004), Martijn & Herben (2003), Fischer de Toledo *et al.* (1998), and Berg (1999). The presumed approaches were used to have an approximation of the signal structure and statistics; however, the acquired estimation from this modelling could not predict the exact signal level at a particular indoor point.

Empirical indoor models have been considered specially dealing with outdoor-indoor paths, and has been characterised mainly by the effect of walls/windows blocking the direct path with great influence from the constitutive variables of the materials and the angle of incidence. In the context of indoor or outdoor-to-indoor propagation, the characterisation of wall attenuation is important: a finite thickness of the surface has to be taken into account for the in-building propagation (transmissions through walls).

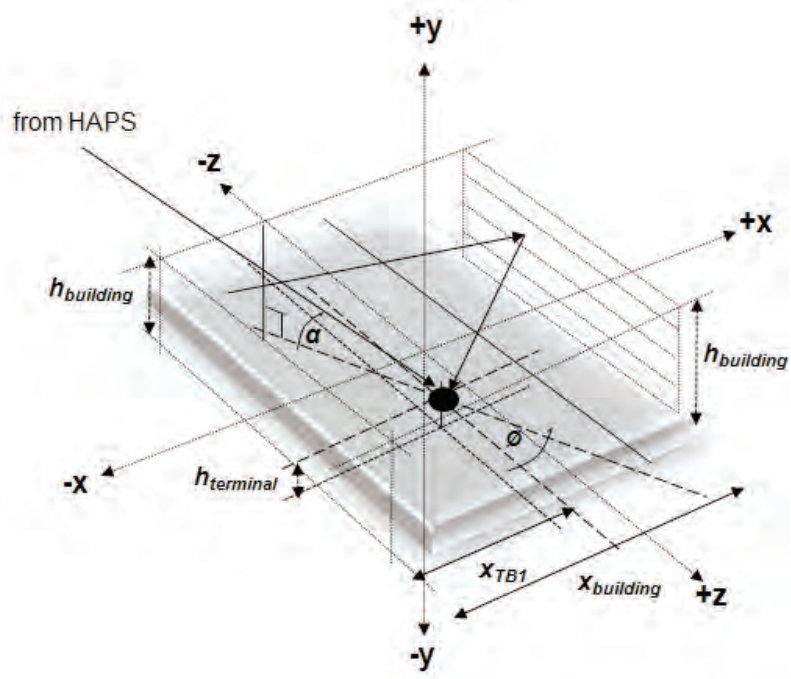

Figure 3.6. Geometrical radio propagation model in the built-up area for downlink HAPS-based communications (not to scale): the geometry at street level.

Simple ray tracing is performed to quantify for robust but easy indoor coverage. Offices on all floors of the building were supposed crowded with typical office furniture, and other possible equipment or obstacle according to the specialised demand of each area. Indoor propagation conditions definitively differ considerably from those found outdoors. In the indoor case, the distances between the building wall and the receiver were much smaller, and mostly the walls, floor, and furniture introduce high attenuation and fading.

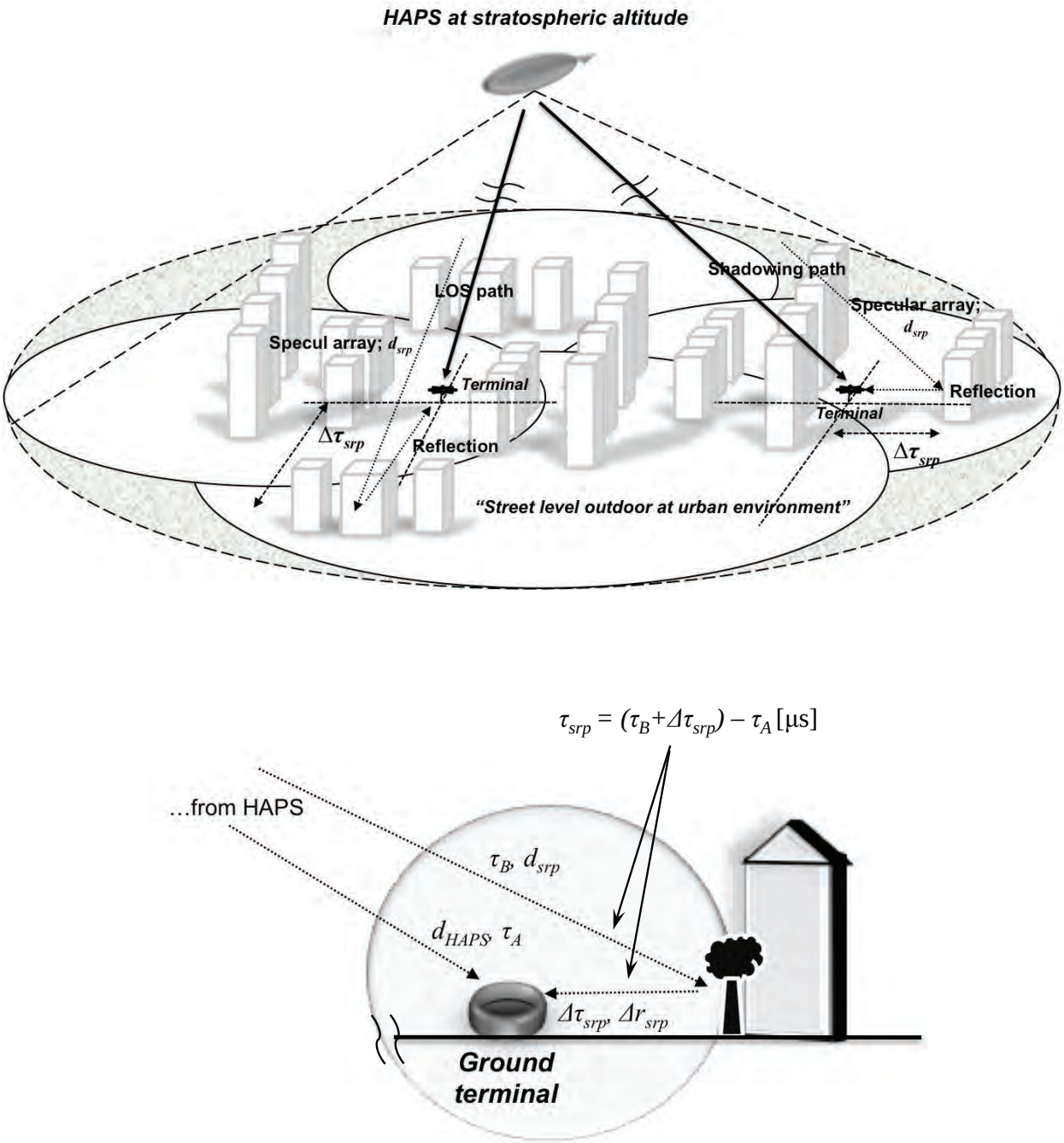

Figure 3.7. Profiles of direct- and specular-reflection paths plus multipath inside the urban built-up area, according to HAPS-channel state situation and to smooth and rough outdoor surfaces. The 3-D and side-perspective representation by the geometry and ray-tracing model in the short-term fading case. The scenarios consider both LOS and shadowing paths.

As long as the height of the transmitter (HAPS) is 21 km above, in the high-density built-up area coverage with different types of buildings and structures, the average values of indoor (penetration) loss may be assumed similar for all buildings from the empirical models.

And, a series of differences in the received signal strength were encountered when comparing rooms at our two concerned channel situations at the outdoor stage, whose variations can be influenced by the situation of the indoor terminal being closest or farthest from the window (or wall) where the signal arrives, and being into a determined floor.

Correspondingly, it has been counted for the important building penetration/entry loss term, where one single external flat wall has resulted in this effect relative to the outdoor strength level; all types of contributions coming through all building's walls were not accounted for due to the need of complex physical models, such as the high order ray-tracing tools. The entry loss has been a function of α (Tila *et al.*, 2001), deducing that the highest entry loss has occurred for the elevations between 15º and 30º, so the entry loss was referred to decrease between 30º and 60º; herein, the expectation is that entry loss decreases with increasing entry angle since the entry angle gets closer to the normal incidence (Pérez-Fontán *et al.*, 2008). The signal through building has been based on the empirical models following the rule of entry loss decreasing with a higher floor level and with less distance to the receiver from the signal entry's exterior wall; higher losses at ground floor were followed due to the street level surrounding, thus signal strength has increased when the receiver was put stood upwards at the building floor.

In addition to the (building) penetration loss concept, further impairments were of interest and are specified for our system design: received signal variability, effects of building height, conditions of transmission, dependence on the path length, effective transmitter (antenna) height, construction materials, room layout, and frequency of operation. It is noted that the interference rejection was neglected in our model, but in Vogel & Torrence (1993) was deduced that may exist with very little values above 1 GHz frequency band. Another presumption was defined with the no bandwidth dependence for loss, which for our study at the IEEE Std 802.16™ with a nominal bandwidth variation was highly helpful.

The description of each indoor space can be explained with several derivations due to the miscellaneous arrangement inside the different existent rooms, and so different path types might occur. The situation of having a corridor or hallway (possible modelling by wave guiding) might imply a more difficult and unworthy design, thus has not been considered. Herein, some deterministic from empirical modelling has been seized, thus a couple of decisive cases were established. In the first instance the receiver was put close to a window (or just obstructed by the external wall) in a quasi-LOS situation (QLOS, or path obstructed by the window so-called obscured LOS (OLOS)). Into small room cases, the QLOS conditions appeared, which can be described by an office room arrangement with a few white-collar

workers having an own room. In another room case, the transmission came from the window going deeper into the room, where the direct visibility between the transmitter and the receiver was definitively lost due to the indoor office obstacles and the type of office room shared by several working personnel. At such last instant of indoor transmission, the receiver has experienced two more local area situations: at the first case, the receiver can be indoors with some inner walls obstructing the sight from transmitter (NLOS situation), and next, the receiver was located deeper in the large indoor room zones where a lot more of partitions are occurring, so-called hard-NLOS condition (HNLOS) —representing more specifically to the room type at a typical small shopping market or exhibition centre.

3.1.2. Channel impairments and characterisation

An adequate HAPS propagation channel model was developed. The geometry approach considered was presumed with elemental rays (or echoes) for the purpose of defining the channel condition; at this stage, the stratospheric propagation link was established to not introduce other atmospheric mitigations, such as the atmospheric refraction, precipitation (rain, fog, snow), cloud cover, and not resulting in additional loss on the signal.

Various impairments can exist to be considered as an important influence on the channel characterisation. The significant part for the present HAPS-based system performance is conformed by the definition of the channel and service environment, i.e., the propagation effects (noise, fading, shadowing) and coverage zone cases were designated; those impairments arising from the system design (e.g., phase noise, channel nonlinearities, motion, intrasystem interference, etcetera) were considered in the ideal or neglected resolutions.

The additive white Gaussian noise (AWGN) existed, being the primary source impairment to which the signal was subjected from thermal noise at receiver. At the next channel impairment, HAPS (stratospheric) channel realised the multipath induced fading: the terminal receiver not only received the direct signal from the HAPS but also the reflected signals from various nearby objects; as the phase of the multipath was differing from that of the direct path, this was leading to a constructive and destructive interferences.

Two propagation channel conditions were defined for the specific urban area coverage: the first condition belongs to the direct-path situation, and the other to the log-normal shadowing situation; for both situations the pertinent propagation parameters for the “strato-

spheric habitat" were needed considering the signal attenuation as random processes due to fast and slow fading variations.

The extrapolation effort from satellite-based to HAPS-based system scenario has been contemplated to conform a complex urban scenario and to connect in a proper fashion to the HAPS-to-ground design and solution. The "multi-mode channel state modelling," in our case, does not stand for a representation about the channel transitions between states (or nonstationary process). It has been assessed two proper single statistical processes that review two independent stationary single-mode channel state modelling occurring in the metropolitan scenario, based on empirical LMSS models to produce the approach to HAPS behaviour; no possible extensions to an adaptable mobile scenario was effectuated due to the need of extensive HAPS communications measurement campaigns or some extended approach from the satellite-based systems, referring as mobile at ground terminal and platform (HAPS).

The HAPS-based system has higher LOS probability because of the consideration as an ultra high-altitude tower compared with the terrestrial one. As a result, HAPS can easily provide LOS communication at high elevation angle α, whereby the links are relatively free of influence of obstacles. Generally, the probability of having LOS path can be described by larger values of α (>40º), and lower values of α (≤40º) that would result in high probability for the shadowing state. Nevertheless, when HAPS is used to serve an urban environment area, buildings can stand on, or even there could be skyscraper where the condition of LOS path would be very difficult to attain. In our case, since a heavily built-up area coverage was considered, the shadowed region was seemly large and was the most severe attenuation factor with predomination, thus shadowing power attenuation was considered as another attenuation factor in addition to the path loss.

On the next issue, the signal's bandwidth is exceeding the coherence bandwidth of the stratospheric channel through which is propagating, the signal has been subjected to the frequency selective effects. Last concern is being increased in interests in the HAPS-based communications as higher rate transmission and new schemes introduced for today applications and services, in other words, the actual period of time when the developing necessities are not only needing narrowband channel models but also broadband channel models to produce a generic channel modelling for the fixed and mobile channel options; the general HAPS-based model to be implemented not only should reflect the physical channel modelling but also to have a model which is able to converge to the narrowband one.

3.1.2.1. Free space path and excess path loss

The determined signal transmission between HAPS and the ground terminal generally could take place via several paths, and the variation of α can define this. Last categorisation might include one direct-ray and potential remaining multipath rays: single reflection from building, single reflection from street, double reflection from building to street, double reflection from building to building, diffraction from rooftop of building, diffraction from rooftop and single reflection from building, diffraction from rooftop and single reflection from street, and diffraction from rooftop and double reflection from building to street; rays outside the mentioned categories can be assumed to leave the original target. Since all surfaces in real propagation environments are finite, also edges and corners have to be considered. In our case, the situation called diffraction can occur when a large body obstructs the radio path between the transmitter and the receiver causing secondary waves to be formed behind the obstructing body and continue to propagate towards the receiver.

The relevant model used, in which specific details of building allocation, trees, etc., for the metropolis environment, gave the signal information approach sorting out an explicit ray-tracing solution of the electromagnetic wave status: it was not required a great deal of measurement data but relatively a generic channel model which can be used in simulations.

The implementation of the ray-tracing algorithm, with a relative large d (d_{HAPS} in our case), has corresponded to the two-ray model. As the stationary receiver was considered to be a gadget, station, or small hardware for easy setup/deployment and equipped with a low gain antenna, the arrival rays collected by the terrestrial antenna have included two coherent components, a direct path (a significant portion of the total energy arrives at receiver by way of a direct wave) and a specular reflected path (remaining power of the transmitted signal), plus the diffuse components (many randomly scattered rays) (Davarian, 1987).

Eventually, it is aware that the product of the antenna fields for the corresponding peers is important in determining the reception power: in the receiver's antenna by following the induction of electric currents created by the wave arrival, the energy in our operating frequency band is directly coupled with the antenna size issue. Equally, antenna size is directly coupled with the field's wavelength (λ), which is basically inversely proportional to the carrier frequency ($\lambda = c/f_c$), that is, higher the frequency, the smaller the antenna size. Consequently, the antenna characteristics (Karapantazis & Pavlidou, 2004), (Miura & Suzuki, 2003) used during our analysis could have played an important role in affecting the performance out-

come; nevertheless, idealist for antennae comes for our whole analysis. Since idealisms for the antenna onboard the platform were considered, it could be complied with an ideal antenna pattern for the HAPS application (denoted by the possible use of a smart antennae or antenna arrays) and with a zero-dBi-gain omnidirectional antenna at the receiver terminal, so local mean received power was directly dependent to α and to the power transmit —the presumed omnidirectional antenna usage has had the relevant aspect of having a multipath power contribution much higher than in the case of a directional antenna assumption.

From the model available for propagation loss predictions, our HAPS-based system can have the calculation with the theoretic general equation

$$PL_{total} = PL_{FSPL} + PL_{shadowing} + PL_{fading}, \tag{3.6}$$

where PL_{total} is the total propagation loss, PL_{FSPL} represents the free space path loss as a function of *Tx-Rx* separation distance, $PL_{shadowing}$ denotes the shadowing loss, and PL_{fading} is the local fading loss.

HAPS has been considered to be an extremely tall base station that can present a propagation path consisting of the free space loss, the diffraction from rooftop, and the multiple reflections from the nearby buildings. Thereafter, based on the theoretical propagation loss, HAPS-based communications path loss can be represented by the sum of the free space loss (FSL), the rooftop scattering loss (RSL) and the multiple screen diffraction loss (MSDL) (Iskandar & Shimamoto, 2006b), (Iskandar & Shimamoto, 2006c). The total propagation loss was supposed as being power-summed since it was desired to predict the local-median value, and the received power was obtained by

$$PL = PL_{HAPS,FSL} + PL_{Terrestrial,RSL} + PL_{Terrestrial,MSDL}. \tag{3.7}$$

The formulation for free space path loss was dedicated to the LOS case in which existed only a direct path in *Tx-Rx*. The theoretical free-space path loss (power transmission ratio) was dependent on frequency and separation distance in *Tx-Rx* as typically expressed by the fixed quantity

$$PL_{HAPS,FSL} = 10 \cdot \log_{10}\left[\left(\frac{\lambda}{4\pi \cdot d_{HAPS}}\right)^2\right], dB, \tag{3.8}$$

λ is in meters and d_{HAPS} represents the *Tx-Rx* distance; latter FSL equation is only a valid predictor for values of d_{HAPS} that are in the far field of the *Tx*-antenna

$$d_{HAPS} = \sqrt{R_{HAPS}^2 + r_{HAPS}^2}. \tag{3.9}$$

Now, the diffraction from rooftop down to the street-level have led to an excess loss to the ground terminal as expressed

$$PL_{Terrestrial,RSL} = \min\left\{10\log_{10}\left[\frac{\lambda}{2\pi^2 \cdot r_{RSL}}\left(\frac{1}{2\pi\psi}\right)^2\right], PL_{EPLMRB}\right\}, \tag{3.10}$$

where PL_{EPLMRB} is the excess propagation loss due to multiple reflections from the buildings' wall along the street and surrounding T, thus

$$\begin{aligned} &\psi = \left|\tan^{-1}\frac{h_{building}}{x1} - \alpha\right|, r_{RSL} = \sqrt{h_{building}^2 + x_{TB1}^2}; \\ &x1 = x_{TB1}, h_{building}\cot\alpha \le x_{TB1}; \\ &x1 = 0; h_{building}\cot\alpha > x_{TB1}. \end{aligned} \tag{3.11}$$

$h_{building}$ is the difference between the building and the terrestrial terminal height, x_{TB1} is the horizontal distance between terminal and the diffraction edge (shadow), and x_{BB} is the width between the supposed buildings at both sides of the street.

At this scenario, x_{TB1} was considered as:

$$x_{TB1} = \min\left\{\frac{x_{BB}}{2}, h_{building}\cot\alpha\right\}, \tag{3.12}$$

with the second term $h_{building}\cdot\cot(\alpha)$ being the width of the building shadow cast onto the street level; when α is close to 90º, shadowing is narrow and the rooftop diffraction loss is relatively small, and in the case of having smaller α, the rooftop diffraction loss might be very high and the user terminal receives multiple reflection signals from the sides of nearby buildings. The condition for considering multiple side-reflections can be satisfied if

$$x_{BB} \le h_{building}\cot\alpha. \tag{3.13}$$

And, the number of reflections N_{RB} caused by the occurred rooftop diffraction and from the opposed building on the other side of street, can be estimated by

$$N_{RB} = \text{int}\left(\frac{h_{building}}{x_{BB}\cot\alpha} - 1\right), \tag{3.14}$$

where the function *int(·)* means the largest integer that is smaller or equal to the variable inside. Thus, the excess propagation loss due to reflection can be computed if the incident angle and the real and imaginary parts of the dielectric constant of the building material were known; but, except for "grazing" reflection where the signal essentially propagates parallel to the building surface, the excess loss can be taken to be 10 dB approximately. And the multiple reflection loss can be

$$PL_{EPLMRB} = -10N_{RB}. \tag{3.15}$$

Subsequently, it has been speculated that the rooftop diffraction loss would be typically of the order of 10 to 40 dB, meaning that more power can be needed for communications between terminal and HAPS in the shady area. Additionally, it has been assumed that at most two reflections must take place before the signal can reach the terminal, where one of the reflections must be from the ground, which has already been disregarded in our model. Now, let us have a reference from an example of a typical urban built-up rise: both the street width and building height are of the order of 25 m and greater, and accordingly, does not N_{RB} exceed 2 until α is below 19º, i.e. in an urban or suburban area with low rises (building heights lower than 10 m and street widths of around 35 m), α would be less than 5.5º before N_{RB} becomes greater than 2. Consequently, at different greater α and coverage area, the excess loss should be of the order of 20 dB or less. Moreover, in the region of typical residential areas, outdoor radio propagation is dominated by LOS propagation and rooftop diffraction; the absence of multiple reflections means that the terminal on the shady side will have to rely on rooftop diffraction to provide coverage, and very significant is the fact that multiple reflections could be rarely effective because of the inter-built-up distances.

Following to the next parameter of multiple screen diffraction loss, which differs from the multiple screen diffraction loss of the traditional radio tower ground base station, the data link transmission is presumed passing a row of buildings until reach the last structure next to the terrestrial terminal. Thus, multiple screen diffraction loss can take the following general form

$$PL_{Terrestrial,MSDL} = 10\log_{10}\left(Q^2\right), \tag{3.16}$$

for which, at the HAPS case, factor Q depends on α relative to the location of the terminal. For most elevation angles, $PL_{Terrestrial,MSDL}$ is essentially zero. At very small α, $PL_{Terrestrial,MSDL}$ increases rapidly. At zero elevation angles, $PL_{Terrestrial,MSDL}$ becomes arbitrarily large so that practically only LOS propagation is possible. It is examined and applied the case of multiple screen diffraction for α with values greater than 3º, and from the consideration of diffraction fringes between two successive screens, leading to the following dimensionless variable

$$\chi = \tan\alpha \cdot \sqrt{\frac{x_{BB}\cdot\cos\alpha}{\lambda}}, \tag{3.17}$$

which corresponds roughly to χ being greater than 1 (for typical average building separation about 50 m) and the multiple screen diffraction loss becomes effectively zero. For this reason

and the long coverage distance from HAPS, multiple screen diffraction is not a significant loss factor in the main HAPS service area (would say at values around and greater than 45º).

After last definitions, the feasible HAPS-based total transmission loss review is

$$PL\,|_{shadowing} = 10 \cdot l\,\mathrm{og}_{10}\left[\left(\frac{\lambda}{4\pi \cdot d_{HAPS}}\right)^2\right] + \min\left\{10 \cdot \log_{10}\left(\frac{\lambda}{2\pi^2 \cdot r_{RSL}} \cdot \left[\frac{1}{2\pi \cdot \psi}\right]^2\right), 10 \cdot \mathrm{int}\left(\frac{h_{building}}{x_{BB} \cdot \tan\alpha} - 1\right)\right\}, \quad (3.18)$$

$$PL\,|_{LOS} = 10 \cdot \log_{10}\left[\left(\frac{\lambda}{4\pi \cdot d_{HAPS}}\right)^2\right].$$

Afterwards, the empirical linear representation for the excess indoor loss representation was considered for a further coverage area approach from HAPS. Hence, the distance away (x_{indoor}) from the outdoor-face wall was supposed, and the penetration loss can be divided into four principal categories of wall loss, room loss, floor loss, and building loss; relative to the median (average) path loss level outside the building.

A great deal of reported penetration loss differs considerably due to different measurement methods and due to different buildings, but there might be a physical explanation of the noticed difference and achieve possibilities of basics for wall penetration losses: waves impinging on the external wall can impinge with a wide range of angles and the loss can be compared to the case of one single wave penetrating perpendicularly through the wall; a pronounce value at NLOS scenario is more probable when one or various dominant waves are arriving at nonperpendicular angles. To the last case the increasing of penetration loss is achieved due to the phenomenon where the outside reference level is resulted from a combination of waves in the direction towards the external wall and from waves reflected from the neighbour buildings (not penetrating through the building).

Hence, the situation of dependence also on the so-called (building) entry angle and azimuth incidence angle, i.e., the dependence of HAPS-path related to the incidence angles at elevation and horizontal orientations. The building entry (elevation) angle is being defined as that (at side-view) between the *Tx-Rx* path and the surface of the building (roof, façade) —the angle between the *Tx-Rx* path and its projection on the building surface having generalisations of lower values at longer *Tx-Rx* path situations with consequences of acquiring higher entry losses.— The azimuthal incidence angle is being defined as the horizontal-orientation incidence angle (top-view) with respect to the external wall.

In addition to the important role of the geometry of the path illuminating the external building face plus the dependence on the orientation incidences (elevation and horizontal) or

delay and angle spreading, the office-buildings have a wide variety of walls and obstacles that are forming the internal and external structure. The values for the building loss are concerning the propagation within the building to account for distances to the locations within the same room or within other rooms. The losses within the building were contemplated due to the partitions going through and due to pieces of furniture in the rooms, and the time-variability due to persons moving around and scatterers in general —the model and measurements (Berg, 1999), (Hashemi, 2002) can show variations very narrow in the Doppler spectra with widths of a very few hertz.

In our case, relying on a received energy component coming through indoors by a single wall (or the direct illumination from HAPS to the building façade) (Oestges & Paulraj, 2004), (Berg, 1999), the building loss expression can be written as following, including the entry loss complex process (outdoor-to-indoor channel modelling),

$$L_{BL} = L_{I,NI} + L_{I,GI}\left[1-\sin\left(\phi_G\right)\right]^2 + \max\left(n_{I,VW}L_{I,VW}, t_{loss}\left[x_{indoorL}-2\right]\left[1-\sin\left(\phi_G\right)\right]^2\right), \quad (3.19)$$

which can be compared from the empirical linear function approximation in Pérez-Fontán *et al.* (2008) resulting in values of 28.5 to 3.42 dB by the expression $L_{BL} = 28.5 - 0.12\phi_G$, in dB, where the building entry loss for 0º (grazing incidence) would be of 28.5 dB.

In the case of high-scattering NLOS scenarios, the expression can be transformed into an average parameter $L'_{I,GI}$, with an approximated value of 6 dB, so

$$L_{BL} = L_{I,NI} + L'_{I,GI} + n_{I,VW}L_{I,VW}, \quad (3.20)$$

in which additional components were counted caused by a reflection from a fixed scatterer (a hill or another building) or by the rooftop diffraction, but with angle of incidences unknown.

The building entry loss can be purely described by

$$L_{BPL} = L_{I,NI} + L_{I,GI}\left[1-\sin\left(\phi_G\right)\right]^2. \quad (3.21)$$

Also, further solutions of having a total received power to the indoor terminal concerning the excess loss through each wall and roof, a total received power can be expressed by

$$PL_{I,tot} = PL_{I,wall1} + PL_{I,wall2} + PL_{I,wall3} + PL_{I,wall4} + PL_{I,roof}. \quad (3.22)$$

From the most recent equations, $L_{I,NI}$ is considered the path loss through the external wall at normal incidence, $L_{I,GI}$ is the additional external wall loss due to incidence angles away from the normal incidence to the wall, $n_{I,VW}$ is the number of penetrated walls, $L_{I,VW}$ is the loss

in the internal walls along the floor, and Φ_G is the grazing incidence with respect to the external wall —latter angle could be possibly taken with further deterministic values of $\sin^{-1}\left(\cos\left(\alpha\right)\cos\left(\phi\right)\right)$for wall-1, $\sin^{-1}\left(\cos\left(\alpha\right)\sin\left(\phi\right)\right)$ for wall-2, $\sin^{-1}\left(\cos\left(\alpha\right)\cos\left(\phi\right)\right)$ for wall-3, $\sin^{-1}\left(\cos\left(\alpha\right)\sin\left(\phi\right)\right)$for wall-4, and ϕ for roof (Glazunov & Berg, 2000).

Values were considered within the boundaries of about 5-7 dB (10-20 dB in Martijn & Herben (2003)) for $L_{l,Gl}$ and 7 dB (Martijn & Herben, 2003) for $L_{l,Nl}$ (4-20 dB in Oestges & Paulraj (2004)). The transmission loss was supposed inside the building (in dB's) per meter (or gradient loss due to furniture and other indoor issues), t_{loss}, to be 1.1 to 3 dB/m (Martijn & Herben, 2003), with a distance $x_{indoorL}$ defined by the gap from the indoor terminal to the wall-signal entrance, and $L_{l,VW}$ with 2-10 dB (Martijn & Herben, 2003) (7.8-10 dB in Oestges & Paulraj (2004)). Besides, walls were roughly classified into light walls, i.e., walls not bearing load (e.g. plasterboard or light concrete walls), and heavy walls, i.e., load-bearing walls (e.g., thick walls made of concrete or brick), so parameter values quoted for our carrier frequency band could be 3.4 for light walls and 6.9 for heavy walls, and loss floor could be of 18.3 dB (Berg, 1999).

Accordingly, a mean penetration loss at ground floor level was assumed with a value of 15.07 dB, or of 12.5-13.4 dB (through a concrete wall building) (Oestges & Paulraj, 2004), (Fischer de Toledo *et al.*, 1998), (Berg, 1999). An average value of penetration loss considering all possible trials could be taken of 17 dB (Fischer de Toledo *et al.*, 1998), or of 20-27.75 dB in (Pérez-Fontán *et al.*, 2008) as a function of the elevation angle of 30º to 45º; furthermore, in a medium-density built-up area coverage, the average building loss factor can vary until 5 dB. And, specifically at 1st floor, the penetration loss would be of 12.5 to 13.4 dB (through a concrete wall building)

The entry loss was considered decreasing upward to the floor height at a rate of 1.4 to 2 dB/floor (on average records) (Fischer de Toledo *et al.*, 1998) —an alternative definition as the floor gain of 1.5 to 2 dB in (Berg, 1999). As a result, last has conveyed to a rate of change of the mean signal per floor about 6.1 dB/floor; it is noticed that with last other possible variations of -13 dB to 7 dB for the limits of the received signal due to remaining alternative dependences, such as that presented from the surrounding environment (urban clutter), the actual floor where the receiver stands up, the condition of the channel state, hence the increases could be obtained (not linear) when the receiver has moved upwards attributed to different causes (Martijn & Herben, 2003). Additionally, the loss considerations for basement

were accounted —considerations for entry losses about 20 to 30 dB were contemplated in either having a small or large (basement) room.

Now, the large-scale signal fluctuations are expected to dominate the statistical nature of the small-scale characterisation, and it can be established that the logarithm of local mean was normally distributed in outdoor, indoor, and outdoor to indoor propagation issues. The long-term fading, understood as fluctuations of the mean value over a distance of a few wavelengths, was related to the condition of transmission at the floor area. As it has been manifested before, the indoor long-term fading has been supposed to follow a Log-normal distribution (Fischer de Toledo *et al.*, 1998), (Berg, 1999) with a standard deviation related to the condition of transmission and *m*-th floor environment, being of ~4 dB in LOS transmission, and of 6-9 dB for partial to complete NLOS conditions; no carrier frequency dependence for the standard variation has been assumed.

In the long-term fluctuations, further accuracies at the direct-path situation were observed. As the received-signal amplitude was modelled as Ricean distributed, the characteristic parameter is the *K*-factor. In our case, *K* was considered substantially zero (for fixed BWA applications) (Oestges & Paulraj, 2004); *K* was reduced due to the small-scale scattering by indoor walls, doors, furniture, etc.

3.1.2.2. Reflection

The frequent reflected path from the ground (from the satellite-based communications design) was not proper in our HAPS-based communications interpretation —a little contrast to the conventional nonmobile HAPS-to-ground link carrying an equipment of high-gain antennas at receiver, where could be completely reject both specular and diffuse components and collect only the direct path. The contribution of the reflected wave has been considered from building structures, as well as possible from trees nearby the receiver. Thus, the method approach has been assumed by a set of rays originated from the same source and reflected from the same set of surfaces to be part of the same wave front.

In certain manner, the multipath has a dependence on the carrier wavelength λ. The front-edge wave has been contemplated as a reflection from an obstacle, or object, if this is smooth and its dimension is large enough compared to λ. In other words, it is constructed that smooth façade with large proportions, comparing to λ, tends to be a specular reflector, which acts in a similar way of a mirror —on the other hand, isolated objects with minor size or

comparable to that of λ, cause dispersion of the energy. Consequently, the importance of defining a smooth or rough surface has been relevant to the current analysis: the criterion of Rayleigh was used interpreting a height h_H that should not exceed a critical height of approximately of 2 to 11 cm in function of the angle of incidence and λ.

Accordingly, assumptions for the exterior surfaces of the buildings along the street held that the majorities have consisted of brick, stone, or concrete, with many glass windows. These types of surfaces have poor reflection coefficient at normal incidence due primarily to surface roughness and irregularities that are sizeable relative to λ, but at grazing incidence the surface can appear smooth and its reflection coefficient has become the highest —the Rayleigh criterion of $h_H \leq \lambda/8 \cdot \cos(\xi)$ determined if a surface was considered smooth, being ξ the angle of incidence and h_H is the height of the surface irregularity; in our analysis ξ = 8º (or greater) was a realistic angle.

As a result, roughness effect has had an influence on the coherent and specular paths by means of the Rayleigh factor

$$\zeta = e\left(-\frac{1}{2} \cdot \frac{4\pi\sigma_H \cdot \cos(\xi)}{\lambda}\right), \tag{3.23}$$

where σ_H is the standard deviation of the surface roughness. It has been deduced that with such factor a major weakness was evidenced on the reflection power of the specular path.

3.1.2.3. Scattering

All latter models can be used certainly to predict the narrowband characteristics. Now, in order to acquire the right predictions of signal for broadband accuracies without requiring the in deep usage of site-specific information and gaining time in computation, the more promising approach of delay spread and fading statistics characterisation must keep the system performance conjecture within a small margin error.

In this proposal, a viable model was useful for developing the information regarding the broadband characteristics by means of the propagation prediction using the echo/ray terminology at local levels of receiver's surroundings. Scattering has occurred due to the radio wave infringing on a large rough surface (or on dense foliage) that causes the (reflected) rays to spread out in various directions, or due to the motion of objects nearly surrounding the terminal. The proposed propagation model was theoretically based on the geometrical fea-

ture of the built-up structures surrounding the ground terminal, and expanded with the statistical estimation from LMSS channel model in order to estimate the system's field capacity; predictions were realised to be fairly different from that of the terrestrial channel but rather similar to the satellite channel.

Echoes that properly intersect to the receiver were analysed, together with the power delay profile (PDP) estimation which was developed by mapping the power of the different rays with respect to the delay time information (Jahn, 1994), (Parks *et al.*, 1996a), (Parks *et al.*, 1996b). The diffuse components were pondered to arrive at an elevation angle near 0º uniformly distributed phase, with amplitude statistically described by a Rayleigh distribution and a maximum Doppler spectrum of $2\upsilon_T/\lambda$.

Two types of reflections were considered, specular and nonspecular; for the former, the distance between the reflection point and the receiver varies, while for the latter it is constant. Now, It was assumed that a change of the HAPS-receiver distance has no significant effect on the relative phases at the receiver in either case, only the variation of the elevation angle could affect phasing: as higher elevation angles are presented, signals are affected less. A primary outdoor propagation model was derived from the attenuated main signal, combined with its multipath and a specular attenuated signal plus multipath, in order to have the correct interpretation of the HAPS signal variations. At the indoor case, multipath was presumed to come from several fixed-location (nonspecular reflection points), and deep nulls in the frequency domain, or in space, have resulted when the summed strength of several multipath components were comparable to the direct signal. And, signal maxima locations were less sensitive to phase changes than signal nulls, so an exact prediction of the HAPS signal level at any particular point cannot be had, but rather to be accurate to the signal structure statistics.

And, a connection can be referred with our proposed model to those with a closest HAPS channel modelling, and so related to the so-called (geometrical) single bounce model or other approaching research (*e.g.*, circular straight cone geometry, 3-D ellipsoid propagation model). It is referred to the distinctions specifically for the specular reflection echo (single bounce path) and the corresponding delay spread. It is differed from those already established models by approaching the probability of the specular ray existence by means of the building blockage inside an impaired scatterer topography resulting in a no uniform coverage over the receiver; in other words, the specular reflection ray was coming from a near scatterer with irregular environment volume and not uniformly distributed in space to the receiver. It is added that the scattering loss depending on the material of the structures was not totally

clarified. Thus, power delay or other related angle calculation for the arrival rays were expressed different from ours coming through unlike assumptions.

3.1.2.4. Diffraction

As a further matter, further improvements for our system are got covering the topic of prediction models of radio wave propagation in built-up areas explicitly taking into account building diffraction effects to improve accuracy.

Therefore, a solution for diffraction modelling purposes was conformed. Buildings were conventionally reviewed as parallel absorbing half planes (knife edges) located at the peak of the building rooftop (Saunders & Bonar, 1994). The attenuation function was provided from the complete solution to the problem of multiple co-linear knife-edge diffraction with an arbitrary number of edges; the solution has focused on the particular resolution for the multiple-edge diffraction integral from Vogler's model employing a method of repeated approximation for the resulting integral equation (Saunders & Bonar, 1994). Following, the terrestrial antenna was placed at an arbitrary height and located some distance away from the row-building edges, and the field was computed at a reference point located at the rooftop of the final building. The field strength at street-level then was calculated by a simple single plane approximation for each of the rays arriving at the receiver. The solution is uniformly valid; so that the source point may be above, level with, or below the diffraction-edge height, and possible bidden in equal easy application to small or large number of edges.

Straightaway, from the shadowing attenuation theory, a more complete received power approach was calculated withal, and the built-up conditions can be clearly defined for single knife-edge diffraction attenuation at the rooftop of the closest building to the ground terminal. Thus, a considerable approach model, proper in the LOS and shady circumstances, has allowed us operative predictions where direct measurements were unavailable and where existent LMSS records can be adopted (Vázquez-Castro *et al.*, 2002), (Saunders & Bonar, 1994).

At the obstructed condition, it was assumed the attenuation from the free space field by the two practical diffracted and diffracted reflected ray (triggered by the building opposite to the main building) were combined with random phase at receiver

$$PL_{Terrestrial,DS} = PL_{HAPS,FSL}\sqrt{A^2\left(\vartheta_{DLOS}\right) + \rho^2 A^2\left(\vartheta_{DDRR}\right)}, \tag{3.24}$$

where ρ is the loss because of reflection, including effects due to polarisation, surface roughness and the material reflection coefficient. And,

$$\begin{aligned} A\left(\vartheta_{DLOS}\right) &= \tfrac{1}{2} F\left(\vartheta_{DLOS}\right) e^{-j\cdot\pi/4} + \tfrac{1}{2}, \\ A\left(\vartheta_{DDRR}\right) &= \tfrac{1}{2} F\left(\vartheta_{DDRR}\right) e^{-j\cdot\pi/4} + \tfrac{1}{2}, \end{aligned} \tag{3.25}$$

where F is the complex Fresnel integral

$$F\left(\vartheta_D\right) = C\left(\vartheta_D\right) + jS\left(\vartheta_D\right). \tag{3.26}$$

The Fresnel diffraction parameters for the (diffracted) direct ray and for the reflected ray are given by:

$$\begin{aligned} \vartheta_{DLOS} &= -\left[\frac{\pi}{2} - \tan^{-1}\left(\frac{x_{TB1}}{h_{building}}\right) - \alpha\right]\sqrt{\frac{2\cdot x_{TB1}}{\lambda}}, \\ \vartheta_{DDRR} &= -\left[\frac{\pi}{2} - \tan^{-1}\left(\frac{2\cdot x_{building} - x_{TB1}}{h_{building}}\right) - \alpha\right]\sqrt{\frac{2\left(2\cdot x_{building} - x_{TB1}\right)}{\lambda}}. \end{aligned} \tag{3.27}$$

In due course, at LOS condition were power-summed the respective direct and specular reflection rays

$$PL_{Terrestrial,DD} = P\left(\vartheta_{LOS}\right) + \rho^2 P\left(\vartheta_{SR}\right), \tag{3.28}$$

with the diffraction parameters defined for the direct ϑ_{LOS} and reflection ϑ_{SR} rays as

$$\vartheta_{LOS} = \left(h_{building} - h_{LOS}\right)\sqrt{\frac{2}{\lambda\cdot d_{LOS}}}, \tag{3.29}$$

$$\vartheta_{SR} = \left(h_{building} - h_{SR}\right)\sqrt{\frac{2}{\lambda\cdot d_{SR}}}, \tag{3.30}$$

where

$$\begin{aligned} h_{LOS} &= \begin{cases} h_{ter\min al} + \frac{x_{TB1}\cdot\tan\alpha}{\sin\phi}; 0 < \phi \le \pi \\ h_{ter\min al} + \frac{\left(x_{BB} - x_{TB1}\right)\cdot\tan\alpha}{\sin\phi}; -\pi < \phi \le 0 \end{cases}, d_{LOS} = \begin{cases} \frac{x_{TB1}}{\sin\phi\cdot\cos\alpha}; 0 < \phi \le \pi \\ \frac{\left(x_{BB} - x_{TB1}\right)}{\sin\phi\cdot\cos\alpha}; -\pi < \phi \le 0 \end{cases}, \\ h_{SR} &= \begin{cases} h_{ter\min al} + \frac{\left(2\cdot x_{BB} - x_{TB1}\right)\cdot\tan\alpha}{\sin\phi}; 0 < \phi \le \pi \\ h_{ter\min al} + \frac{\left(x_{BB} + x_{TB1}\right)\cdot\tan\alpha}{\sin\phi}; -\pi < \phi \le 0 \end{cases}, d_{SR} = \begin{cases} \frac{\left(2\cdot x_{BB} - x_{TB1}\right)}{\sin\phi\cdot\cos\alpha}; 0 < \phi \le \pi \\ \frac{\left(x_{BB} + x_{TB1}\right)}{\sin\phi\cdot\cos\alpha}; -\pi < \phi \le 0 \end{cases}; \end{aligned} \tag{3.31}$$

the diffracted ray power was then expressed in terms of the Fresnel cosine $C\left(\vartheta\right)$ and sine $S\left(\vartheta\right)$ integrals

$$P\left(\vartheta\right) = \tfrac{1}{2}\cdot\left(\tfrac{1}{2} + C^2\left(\vartheta\right) - C\left(\vartheta\right) + S^2\left(\vartheta\right) - S\left(\vartheta\right)\right). \tag{3.32}$$

Latter expressions were assumed to have HAPS-to-building distance very much greater than the building-to-terminal distance, also supposed that only one building has contributed to the diffraction process and has defined that the higher the building height was, the more would has counted for the shadowing case attenuation.

Typical extension of vegetation areas in cities is generally too small, but realistically existent. Then, a similar analysis has also been applied to potential shadowing by trees rather than buildings.

In our case, the effect of foliage was considered by adding contributions from the penetration through vegetation (empirical approach) and diffraction over vegetation effects (Davarian, 1987). The foliage has been accounted for leaves very thin from real vegetation canopies behaving like Rayleigh scatterers, without considering the influences of stem and moisture. Thus, diffraction over greenery has been specifically modelled by single knife-edge diffraction at 1.2 m average height, and penetration through greenery was defined to be feasible with 5 dB by the following approach

$$PL_{Terrestrial,\,foliage} = g \cdot \sum_{i=1}^{n} l_i, dB, \tag{3.33}$$

where g = 0.2dB/m, and l_i stands for the longitudes of the i-th vegetative areas, which were taken as an alternate arrangement of n=5 greenery areas of 5 m in longitude for each one located through the signal transmission path.

Eventually, the possible attenuation for such specular reflection path was evaluated by

$$L_{srp,FSL} = 20\log_{10}\left(\frac{d_{srp}+\Delta r_{srp.}}{d_{HAPS}}\right), dB. \tag{3.34}$$

Straightaway, from the last attenuation theory, the received indoor power approach was calculated. The condition was defined for the single knife-edge diffraction attenuation at the rooftop of the closest building (or vegetative area) to the indoor receiver, and the approach model, proper in the LOS and shady circumstances, was related to the operative predictions where direct measurements were unavailable and where existent LMSS records were adopted (Pérez-Fontán & Mariño Espiñeira, 2008), (Karlsson *et al.*, 1994).

Further outdoor variables were considered, the x_{indoor} is the distance from indoor receiver to the wall illuminated by the HAPS $x_{indoorL}$ and the opposite one $x_{indoorR}$, $h_{building}$ is the difference between the building and the receiver height with dependence on the m-th floor height, and x_{TB1} is the horizontal distance between receiver and diffraction edge —corresponding to the sum of x_{BB} (width of street) and $x_{indoorL}$.

A number of reflections N_{RB} can also appear, usually caused by the opposed building from the rooftop diffraction occurrence; in this proposal the reflections were not regarded in the 'reflection' essence as in Palma-Lázgare & Delgado-Penín (2010b) but was taken as a reference for the additional loss for the specular ray (small-scale term) computed with -10 dB.

At the obstructed channel state, it was assumed that the attenuation from the free space field and the two possible diffracted rays were combined with equal random phase at receiver

$$PL_{S,Terrestrial} = PL_{HAPS,FSL}\sqrt{A^2\left(\vartheta_{DLOS}\right) + A^2\left(\vartheta_{SDR}\right)}, \tag{3.35}$$

$$\begin{aligned} PL_{HAPS,FSL} &= 10\log_{10}\left[\left(\frac{\lambda}{4\pi d_{HAPS}}\right)^2\right], \\ d_{HAPS} &= \sqrt{R_{HAPS}^2 + r'^2_{HAPS}}, r'_{HAPS} = r_{HAPS} - h_{terminal} - h_{floor}. \end{aligned} \tag{3.36}$$

$$\begin{aligned} A\left(\vartheta_{DLOS}\right) &= \tfrac{1}{2}\cdot F\left(\vartheta_{DLOS}\right)e^{-j\cdot\pi/4} + \tfrac{1}{2}, \\ A\left(\vartheta_{SDR}\right) &= \tfrac{1}{2}\cdot F\left(\vartheta_{SDR}\right)e^{-j\cdot\pi/4} + \tfrac{1}{2}, \end{aligned} \tag{3.37}$$

where F is the complex Fresnel integral

$$F\left(\vartheta_D\right) = C\left(\vartheta_D\right) + jS\left(\vartheta_D\right). \tag{3.38}$$

The Fresnel diffraction parameters for the (diffracted) direct and reflected rays are given by:

$$\vartheta_{DLOS} = \vartheta_{SDR} = -\left[\frac{\pi}{2} - \tan^{-1}\left(\frac{x_{indoorL} + x_{BB}}{h_{building}}\right) - \alpha\right]\cdot\sqrt{\frac{2\left(x_{indoorL} + x_{BB}\right)}{\lambda}}. \tag{3.39}$$

In due course, at LOS condition, the respective direct and reflected rays were power-summed (Palma-Lázgare & Delgado-Penín, 2010b)

$$PL_{D,Terrestrial} = P\left(\vartheta_{LOS}\right) + P\left(\vartheta_{SR}\right), \tag{3.40}$$

with the diffraction parameters defined for the direct ϑ_{LOS} and reflected ϑ_{SR} rays as

$$\begin{aligned} \vartheta_{LOS} &= \left(h_{building} - h_{LOS}\right)\sqrt{\frac{2}{\lambda\cdot d_{LOS}}}, \\ \vartheta_{SR} &= \left(h_{building} - h_{SR}\right)\sqrt{\frac{2}{\lambda\cdot d_{SR}}}, \end{aligned} \tag{3.41}$$

where

$$h_{LOS} = h_{SR} = \begin{cases} h_{ter\,\min al} + h_{floor} + \frac{\left(x_{indoorL} + x_{BB}\right)\cdot\tan\alpha}{\sin\phi}; 0 < \phi \le \pi \\ h_{ter\,\min al} + h_{floor} + \frac{\left(x_{indoorR}\right)\cdot\tan\alpha}{\sin\phi}; -\pi < \phi \le 0 \end{cases},$$
$$d_{LOS} = d_{SR} = \begin{cases} \frac{x_{indoorL} + x_{BB}}{\sin\phi\cdot\cos\alpha}; 0 < \phi \le \pi \\ \frac{\left(x_{indoorR}\right)}{\sin\phi\cdot\cos\alpha}; -\pi < \phi \le 0 \end{cases}; \quad (3.42)$$

the diffracted ray power was then expressed in terms of the Fresnel cosine $C\left(\vartheta\right)$ and sine $S\left(\vartheta\right)$ integrals from Equation 3.31.

3.1.2.5. Mid- and short-term random variations

3.1.2.5.1. Slow-fading

The mid-term fading was materialised due to shadowing and distance dependence.

Path loss (IEEE Std 802.16™, 2009) at our case presenting HAPS-wireless channel can be as lower as the path loss for an equivalent terrestrial fixed wireless channel —and possibly as much higher as the path loss in the case of a mobile wireless channel due to the use of a low height omnidirectional antenna at the receiver unit—. The situations having a higher path loss are defining a higher system gain and the high variance of the path loss can cause interference.

The transmitted signal through the urban environment is experiencing random variations due to the blockage from urban objects in the signal path and giving rise to random variations of the received power at a given distance (Goldsmith, 2005). These variations were supposed to be caused by changes in the reflecting surfaces and scattering objects, and random attenuation due to such effects was needed. As the mentioned changes were generally unknown, the implementation of statistical (log-normal) modelling is characterising this attenuation. Hence, our modelling is accurately confirmed by proper empirical application of the variations of received power at outdoors and indoors radio propagation environments.

3.1.2.5.2. Fast-fading

A reasonable model for a given broadband measured radio channel can be approximated by the statistical properties of the physical channel (Mohr, 1995), (Castro *et al.*, 1999).

The HAPS broadband channel founded on satellite measurements can show the following behaviour (Castro *et al.*, 1999): echoes can have very short delays from the vicinity of receiver at the most modest case corresponding to where a very strong direct path exists, but the environment with a strongest echoes can be defined by the urban environment where the surfaces of building and the heavy traffic form the reflectors even for high angles of incidence (or elevation angles).

Three effects and one note could influence the broadband channel modelling:

- The operational scenario, i.e., end-user/terminal's behaviour effects, direct path suffering from shadowing or blockage.
- The foreground environment changes (traffic and surroundings).
- The background environment changes (HAPS motion). Echoes with long delays can influence on modelling; such movement also can be scaled if a HAPS-communication constellation is used.
- A short-term description, in general, has a correlation duration corresponding to 40λ; mid-term variations of the echoes are mainly determined by the lifetime of the echoes.

Therefore, at the channel state situations formed at our communication system, the frequency-selectivity was generated and can vary very fast. The tap model for the broadband channel was generative one and had a physical background from discrete reflectors —the reflectors were located in different distances to the receiver at built-up geometry structure, which can cause very close echoes in time implying different arrival times of the main paths; thus the impulse response of the received signal was generated by a superposition of the reflected impulses.

At this multipath component routine, the stratospheric model mainly corresponded to a transversal filter structure described by tap delays, statistics of the tap amplitudes and their corresponding Doppler spectra —the derivation came from a set of broadband measured complex impulse responses and mathematical heuristic approach standing for a given number of taps with constant delays: every tap was described by its complex time-varying amplitude including its statistic and Doppler spectrum.

The power of one impulse response can be denoted by $P(t,\tau)$ where the excess delay is τ, t is the time variation, and a series of continuous impulse responses was defining the power delay profile (PDP), where the phase information was not able to be obtained by measurements and a uniform distribution was presumed.

The expected value with respect to time of a variable x is denoted by E{x}, and the calculation of the average PDP (or delay power spectral density (PSD)) can be represented by $P(\tau) = E\{P(t,\tau) \mid \tau\}$, with the average excess delay defined by $\tau_e = \frac{\int_0^\infty \tau \cdot P(\tau)\,d\tau}{\int_0^\infty P(\tau)\,d\tau}$ and the delay spread (RMS delay) by $\tau_{rms} = \sqrt{\frac{\int_0^\infty (\tau-\tau_e)^2 \cdot P(\tau)\,d\tau}{\int_0^\infty P(\tau)\,d\tau}}$.

3.1.2.5.3. Delay spread, Doppler spread, coherence bandwidth, and coherence time

The operation over broadband wireless channels (IEEE 802.16™, 2009) implies to operate even in fading channels where significant multipath can be present. The RMS delay spread for the HAPS channel around the ultra high frequency range can present values between several hundreds of nanoseconds to several tens of microseconds —the worst large delay spreads can be presented in both vehicular and pedestrian mobility situations due to the small height of the receiver antennas, and the fact that the mobile unit is typically using omni-directional antennas.

The set of HAPS-channel variables and modelling specified and denoted the statistical parameters of such microscopic effects, and to complete the channel model, the macro-scopic channel effects and their statistics are combined with the last parameters concerning the path loss and shadowing (excess path loss).

In addition, the elevation angle parameter must be mentioned. The azimuth angle con-sideration had a significant effect on performance, especially at blockage/shadowing channel state. Azimuthal data were not available for a number of measurements pertaining to blockage/shadowing but could be assumed with a uniformly distributed azimuth angle in the derivations of blockage statistics for a given elevation; a worst case was considered for the azimuth angle occurring when the LOS-link is perpendicular to the terminal's transmission di-rection — the implicit azimuthal dependence from the scenario geometry could be removed by the integration over the full range of azimuth angles.

Now, the fading spectrum can be determined by the spatial distribution of the scatter-ers and the antenna properties: if the scatterers are uniformly distributed in a plane the result-ing fading spectrum can be the Jakes spectrum, and other authors can considered the case

where the scatterers can have a distribution in three dimensions. Herein, the system's performance cannot be highly sensitive to the precision of fading spectra shape due to the fixed terminal situation, and it is not apparent to gain much by finding the exact approximation of the fading PSD.

The statistics of the wireless channel by means of first and second order moments were giving their main behaviour in the HAPS-based system. The HAPS wireless channel was assumed to be wide-sense stationary due to the independence of the first order moments of time and the dependence of the second order moments on the time difference Δt (Hutter, 2002). The channel fulfilled same features with respect to the frequency variable so exhibiting uncorrelated scattering. The combination of both latter characteristics was defined for the WSSUS channel case.

Therefore, the autocorrelation function can be defined for the WSSUS channel only depending on Δt and the frequency difference Δf

$$E\left\{h\left(f,t\right)h^{*}\left(f+\Delta f,t+\Delta t\right)\right\} = R_{h}\left(\Delta f,\Delta t\right). \tag{3.43}$$

By applying the double Fourier transform can be obtained the channel description in the time-delay Doppler domain, and the corresponding autocorrelation function can be referred to its scattering function, which is the important system function providing the energy distribution along the time-delay variable τ and the Doppler frequency v

$$S\left(\tau,v\right) = \int\int R_{h}\left(\Delta f,\Delta t\right)e^{j2\pi\Delta f\,\tau}e^{j2\pi\Delta t v}\,d\Delta f\,d\Delta t. \tag{3.44}$$

Concerning the mean Doppler power spectral density (PSD), which provides the description of the integral effect of the time-variant channel's nature, can be expressed by

$$P\left(v\right) = \int_{-\infty}^{\infty} S\left(\tau,v\right)d\tau; \tag{3.45}$$

the mean time correlation function $R(\Delta t)$ can be described as the time-variant behaviour of the channel in the time domain, and obtained as the Fourier transform of $P(v)$ finding $R(\Delta t) = R_h(0,\Delta t)$.

Consequently, based on the time correlation function, the key parameter of coherence time $T_{coherence}$ can be derived. The coherence time is referring to the time difference for which $R(\Delta t)$ attains 50% of its zero-lag value, and is inversely proportional to the maximum Doppler frequency $f_{D,max}$. Following last observations in literature, examining such values a simple rule-of-thumb can be used if the actual Doppler spectral density was certainly unknown

$$T_{coherence} \approx \frac{0.25}{f_{D,\max}}. \tag{3.46}$$

The PDP can describe the average frequency-selective channel's behaviour

$$P(\tau) = \int_{-\infty}^{\infty} S(\tau, v)\, dv; \tag{3.47}$$

this can exhibit the exponential decay $P(\tau) \propto e^{-\tau/\tau_0}$ with τ_0 as the decay constant. The parameters describing such PDP are the first and second order moments, mean time $\bar{\tau}$ and delay spread σ_τ; as an exponential decaying power-delay profiles was presented, both parameters can equal to the decay constant $\bar{\tau} = \sigma_\tau = \tau_0$.

Next, the mean frequency correlation function *R(Δf)* can describe the frequency-selective channel's behaviour in the frequency domain with $R(\Delta f) = R_h(\Delta f, 0)$ from the Fourier transform of $P(\tau)$; hence, the parameter of coherence bandwidth $BW_{coherence}$ can be determined as the frequency where frequency correlation function attains 50% of its zero-lag value, and in our case of having exponentially decaying PDP's the coherence bandwidth can be given by

$$BW_{coherence} = \frac{1.1}{\tau_m} \approx \frac{1}{\tau_m}, \tag{3.48}$$

τ_m is established as the maximum excess time delay; also can be the relation $\tau_m = 6.9\tau_0$.

3.1.2.5.4. Envelope and phase fluctuations

Even the HAPS is assumed still at stratospheric, it can be said that no perfect stationarity can be gained and could exhibit cyclical and drift motions changing the distance and elevation angle between transmitter and receiver; if these nonstationary effects would affect the relative phase between the received waves, then the signal level could be considered a time varying case.

The referred phase fluctuations can make the reference to the presented model where the deeper the fade threshold is, the larger the phase variance can be. These fluctuations may be compared to the literature's small phase variations measured at urban zones to those that represent larger phase variances with a severe shadowing condition. As a general fact, the distributions of phase fluctuations can have such small variances that they will not affect

the demodulator at all (Saeed *et al.*, 2003); from the latest, the channel HAPS-channel characterisation can be estimated by amplitudes only, without regarding to the phase fluctuations.

3.2. The composite of the stratospheric channel

The acquisition of the parameters and modelling, in our case, are from the given environment and elevations considered from empirical and (averaged) measurement recordings. The registered data for our system's channel modelling were performed from the satellite based narrowband and broadband research literature, predominantly.

Hence, the overall representation for the HAPS-channel modelling has been taken as the equivalent complex channel impulse response (CIR) expression (Pätzold, 2002)

$$\tilde{c}(\tau,t) = \sqrt{L \cdot f_{CS}\left(t\right)} \cdot \tilde{h}\left(\tau,t\right), \tag{3.49}$$

where the first factor represents the long-term situation, and the second factor counts for the short-term statement. Equation 3.49 is valid for greater values of 1 km, where L is the mean loss, and $f_{CS}(t)$ belongs to the channel state situation, *e.g.*, the shadowing state (at the locality of the receiver) through time t the function can be modelled as a Gaussian variable with 0 dB mean and a standard deviation, the Log-normal model.

In order to model the HAPS-to-terminal channel propagation for optimisation, our design has comprised of two cascaded stages (Figure 3.8 and 3.9) associated to the HAPS-to-ground path (HAP-process) and to the effects surrounding the terrestrial terminal relative to its neighbouring scatterers (terrestrial-process)

$$PL = PL_{HAPS} + PL_{Terrestrial}, \tag{3.50}$$

in which free space attenuation and multipath fading effects counted for the major fading factors.

On the other hand, when concerning the communications coverage at indoors, the transmission inside buildings is involving a propagation environment that had differences from the familiar street-level situation studied in connection with the HAPS (Palma-Lázgare & Delgado-Penín, 2010b).

The propagation model into buildings (ITU-R P.1411-3, 2005), (Pérez-Fontán & Mariño Espiñeira 2008) has involved two major predictions of the received signal level: building-outside conditions, building penetration loss and indoor layout. For instance, main factors of

building and room losses are used as additional parameters for a nonprecise predicted signal loss from the surroundings outdoor local area as in Martijn & Herben (2003): the building loss can be defined as the difference between the average signal strength in the area around a building and the average signal strength on the ground floor of that building, and the room loss can be defined as the difference between the average signal strength in the outdoor area adjacent to a room located on the ground floor of a building and the average signal strength in that room; at higher floors, the received signal strength can be in general higher than at ground floor, thus may cause higher interference levels related to the building loss by means of the so-called floor height factor.

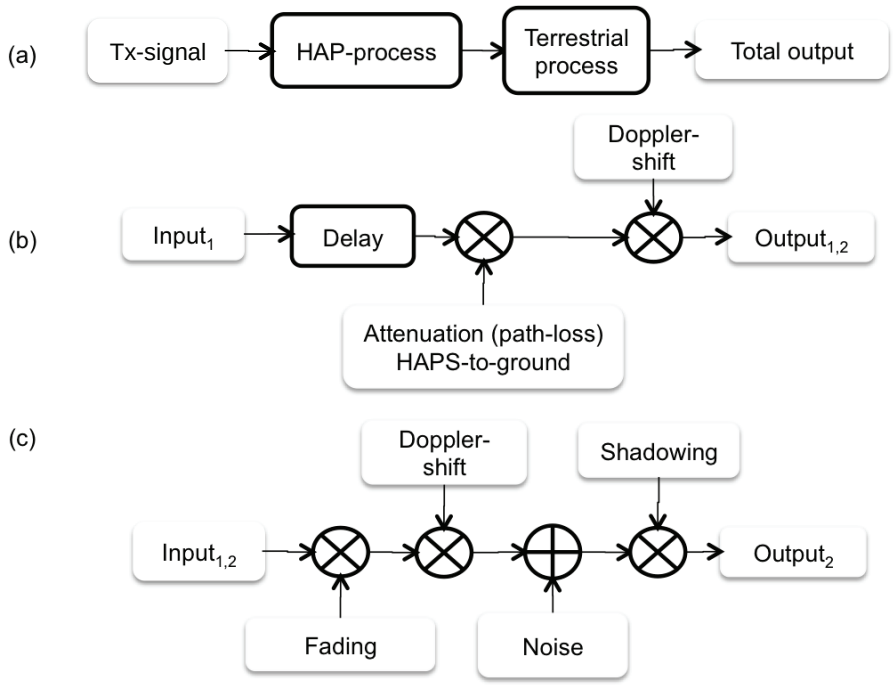

Figure 3.8. (a) The general block perspective of the assumed HAPS-channel modelling (or stratospheric channel) conformed by: (b) the HAP-process, and (c) the terrestrial-process (Parks, 1996b).

Hence, a two-step model was determined, i.e., the overall outdoor-indoor propagation loss has been developed through the following expression

$$L_{Total,dB} = L_{Outdoor} + L_{Indoor}, \tag{3.51}$$

where the average power was resolved to have the outdoor/outdoor-indoor path contributions, together with the multipath effects of the surrounding buildings, which is the reference of 0 dB for the applied absolute values (Pérez-Fontán & Mariño Espiñeira 2008).

The HAPS-channel modelling showed was characterised into two stages that represent the long-term and short-term conditions. The long-term fading brings about the attenuation, or path-loss, where signal suffers from the long distances between transmitter and receiver-end; in our case, it is considered a random environment-state static receiver primarily shadowed by urbanism identification or possible existent foliage. The short-term fading has concerned in the dynamic variations in amplitude and phase of the received signal as a result of the very small changes in the short spatial surroundings at ground.

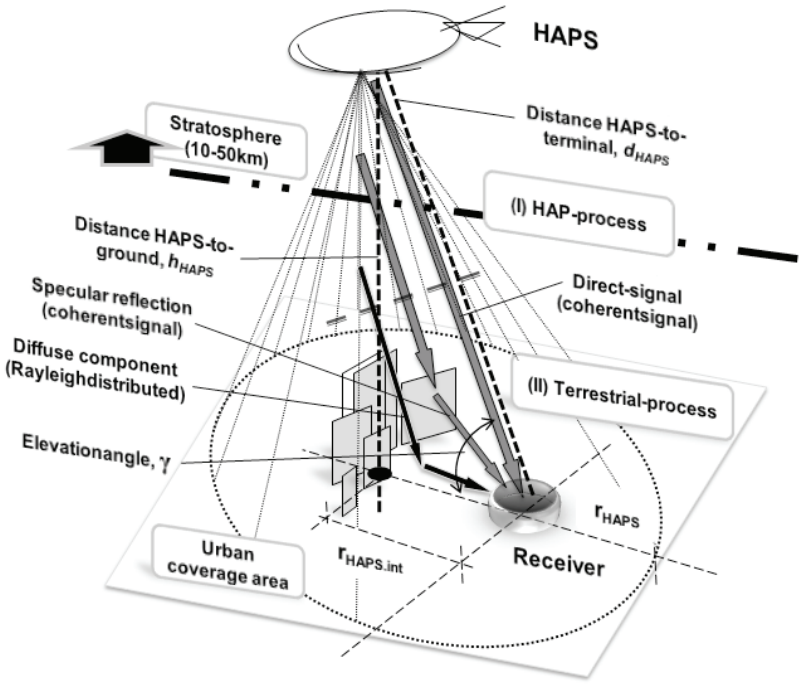

Figure 3.9. The global scenery for contributions from the presumed HAPS-based system (Davarian, 1987), (Parks, 1996b), (Evans *et al.*, 1996), (Vázquez-Castro & Pérez-Fontán, 2002), (Palma-Lazgare *et al.*, 2008).

Figure 3.9 and Figure 3.10 give the visualisation of the physical propagation environment assumed for our HAPS-based system, where the terrestrial receiver was presumed with an ideal low gain antenna that has collected the following four main rays: a direct path (r_1), a specular reflected path (r_3), and a diffuse path splitting over the first diffuse component (r_2) and the second diffuse component (r_4); if the receiver terminal would had been equipped with a high-gain antenna, then it could have had completely rejected the last three components and collected only r_1, not our case. Thus, the representation of the received signal was declared as the sum of such four vectors: the two coherent components (direct and reflection wave) and the two diffuse ones (frequency-selective fading waveform)

$$\bar{R} = \bar{R}_1 + \bar{R}_2 + \bar{R}_3 + \bar{R}_4, \tag{3.52}$$

where *R* denotes the signal arrival at the terrestrial receiver, with the assumption of having the changes in the reflection ray occurring very slowly when arrive at the supposed non-negative elevation angle (Davarian, 1987), (Vucetic & Du, 1992).

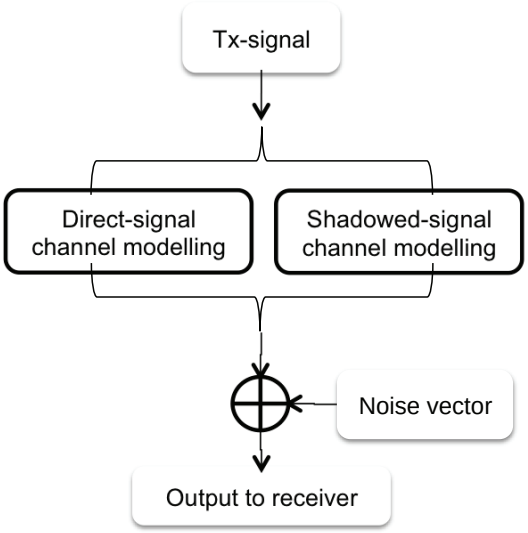

Figure 3.10. The state-oriented channel modelling.

Next, HAPS communication systems is assumed to offer high flexibilities for terrestrial users and simultaneously made from high-degree propagation design by the complex nature of the outdoor/indoor channel, specifically, if it was looked for provisions at a wide range of services and communications through many different environments. Hence, the signal can be corrupted by noise, distorted by Doppler shifts and obstructed by both stationary and rapidly moving objects. An accurate multipath fading channel model can be represented in the baseband as the direct component (or obscured LOS at indoor case) and the sum of discrete signal components varying in number, amplitude, and phase (each signal component is resulted from the propagation along a different path with different levels of attenuation and different delays relative to the main component from *Tx* to *Rx*). And a generalisation to represent such fading channel can be given by

$$h(\tau;t) = L(t)\delta(t) + \sum_i a_i(t) e^{-j2\pi f_c \tau_i(t)} \delta\left[\tau - \tau_i(t)\right]. \tag{3.53}$$

In the latter generalised expression *L(t)* is representing the time-varying amplitude of the direct component, a_i is the time-varying amplitude/magnitude of the *i*-th multipath com-

ponent, τ_i is the delay of the i-th multipath component, and f_c is the carrier frequency —the direct component may be characterised by a Rayleigh, Rice or log-normal distributions depending on the extent of obstruction of the LOS signal, and the multipath components are typically Rayleigh if no strong reflectors exist and Ricean/Nakagami if some small number of strong reflectors exist; this model must be capable of simulating the significant changes in the environment experienced by the receiver, at a fixed or as it is moving relative to *Tx*, *e.g.*, a representation done by a finite set of states similar to the narrowband channel model implementations.

3.2.2. The state-oriented channel model

Existent extended models for HAPS can be found, that were developed through the recent decade of 2000's (Djuknic & Okunev, 1997), (Tozer *et al.*, 2000), (Mondin *et al.*, 2001), (Husni *et al.*, 2001], (Stephen & Makrinos, 2005), (Oodo *et al.*, 2005), (Jamison *et al.*, 2005], (Falletti *et al.*, 2006), (Kang *et al.*, 2007), (Iskandar *et al.*, 2008). Beside the design for the HAPS-based system under the COFDM-based and IEEE 802.16™ standardisation margins (Czylwik, 1998), (Heiskala & Terry, 2001), (Grønsund *et al.*, 2007), (Pedro-Eira *et al.*, 2009), the modelling is facing with a further matter, i.e., the stratospheric channel modelling for which there is no prior database; and, addressing the adequate margins to combat such predominant issues were considered.

Our stratospheric channel modelling was based on the terrestrial and satellite communication designs due to its comparable signal propagation condition and path-loss similarities. Consequently, it has been considered that HAPS-based communications behaves practically in the same way as in the LMSS case in which similar elevation angles are used, the only difference is the link length which sets the FSPL reference level (Hoeher *et al.*, 1996), (Vázquez-Castro & Pérez-Fontán, 2002), (Iskandar & Shimamoto 2006b), (Palma-Lazgare *et al.*, 2008), (Palma-Lazgare & Delgado-Penín, 2008b).

Our study specifically addresses parameters of statistical-geometrical modelling and multipath effect at 1.820 GHz in the environment defined by a clutter density in a dense urban area which belongs mainly to elevation angles between 29º and 90º (ITU-Q/2, 1998), (ITU-R 39.8, 1999), (Husni *et al.*, 2001), (Kang *et al.*, 2007).

On the next subtopics, the approach of the stratospheric channel modelling has been related to our study with a number of recorded data gathered into the context of the LMSS

research literature, and for which had carried out the state-oriented model estimate defining the received signal level into the LOS and shadowing channel propagation paths. So that, it has been enclosed to two feasible aims for the channel propagation events: our proposal analyses were built up from LMSS-based system channel model states that were fine-tuned to the stratospheric case and accommodated to the broadband capabilities.

The last two conditions were combined to fit a more accurate and broad range of the HAPS-based system notions into the norms and to develop the appropriate model of the HAPS channel propagation variations. In addition, it is suggested to use the model on having a significant role into the fixed BWA (FBWA) implementation based on a proficient and regulated communication system supported by a stratospheric platform station.

Another essential assumption has been made for all of our analyses: it was defined that some long- and short-term variables have been modelled in similar way for every state-classification, and the reason for this is that if it were employed different approaches for each environment-situation; it have had a bad effect affecting the obtainment of reliable results defining non-comparable states (Pérez-Fontán *et al.*, 1998), (Fontan *et al.*, 2001), (Vazquez-Castro & Pérez-Fontán, 2002).

Upon establishing that shadowing plus multipath determined our HAPS channel modelling characterisation, not anymore a single probability distribution has described the HAPS channel behaviour.

The long-term observations clearly suggested us that typical distributions used in radio propagation could not have been used directly to characterise the channel, and rather a combination of signal states was required to have the corresponding overall signal variations. Hence, the overall probability density function (pdf) has followed the expression

$$f_{overall}(r) = p_{LOS} \cdot f_{LOS}(r) + p_{shadowing} \cdot f_{shadowing}(r), \tag{3.54}$$

where f_{LOS} is the pdf of the amplitude variations and p_{LOS} is the radio-link's probability when LOS condition communication is occurring, and $f_{shadowing}$ is the pdf of the signal variations and $p_{shadowing}$ conforms the link's probability when the communication system is in shadowed channel conditions. Thereby, it is distinguished from each state the time interval with high received signal power and the time interval with low power level; each "good and bad" state was studied in separated mode represented by the area with unobstructed view from HAPS and the moment where the direct HAPS-signal was shadowed by obstacles, respectively.

The received complex signal envelope was expressed in the particular terms of Loo's (Loo, 1985), (Loo & Butterworth, 1998) and Lutz's models (Lutz *et al.*, 1991), (Belloul *et al.*, 2000)

$$R(t)e^{j\theta(t)} = c_{Loo}(t)e^{j\alpha(t)} + c_{Lutz}(t)e^{j\beta(t)}; \tag{3.55}$$

and with no motion considered, neither in the platform nor in the terminal, a constant signal level has been supposed at LOS or at shadowing state remaining in only one particular state throughout the time.

The previous approach can be validated for the link budget studies, where link margins and availability levels are the wanted outcome. Nevertheless, when more details are required, the inclusion of duration about the state events or the time dispersion caused by the radio-channel, which is occurring in our case, an implemented approach producing time-series was necessary to establish such issue influences on link and system performance, which has been done in the system's simulation (Chapter 4).

3.2.2.1. Line-of-sight path

At direct-signal state and involving a specular reflection signal, it was derived from Loo's model. It was assumed the LOS component under shadowing conditions as a log-normal distribution plus the Rayleigh distributed multipath effect; these two random processes were assumed correlated. At this first case, shadowing was not presented and the multipath signal was superimposed on the unobstructed transmitted signal power from HAPS, so having the total received signal amplitude forming a Ricean process.

For the state-oriented channel model, it was defined the proper language for the direct-path state with the sum of a log-normal distributed random phasor and a Rayleigh phasor —the Loo's model is assuming that the direct signal's variations (received voltage) can be modelled by means of a log-normal distribution, whereas multipath can be modelled by means of a Rayleigh distribution; this is the same as assuming a Rice distribution in which the direct signal changes according to a log-normal law—

$$f_{Loo}(r) = \frac{r}{b_0\sqrt{2\cdot d_0}} \cdot \int_0^\infty \frac{1}{z} \exp\left[-\frac{\left(\ln z - \mu\right)^2}{2d_0} - \frac{r^2 + z^2}{2b_0} \right] \cdot I_0\left(\frac{r\cdot z}{b_0}\right) dz, \tag{3.56}$$

where $2b_0$ is the average multipath power, d_0 is the variance of the direct signal variations, and μ is the mean value. Now, with the log-normal part in LOS condition, a temporarily constant Rice pdf envelope is had as

$$f_{Rice}(r) = \frac{r}{b_0} \cdot e^{-(r^2+z^2)/2b_0} \cdot I_0\left(\frac{r \cdot z}{b_0}\right); \tag{3.57}$$

r is the signal envelope, z is the direct LOS component, I_0 is the modified Bessel function of zero-*th* order, μ and $\sqrt{d_0}$ are the mean and standard deviation of the shadowing component respectively, and b_0 is the standard deviation of the multipath component. At small values of the signal envelope $r \ll \sqrt{b_0}$, the statistical *pdf* was Rayleigh distributed plus phase variations assuming a simple Gaussian model (zero-mean Gaussian distribution)

$$f_{Rayleigh}(r) \approx \frac{r}{b_0} \cdot e^{-r^2/2b_0}, \tag{3.58}$$

μ, d_0, and b_0 were referred to the LOS level (LOS ≡ 0 dB) being related to α, ψ, and *MP* as following

$$\alpha = 20\log10(e^{\mu}), \psi = 20\log10(e^{\sqrt{d_0}}), MP = 10\log10(2b_0); \tag{3.59}$$

the diffuse multipath was classified in *near echoes* and *far echoes* and introduced in terms of its average power *MP*, which was the alternative to the carrier-to-multipath ratio *K* parameter.

Therefore, the following proper function was referenced in order to approach for the presented LOS situation

$$\begin{aligned} &f_{CS}(r)|_{LOS} = p_{vis}(\alpha,\phi) \cdot f_{LOS}(r), \\ &p_{vis}(\alpha,\phi) = (\sin\alpha)^{0.01}; \phi = 0^{\circ}. \end{aligned} \tag{3.60}$$

where p_{vis} is the probability of visibility.

3.2.2.2. Log-normal shadowing

At shadowing state (and comprising again a specular reflection signal), the variations were specifically due to built-up obstruction effects. The overall signal variations due to shadowing and multipath effects were assumed to follow the Lutz's distribution, thus having a Log-normal/Rayleigh characterisation.

Now, at the second remaining state of shadowed path condition was supposed that

$$f_{Lutz}(r) = 1 - A_{tss} \cdot f_{Rice}(r) + A_{tss} \cdot \int_0^{\infty} f_{Rayleigh}(r \mid r_0)\, f_{log\,normal}(r_o)\frac{1}{z}dr_0, \tag{3.61}$$

where

$$f_{Rayleigh}\left(r \mid r_0\right) = \frac{1}{r_0} e^{-r/r_0}, \tag{3.62}$$

$$f_{log\ normal}\left(r_0\right) = \frac{10}{\sqrt{2\pi} \cdot \sigma\ ln10} \cdot \frac{1}{r_0} e^{-\left(10\log r_0 - \mu\right)^2 / 2o^2}, \tag{3.63}$$

in which r_0 is the time-varying short-term mean received power, A_{tss} is the time-share of shadowing, and μ is the mean power level and σ^2 is the variance of the power level due to the slow shadowing process.

Once the major parameters were declared and the receiver have an elevation angle little less than 45º, the parameter of shadowing effect has been taken part into a time-share of shadowing about 50%. And, it can be presented one more analysis to be counted for channel performance in shadowing conditions by the terms of visibility and building height distribution.

Visibility was supposed as the probability of the channel of having LOS situation at each elevation angle and 360º of azimuth angle ø, a variable referenced in Figure 3.6. Accordingly, the equation for visibility was based on the significances of α and ø (Iskandar *et al.*, 2006a), (Iskandar *et al.*, 2006b)

$$p_{vis}\left(\alpha, \phi\right) = \left(\sin\alpha\right)^{\sin\phi}; \phi = 30^o, 60^o, 90^o, \tag{3.64}$$

where ø was reached in our system at ≤10º in LOS and >75º in shadowing, being ø = 0º in the negative *z*-axis direction and ø = 90º in the negative *x*-axis direction, as shown in Figure 3.3; respectively, the visibility has agreed with the direct path at ø = 0º and shadowing situation being an increasing function following high values in ø. The propagation impairments at LOS situation has gone along with the α variations, and in obstructed situation different ø have resulted in different fading due to the dominant multipath power variations with worse effects at α < 45º —the potential worst case has occurred when ø = 90º, in which a distributed Rayleigh characterisation was roughly an enough approach.

The received signal has also been judged in shadowing conditions when the building height h_{mbh} exceeded some threshold height $h_{threshold}$ relative to the point of the direct ray height (Saunders & Bonar, 1994), (Saunders & Evans, 1997). The shadowing probability term $p_{building}$ was expressed by the *pdf* of the building height $f_{building}(h_{mbh})$

$$p_{building} = p\left(h_{mbh} > h_{threshold}\right) = \int_{h_{building}}^{\infty} f_{building}\left(h_{mbh}\right) dh_{mbh}. \tag{3.65}$$

A suitable form for $f_{building}(h_{mbh})$ was fitted to a Rayleigh distribution with the parameter $\sigma_{building}$, and such fit has been acceptable although the Rayleigh distribution tended to over-emphasise the effects of the building height; the Rayleigh distribution has had the particular advantage in our scheme for being of analytic simplicity. Nevertheless, for the case where explicit distributions for the building height were unavailable, the parameter $\sigma_{building}$ has been related instead to a qualitative classification of the environment situation. And, $p_{building}$ was expressed as

$$p_{building} = \int_{h_{mbh}}^{\infty} \frac{h_{mbh}}{\sigma_{building}^2} \cdot e^{\left(-h_{mbh}/2\sigma_{building}^2\right)} dh_{mbh} = e^{\left(-h_{threshold}^2/2\sigma_{building}^2\right)}. \tag{3.66}$$

The simplest definition of $h_{threshold}$ was obtained by considering the geometrical block of the building face, i.e., $h_{threshold} = h_{LOS}$, which was defined as the height of the direct ray above the building face relative to the local ground level. In a more sophisticated approach, the shadowing has been considered to occur whenever the building obscured a significant proportion about 0.7 of the first Fresnel zone radius $R_{FZ,LOS}$ of the direct ray. Given that the distance between HAPS and building is much greater than the building-to-terminal distance, $R_{FZ,LOS}$ was given by

$$R_{FZ,LOS} = \sqrt{\frac{\lambda \cdot x_{TB1}}{\sin\phi \cdot \cos\alpha}}, \tag{3.67}$$

thus $h_{threshold}$ was obtained as

$$h_{threshold} = h_{LOS} - 0.7 \cdot R_{FZ,LOS}, \tag{3.68}$$

Subsequently, the overall shadowing pdf can be expressed by

$$f_{CS}\left(r\right)|_{shadowing} = p_{vis}\left(\alpha,\phi\right) \cdot P_{building} \cdot f_{shadowing}(r). \tag{3.69}$$

3.2.2.3. Multipath fading

The short-term fading was conformed by the hypotheses of a direct ray and a specular reflected ray (a reflected signal caused by the 'reflection body' inside the small vicinity of the receiver) plus multipath derived from such two main rays (Palma-Lazgare *et al.*, 2008), (Palma-Lazgare & Delgado-Penín, 2008a) (Figure 3.7).

Our radio communication model is particularised for the case where both ends of the link remain stationary. Later situation can be extended (not in this study) that in the cases where the channel time-variations when at least one of the link ends is moving (i.e., the spatial-variations) can dominate over the time-variations when both ends are stationary (Pérez-Fontán *et al.*, 2006), and also regard to the relative phase changes. At our presented stationary situation, such phase vitiations do not occur as fast in the case of the moving terminal case, however, the experienced research material tells that still slow signal variations could be observed; those variations again being caused by ray interference at much slower rates, possibly due to the movement of the various scatterers giving rise to the multipath phenomena. As a result, it is possible to assume main rays and associated multipath contributions to be the same, and, for a static user terminal such structure is remaining constant.

As it is known, the HAPS communications channel can exhibit both time variance, due to the motion of the HAPS itself and the receiver terminal, and frequency selectivity due to multipath propagation. The stratospheric channel can be certainly characterised by both Doppler spread and delay spread. The total Doppler spread can be composed of two components, the first related to the motion of the HAP, and the second to the motion of the receiver terminal. Herein, it is an important notice when the terminal is not moving all multipath coming from the HAP will practically demonstrate the same Doppler shift, this is due to the relatively high altitude of the platform which means that the first component (central moment) of Doppler spread virtually corresponds to a large Doppler shift; the largest Doppler shift is exhibiting a deterministic variation in time parameterised by the maximum elevation angle α from satellite/HAPS-to-user terminal in the considered urban scenario. If it is assumed that the platform is not moving, the multipath coming from/arriving at the platform will demonstrate unequal but relatively small Doppler shifts meaning the second Doppler spread component can exhibit a relatively small value and be modelled in accordance to the approaches employed in terrestrial radio systems.

As far as small-scale fading is concerned, its characterisation was chiefly determined by two parameters: the PDP and the Doppler spectrum (coherence bandwidth and coherence time); while multipath delay spread led to time-dispersion and frequency selective fading, Doppler spread led in our case to low frequency dispersion and no time selective fading because of the presumed stationary situation.

The Doppler spectrum was assumed quiet narrow in the concerned stationary case, thus it can make no difference whether either spectrum is used for modelling, and a Butter-

worth shaped spectra filter is chosen for the ease in its implementation and its slower roll off showing no ripples than other filters

$$G^2(f) = \left|H_{Butt}(f)\right|^2 = \frac{A^2}{1+(f/f_c)^{2k}}, \tag{3.70}$$

where the transfer function *H(f)* has a gain *G(f)* of an *k*-order Butterworth low-pass filter, *A* is the DC gain at zero frequency and f_c is the cut-off frequency of approximately -3dB frequency with slope of 2*k* (dB/decade); due to lack of experimental data for the distribution of angles-of-arrival (AOA's), a realistic assumption of a uniform azimuth distribution was employed for the echo-representations.

The maximum Doppler shift $f_{D,max}$ has been associated to the dynamic environment relative to the local scattering objects, and since the platform could have an elevation angle within 90º to 30º, the effective shift for the fixed terminal case can experience of $f_{D,max}\cdot\cos(\alpha)$, with

$$f_{D,\max} = \frac{\upsilon_{UT}}{\lambda} = f_c \cdot \frac{\upsilon_{UT}}{c}, \tag{3.71}$$

where υ_{UT} is the velocity of the surrounding objects. Late considerations have resulted in a continuous distribution of frequencies in the spectrum of the signal leading to Doppler shifts placed at the origin close to the unit, and deducing that most of energy was contained in a bandwidth of twice the incident Doppler $2\cdot f_{Dmax}$.

Additionally, due to the conceivable nature of the path, the transmitted frequencies were inferred to undergo Doppler frequency shifts, and the Doppler frequency shifts were primarily influenced by wind speed and traffic density. For fixed wireless channels the Doppler power spectral density (PSD) of the variable component can mainly be distributed around *f* = 0 Hz (IEEE 802.16™, 2009), and the approximation for the shape of the spectrum could be affirmed by

$$S(f) = \begin{pmatrix} 1 - 1.72 f_{Ds}^2 + 0.785 f_{Ds}^4, f_{Ds} \le 1 \\ 0, f_{Ds} > 1 \end{pmatrix}, \tag{3.72}$$
$$f_{Ds} = \frac{f}{f_{D,\max}}.$$

Power delay profiles (PDPs) were possible classified into categories representing those PDPs with no features other than in the first delay bin, PDPs with additional features in delay bins 2nd, 3rd, 4th,… etc. (i.e., with time dispersion), and those PDPs where long delays were

observed (far-echoes) (Pérez-Fontán *et al.*, 2006); late wideband assumptions were extracted from the literature recorded ones, where the long delay profiles could occur in an unusual but realistic manner and so were not disregarded.

The channel modelling was represented as time varying, and such statistical properties were analysed with the Bello's functions (Bello, 1993) as the base of our short-term variations. It is reorganised last statistical characterisation and simplified the channel to the wide sense stationary uncorrelated scattering (WSSUS) function as shown in Figure 2.7 with a tapped-delay-line model of 11 bins. Therefore, it is declared further ideal transmission conditions that have been considered. The different paths were treated as ideal deltas affected by attenuations. The noise floor were approximated to very low values relative to the direct signal level and has been neglected; nevertheless, such induced fading anomaly could have been theoretically considered as a function of the incident Doppler and the higher fading rate, and the larger it can be so the error floor would be.

The time-dispersion effect was introduced by using an exponential distribution to represent the excess delays of the received echoes, and such multipath contributions were partitioned in two classes: those originated by the direct ray (from those scatterers in the vicinity of the user terminal) and those due to the specular ray (a very few far-echo events have been recorded (Jahn, 1994), (Jahn *et al.*, 1996), [Parks *et al*, 1996a], (Parks *et al.*, 1996a), (Evans *et al.*, 1996), and were assumed in our model even their low probability of occurrence) (Palma-Lazgare *et al.*, 2008), (Palma-Lazgare & Delgado-Penín, 2008a). Thus, the exponential distribution is corresponding to the expression

$$p_{exponential}(\tau_i) = \frac{1}{\tau_e} \cdot e^{-\frac{\tau_i}{\tau_e}}, \tag{3.73}$$

with τ_e being the average of the distribution.

In the HAPS channel the time-dispersion were confirmed smaller than that of the terrestrial (cellular) channel, and multipath echoes were not significantly spread in time in most time. The modelling of the diffuse contributions was recounted to the term of average multipath power *MP* describing the diffuse multipath power generated by the main signal; the total average power of the *i*-th ray power sum (multipath rays) equalled to

$$10 \cdot log\left(\sum_i a_i^2\right) = MP[dB] \tag{3.74}$$

where a_i is the amplitude of the *i*-th multipath echo; the appropriate normalisation of the relative powers of the direct and multipath components was allowed in the last expression where the LOS condition implies a direct signal amplitude of 1 or 0 dB (20·log(1)).

Another parameter was required to quantify the broadband transmission named the multipath power decay profile representing the rate at which the multipath contributions weakened as their excess delay has increased; the linear decay rate *Sp* (in dB/μs) has quantified for this slope.

In addition, it can be considered one more distribution standing for the number of occurrences discussed by the Poisson distribution (Jahn, 1994), (Jahn *et al.*, 1996), (Fontan *et al*., 2001), (Palma-Lazgare *et al.*, 2008), (Palma-Lazgare *et al.*, 2008a). In which, a fixed and sufficiently large number of rays, 50 or greater, were conceivably assumed eliminating the need of using such distribution; the criterion for latter presumption was primarily to generate smooth continuous Doppler spectra.

Since the broadband transmission has been determined by the WSSUS model, the short-term factor considerations were defined for our case by the tapped-delay-line (TDL) representation (Jahn, 1994), (Erceg *et al.*, 1999), (Fontan *et al.*, 2001), (Dovis *et al.*, 2002) as an equally spaced array from 0 to $\boldsymbol{\tau}_m$, with the term of $\boldsymbol{\tau} = 0$ corresponding to the main component delay and the fixed *i*-tap-delays for the remaining multipath echoes. Subsequently, the HAPS channel impulse response (CIR) was expressed by the sum of *n*-echoes within the framework of the two-discrete PDP classification near- and far-echoes, $N_{echoes,ne}$ and $N_{echoes,fe}$, the term of complex attenuation (and phase) A_i for each *i*-th echo, $\boldsymbol{\tau}_i$ delays (with $\boldsymbol{\tau}_i = \boldsymbol{\tau}_{i,ne}$, or $\boldsymbol{\tau}_i = \boldsymbol{\tau}_{i,fe}$ for near- and far-echo tap-delays respectively), and the Doppler frequency shifts $\boldsymbol{\nu}_i$

$$h(\tau_i;t) = \sum_i A_i(\tau_i(t)) \cdot \delta(\tau - \tau_i(t)) \cdot e^{j2\pi\nu_i t},$$
$$h(\tau_i;t) = \sum_i A_i(\tau_i(t)) \cdot \delta(\tau - \tau_i(t)) = \sum_i a_i(\tau_i(t)) \cdot e^{j\phi_i(t)} \cdot \delta(\tau - \tau_i(t)). \quad (3.75)$$

It is now defined that signals travel at a finite speed. Henceforth, an upper limit was defined by the speed of light at receiver sensing a time delay $\Delta\tau$ related to the propagation speed and the distance *d*, $\Delta\tau = d/c$. This was indicated in the used term of the specular reflection path which was conditioned to the founded term horizontal distance Δr_{srp}, a distance from the 'reflection body' to the receiver, and elevation angle α; ergo the physical space delay of the reflection path, as shown in Figure 3.6 and Figure 3.7 can be determined by

$$\begin{aligned}\Delta\tau_{srp} &= \tau_B - \tau_A \\ &= \tfrac{1}{c}\left\{ d_{srp} - d_{HAPS} \right\} \\ &= \tfrac{1}{c}\left\{ \left[\sqrt{\left(\Delta r_{srp} + R_{HAPS}\right)^2 + r_{HAPS}^2} + \left|\Delta r_{srp}\right| \right] - \left[d_{HAPS} \right] \right\};\end{aligned} \tag{3.76}$$

$\Delta r_{srp} << R_{HAPS}$, c is the speed of light, d_{srp} is the distance from HAPS to the 'reflection body' for the specular reflection path, and τ_A and τ_B (in μs units) are the total arrival delay from HAPS to terminal for the direct path and from HAPS to reflector (object) for the specular path, respectively; furthermore, the variable τ_{srp} was taken as the differential arrival from HAPS to terminal for the specular path with $(\tau_B + \Delta\tau_{srp}) - \tau_A$ (in μs units) referred to Figure 3.7.

Into the next topic concerning the indoor small-scale fading statistics, it can be assumed that the indoor received signal is relatively stable in time (Vogel & Torrence, 1993). In the long-term fading, the path amplitude statistics were not stationary because of the variation of the surrounding obstacles exhibiting cyclical and drift motions changing the distance and elevation angle between transmitter and receiver and affecting the relative phase between received waves, so the signal level was time varying. Appropriately, the short-term fading was defined to be independent for each floor, and the signal transmission in the indoor radio channel was impaired because of the attenuation and the dispersive nature of the transmission indoor medium: the channel response was dispersive and time-variant due to multipath propagation and changing environments, so the relative delays among different propagation paths defined a frequency-selective channel. Therefore, countermeasures were needed to combat such severe channel distortion when we were assumed transmitting at relatively high rates. Nevertheless, the large variety of indoor environment situations could not make a unique possibility to base the system's performance evaluation on a well-defined channel modelling, hence it can be considered simplified models to have a general but accurate perspective of prediction.

And, the short-term fading was understood as the fast fluctuations of the signal level caused by movements in each of the floor. Hence, assumptions for contemplating people moving nearby of receiver could produce variations of less than 0.5 dB, whereas a person blocking the transmission path could produce fades of 6 to 10 dB (Vogel & Torrence, 1993) —the employee's physical complexion was not pondered.

It was regarded that multipath has been received from several fixed indoor locations with the disappearance of the direct path (Vogel & Torrence, 1993), and has accounted for a reduction of energy due to diffuse components scattered by furniture and building material in

all directions. The delay and distance of echoes between illuminated wall and receiver were mostly implied, plus to experience particularly multiple reflections from the furniture close to the walls. As a result, the overall indoor delay spread could experience the orders of tens/ hundreds of nanoseconds.

The delay spread was related to the size of the room, the larger room, the higher value of delay spread. For instance, the dependency on the room dimension and environment has resulted, with an exponential function: in predictions of 19.3 ns in average RMS delay spread and standard deviation of 3.4 dB inside small rooms, at an open environment the average RMS delay spread was supposed of 27.7 ns with a standard deviation of 4.1 dB, and in large environments the average RMS delay spread was 67.4 ns with a standard deviation of 4.3 dB.

Herein, closed room scenarios were defined to show similar behaviour, a less dispersion of the delay since the scatterers are closer to the receiver, while the open environment showed more different statistics due to a greater dispersion of the delay or greater separation between scatterers. In the quasi-LOS (QLOS) case, the rays which contribute most to the impulse response do not come from the scattering close to the receiver (as in the NLOS and hard-NLOS (HNLOS)) but rather come from the outside (Fernández *et al.*, 2007); last assumption was related to the decrease or increase of the entry loss variable (Pérez-Fontán *et al.*, 2008b): with a lower entry loss the entering rays carry more power and, some of them can be reflected within the room before arriving at receiver resulting in longer propagation time (higher delay spread).

Accordingly, quasi-LOS (QLOS) areas have fitted the discrete model of two taps, and in contrast, the NLOS and HNLOS area type might have been modelled using more taps due to the greater delay possible presented (Fernández *et al.*, 2007). The indoor broadband channel modelling must have been efficient for the system simulation with the possible lowest number of taps; and specifically, the wideband approach has been based on the scattering process with two paths, rarely three, sufficient for evaluation optimisation of OFDM and *M*-QAM modulation (Berg, 1999).

Thus, the TDL model was implemented with an adequacy to the WSSUS defining a consistency for the indoor characterisation with delays τ_i and time-varying (complex) gains α_i; the coefficients have presented a highest value (high correlation) as expected for the first path representing the stable path, and for excess delays greater than zero the correlation decreases drastically —multipath components undergo more reflections, and hence, were more

random and less correlated. However, the uncorrelated scattering assumption cannot be always verified, and generally correlation might be caused by a limited number of scattering surfaces regularly positioned, and either small (0.3) or high correlation values between the amplitude of adjacent multipath components can appear.

At this point, all last indoor assumptions have been considered for the existences within a different building's material wall case, where walls, furniture, etc., can be made of brick, metal, wood, and concrete construction; herein, it has been deduced to have similarities in the mentioned indoor issues among such construct materials.

As $\delta(\tau)$ can be assumed the indoor equivalent baseband impulse response of the band-limited receiver front-end, such characterisation was represented with a limited equidistant *k*-th tap taken into the interval $T = 1/BW$

$$h(t,\tau) = \sum_{i}^{M} \alpha_i(\tau_i(t)) \cdot \delta(\tau - \tau_i(t)), \tag{3.77}$$

$$h(t,\tau) = \sum_{n} h\left(t, nT\right) = \sum_{n} h\left(t, \frac{n}{BW}\right), \tag{3.78}$$

$$\begin{aligned} h(t,\tau) &= \sum_{k=1}^{N=2} a_k\left(t\right)\delta\left(\tau - \tau_k\right) \\ &= \sum_{i=0}^{M} \alpha_{i,0}\left(t\right) \cdot e^{j\phi_{i,0}(t)} \cdot \delta\left(\tau - T_0 - \tau_{i,0}\right) + \sum_{i=0}^{M} \alpha_{i,1}\left(t\right) \cdot e^{j\phi_{i,1}(t)} \cdot \delta\left(\tau - T_1 - \tau_{i,1}\right); \end{aligned} \tag{3.79}$$

and, following the values for the *k*-th taps were configured by sampling the channel impulse response (CIR) with *D*-time samples

$$h_i\left(\tau_k\right) = \sum_{m=(k-1)D}^{kD-1} h_i\left(\tau_m\right), k = 1, \ldots, N_{tap}. \tag{3.80}$$

The $a_{i,k}$ are statistically independent positive random variables whose path voltage gains (mathematically approach to complex ray gains forming a Gaussian process) were the amplitudes represented with the respective Rayleigh distribution with phases uniformly distributed over [0, 2π), and independent of the associated delays —or equivalently the exponential pdf for the path power gain. The latest corresponds to the complex Gaussian process, where the so-called tap was the sum of many independent rays arriving within the time resolution invoking the central limit theorem: continuous Rayleigh model or Gaussian WSSUS model.

In this study, the indoor multipath fading concept was also introduced by the ray/echo clustering (Saleh & Valenzuela, 1987), i.e., multipath contributions tended to reach the receiver in groups with similar delays and angles of departure and arrival. Each of the external wall and roof can rise to a multipath structure/group or cluster spread in time-delay axis —in various instances it can be possible that a second or even third sub-clusters are received due to the same incoming wave due to scattering on large features within the indoor environment, these sub-multipath groups can very well correspond to contributions from the same element in the indoor propagation environment, for example, a piece of furniture for multipath generation can behave in such way; one does not be in confusion with the different situation that corresponds to the situation occurring in the outdoor channel modelling.— On that account, the indoor cluster arrival echoes were adopted with a simple overall impulse response $h_I(t,\tau)$ and restricted to the presumed empirical-statistical indoor models.

The considerations were defined and was presumed that at least one cluster $h_I(t)$, or measured PDP, has reached the indoor receiver, other remaining cases were showing that two or even five arriving clusters could be pondered due to the combination of the external walls and roof multipath clusters

$$h_{I,tot}(\tau) = h_{I,wall1}(\tau) + h_{I,wall2}(\tau) + h_{I,wall3}(\tau) + h_{I,wall4}(\tau) + h_{I,roof}(\tau). \quad (3.81)$$

So, the overall received power can be

$$p_{I,tot} = p_{I,wall1} + p_{I,wall2} + p_{I,wall3} + p_{I,wall4} + p_{I,roof}; \quad (3.82)$$

normalisation was required for the excess delays, and all excess delays are referenced to be expressed to the first signal arriving at the receiver: the received power for such walls/roof was normalised with respect to the direct path (LOS) power by $p(r) = 1/pl$, where $pl = 10^{L_{BPL,LOS}/10}$ is the linear unit excess path loss through a given wall going to the indoor terminal. Furthermore, previous equations denote the scenario referring to the indoor terminal in the building which can be illuminated from the transmitted signal penetrating through the four-external walls and roof presumed: the roof contributions represents remarkable worth whenever the indoor terminal could be located on the last floor, two external walls were mainly visible from the HAPS and the remaining (two) walls were indirectly illuminated from reflections of surrounding buildings.

Following, the number of arrivals and the times of arrivals (cluster and echoes) can be characterised by means of Poisson and exponential distribution, where the cluster arrival rate

is denoting the parameter of inter-cluster arrival time and the echo arrival rate is referring to intra-cluster arrival time.

In our model, since the physical realisation that rays arrive in clusters, the cluster arrival times (the first rays of each cluster) were modelled as a Poisson arrival process with a fixed rate, where with a fixed time value of 300 ns was possible for this Poisson distribution case to be associated to a *P(1)* = 0.37 to 0.34 meaning to have one additional cluster into the considered 300 ns time-period. Within each cluster, the arrival times of the subsequent rays were configured using a number of echoes greater than 50, and the number of arrivals were not compulsory characterised neither accounted for a Poisson distribution.

Consequently, each tap has been represented by the average of the received components, and characterised by means of an exponential distribution. The latest realisation was distinguished (Pérez-Fontán *et al.*, 2008), (Saleh & Valenzuela, 1987) with the received echo structure expected to present a decay rate as a function of the associated arrival times of the *k*-cluster and *i*-ray number within such *k*-th cluster, with a negative power exponential law (path power gains) $\overline{a_{i,k}^2}$ expressed in linear units —an equivalent to the Rayleigh pdf for the path voltage gain with the amplitude of each echo being $a_{i,k}$ —, or a linear law for powers in dB expressed as

$$\begin{aligned}
&\overline{a_{i,k}^2} = \overline{a^2\left(\tau_k,\tau_{i,k}\right)} = \overline{a^2\left(0,0\right)}\cdot e^{-\frac{\tau_{k,indoor}}{PDc}}\cdot e^{-\frac{\tau_{i,k,indoor}}{PDr}},\\
&\overline{A_{i,k}^2} = \overline{A^2\left(\tau_k,\tau_{i,k}\right)} = \overline{A^2\left(0,0\right)} - Sp_{k,indoor}\tau_{k,indoor} - Sp_{i,k,indoor}\tau_{i,k,indoor},\\
&\overline{a^2\left(0,0\right)} = e^{\overline{A^2(0,0)}/10\log(e)}, Sp = \frac{\log\left(10\cdot e\right)}{PD}.
\end{aligned} \tag{3.83}$$

The first factor $\overline{A^2\left(0,0\right)}$ is the average power gain (linear units) of the first ray in the first cluster, $Sp_{i,k,indoor}$ and $Sp_{k,indoor}$ in dB/μs are the power decay slopes, and the *PDc* and *PDr* are the time constants (in ns) for the linear unit (power delay) decay rate of the clusters (envelope) and within the clusters, respectively; $\tau_{i,k,indoor}$ are the arrival times within cluster *k* and $\tau_{k,indoor}$ are the cluster arrivals. On the average, rays within a cluster decay were approximated with a time constant of 20 ns (*PDr*), and the clusters decay on average were approximated to a time constant of 60 ns (*PDc*) (Saleh & Valenzuela, 1987) considering that the decaying exponential was leaded by a highest peak and later successive smaller cluster peaks appeared.

Since the short-term fading has been accepted to follow a Rayleigh characterisation, up to about 200 ns delay spread (Saleh & Valenzuela, 1987) and RMS values about 40-155 ns were contemplated in the model —50 ns RMS valued was expressed in (Saleh & Valenzuela, 1987). Or another possibility has been described for the RMS delay spread value through the experiments at three different frequencies in (Devasirvatham *et al.*, 1990) about the bounds of 100 to 270 ns, plus time delay values considerably lower than the typical values at outdoor channels in the urban environment. However, a last assumption has been pondered from measurements in (Karlsson *et al.*, 1994) where was believed about a farthest power component covering a delay pronounced up to 400 ns due to a reflection in the back (last) wall.

On another issue of modelling, definitively the presumed taps were overlapping. For instance, if for some *i* the $\tau_{ik} \geq T_{k+1} - T_k$ is presented, then the *l*-th and the (*l+1*)-th clusters overlapped for all subsequent values of *i*. The supposition also has had that *PDc* > *PDr*, with the expected power of the rays in a cluster decaying faster than the expected power of the first ray of the next cluster. Thus, if $\Delta\tau \equiv T_{k+1} - T_k$ was sufficiently large such that $e^{-\Delta\tau/\mathrm{PDr}} \ll e^{-\Delta\tau/\mathrm{PDc}}$, then the *k*-th and (*k+1*) clusters could appear disjointed (Saleh & Valenzuela, 1987).

The latter expression for broadband model could be more completed to include the angles of arrival (an extension of Saleh & Valenzuela's model) where can be defined that ray clusters are not only spread in time and delay, but in angle of arrival θ; so with the overall impulse response $h_I(\tau) = \sum_k \sum_i a_{i,k} e^{j\phi_{i,k}} \delta\left(\tau - \tau_{k,indoor} - \tau_{i,k,indoor}\right)$, $e^{j\Phi t}$ has a statistically independent random phase related to each ray arrival and uniform over [0,2π), could be obtained extension to $h_I(\tau,\theta) = \sum_k \sum_i a_{i,k} e^{j\phi_{i,k}} \delta\left(\tau - \tau_{k,indoor} - \tau_{i,k,indoor}\right) \cdot \delta\left(\theta - \Theta_{k,indoor} - \theta_{i,k,indoor}\right)$. However, at the HAPS situation were not possible gathering further empirical information of AOA's at the specific indoor application, and were considered uniformly distributed between 0 and 2π.

At last, the indoor signals have been translated to the meanings of travelling at a finite light speed and sensing the time delay $\Delta\tau$ related to the propagation speed *c* and the distance *d*. The application of last was indicated with the presumption of a specular reflected path, conditioned to the horizontal distance $x_{indoorR}$ a maximum distance from a 'reflection body' inside the building in the same room where the receiver could be localised at such moment. And, the arrival time of the swallow specular reflected path was redefined by

$$
\begin{aligned}
\Delta\tau_{srp,indoor} &= \tau_B - \tau_A \\
&= \tfrac{1}{c}\cdot\left\{ d_{sp} - d_{HAPS} \right\} \\
&= \tfrac{1}{c}\left\{ \left[\sqrt{\left(x_{indoorR} + R_{HAPS} \right)^2 + r'^2_{HAPS}} + \left| x_{indoorR} \right| \right] - \left[d_{HAPS} \right] \right\}, \\
\tau_{srp,indoor} &= \left(\tau_B + \Delta\tau_{srp,indoor} \right) - \tau_A, [\mu s].
\end{aligned}
\tag{3.84}
$$

2

The preface to wireless communications via HAPS

2.1. An overview

The origin of HAPS-based wireless systems comes principally from the military research, where in such case are called unmanned aerial vehicles (UAVs). The big three options in the use of telecommunications are by means of the terrestrial wire (copper wire, coax and fibre optic cable), wireless terrestrial, and satellite communication systems (SACRI, 2006). In the last years, a new set of options has been added in the form of HAPS mostly operating at stratospheric altitudes or other lower altitudes.

In the 96‘s early, the ITU-R Study Groups and the Radiocommunication Bureau as well as the Radio Regulations Board in 1997 and the World Radiocommunication Conference 1997 (WRC-97), commenced for considerations of the HAPS emerging technology, or stratospheric stations as they were mainly called in the early studies (Aubineau *et al.*, 2010). Hence, the HAPS’ radio regulatory aspects were initiated and reflected in the ITU Radio Regulations and in Conference Resolutions being associated to the frequency-sharing studies, which are still continuing and in preparation for agenda item 1.20 at WRC-12.

HAPS is whether treated as a very low satellite or a very tall mast. HAPS is a vehicle holding a fixed position in the Earth’s stratosphere layer. It is presumed located at an altitude of 17-50 km and must offer an ideal platform from which to support a congregation of broadband communications within the area of wireless network services (Figure 2.1).

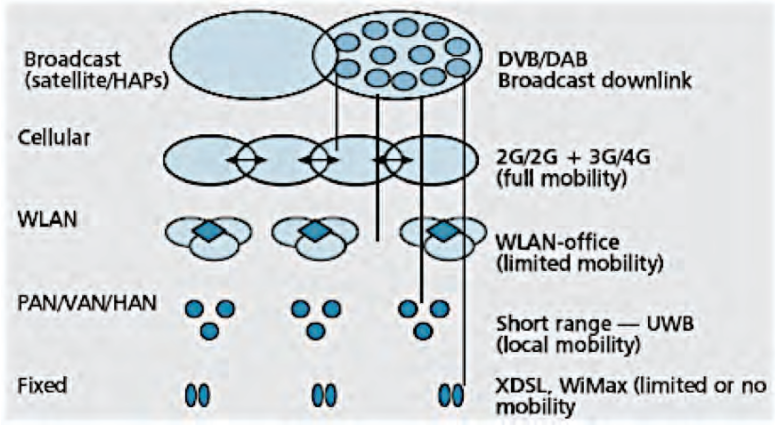

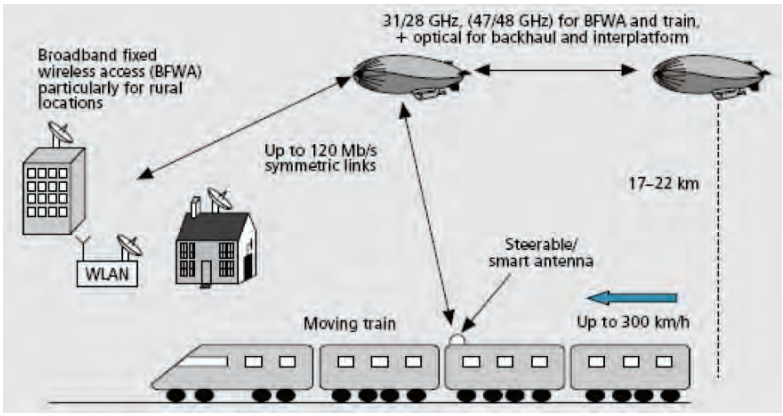

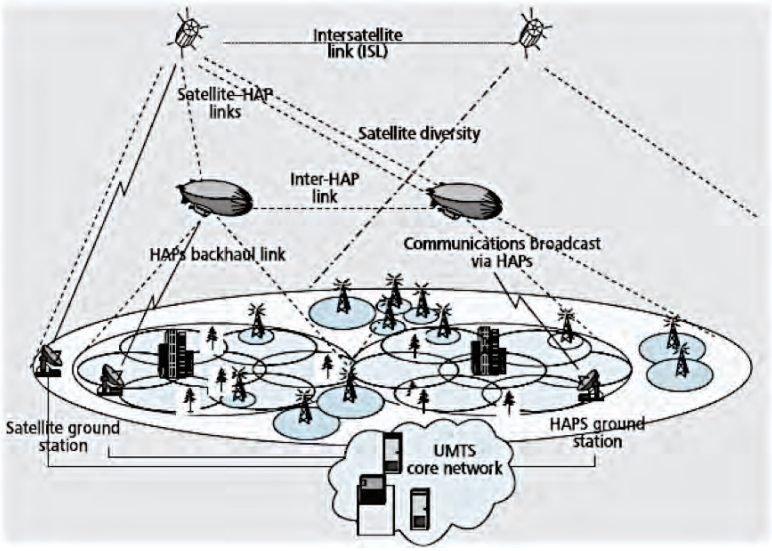

Figure 2.1. Layered networks, general HAPS network (HAPN) architecture and communication scenario (Evans *et al.*, 2005), (Grace *et al.*, 2005).

The many role applications that have been put forward suggest a richness of a fairly-soon development in the radio communication field. HAPS can inform, influence and work together with other standardisations and regulatory bodies for broadband communications. And apart from these extensive promises, the provision of broadband services is expected to be the major economic stimulus to continue the development of this project.

Nowadays, HAPS are based on lighter-than-air (LTA) airships, vehicles, or conventional aircrafts, and are at various stages of research and possible implementation. Another development at a glance is the provision military research with the so-called UAVs, being in parallel with the logistics of civilian communications from HAPS.

HAPS has many similarities and differences with fixed, terrestrial wireless, and satellite systems, from which can represent a better design compromise and an economically attractive way for the provision of time-space coverage communications. However, the full potential to be offered by unpiloted solar-powered stratospheric platforms is still a little way off, but it can be reviewed in recent advances at testbeds and research programmes. In this thesis, particularly the platform's civil broadband communications payload is referred for development.

2.1.1. HAPS technologies

Throughout the evolution of HAPS, with a couple of examples in Figure 2.2, three types of vehicles can be identified:

- Unmanned airships with propulsion systems. These are normally huge (200 m long with a payload of 1000~2000 kg) solar-powered balloons fed with helium (He), which can be semi-rigid or non-rigid. The basic construction material is the resilient He leak-proof laminated plastic. Lightweight solar cells (<400 g/m^2) lie on the upper surfaces of the airship. Three different aerial platform technologies are used for prototypes: tethered platform, stratospheric balloon, and full HAP, which are supported by a common test/measurement methodology. Flight duration can reach up to 5 years.
- Unmanned aircrafts. Also known as high altitude long endurance (HALE) platforms, these solar-powered aircraft are smaller than airships, they cannot carry fairly heavy payload and are power-limited, especially during long-night periods. A variant are fuelled unmanned aircraft, often referred to as unmanned aerial vehicles (UAVs), which gener-

ally fly at modest altitudes and are used essentially for military short-time surveillance with flight durations of about 6 months.

(I)

(II)

Figure 2.2. UAS images, licensed for private non-commercial use only (AeroVironment, 2011): (I) AeroVironment's Global Observer (GO) unmanned aircraft at test program (august 2010) to culminate in a week-long flight in the stratosphere using liquid-hydrogen fuel. (II) AeroVirnonment solar plane, Corporate Helios flying, a prototype precursor to GO production concept HALE UAS 2001.

- Manned aircrafts. They are conventional fuelled aircraft with average flight duration of 4~6 hours. Not environmentally friendly, and within a position (radius) of approximately 10 km.

HAPS are also known as stratospheric platforms (SPF) airships, or stratospheric platform systems (SPS).

The recent worldwide LTA vehicles, HAP stations (HAPS), are a technology built on an aerial object such as unmanned airship, essentially helium (He) filled balloons flying in the stratosphere at an altitude capable of long endurance on-station. This untethered platform is at a specified, stabilised, quasi-stationary point relative to the Earth. It can be moved to desired positions, depending upon the region of operation and the statistics of winds at those altitudes, worldwide varying, in order to have the potential to be rapidly deployed. The HAPS altitude around 22 km is principally proposed (Figure 2.3), and the main reasons for this range selection are twofold: first, these altitudes are above aviation airlines, and second, average wind speed is sufficiently low otherwise the extremely low ambient density of greater altitudes would render the placement of a vehicle unfeasible.

An airship (HAPS-based) is more susceptible to wind or pressure variations and they have to compensate for the drift. However, it is rather difficult to finely control the altitude of an airship remotely: an aircraft usually flies on a tight circle (about 2 km radius or more), while airships can theoretically stay still and they only need to compensate for the winds. The ITU has specified HAPS should be kept within a circle of 400 m radius, with height variations of ±700 m, so its service is available almost all the time.

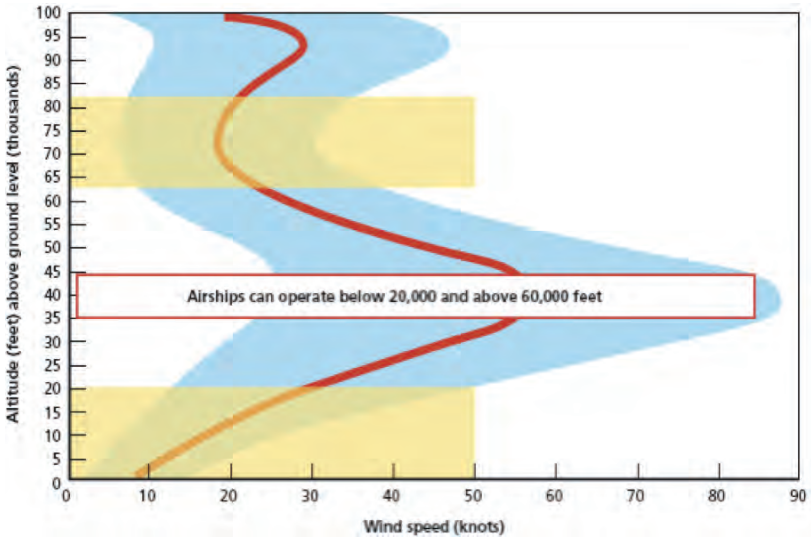

Figure 2.3. Wind-speed profile with height. Values vary with season and location, but generally follow this rough distribution (Source: NASA) (Jamison *et al.*, 2005). *1 knot = 1.852 km/h; 1 ft = 0.3048 m*

A single aerial platform can replace a large number of terrestrial masts, along with their associated costs, environmental impact, and backhaul constraints. Site acquisition problems can be eliminated. Accordingly, HAPS can enable services that take advantage of the best features of both terrestrial and satellite communications; HAPS' payload can be a complete base-station or simply a transparent transponder (Tozer & Grace, 2001).

Thus, HAPS are being designed to supply a wireless/optical base for communications and broadcasting, as well as Earth observation and monitoring —referring these assistances into the next generation services; HAPS can aim to stationary users on the ground as well as to users on moving vehicles at high speeds (in Figure 2.1 is depicted such general HAPS communication scenario).

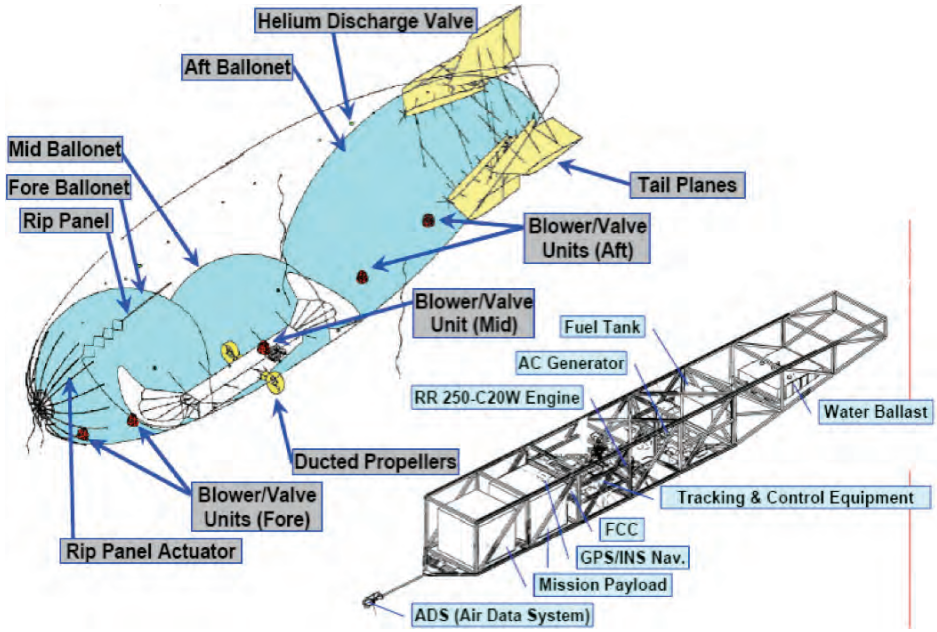

Figure 2.4. Prototype airship structure (courtesy by SPF project of Japan) (Nakadate, 2005).

A typical HAPS design should seek high reliability, low power consumption, and light payload, thus leading to an architecture that places most of the system complexity on the ground segment. This is the case of a transparent HAPS, namely a HAPS that acts as a relay station, transferring information from an uplink to a downlink channel. However, a HAPS can be a processing device incorporating a level of functionality itself, such as a multichannel transponder, user and feeder-beam antennas, antenna interfaces, DSP system, etc., and often referred to as an on-board processing (OBP) system (Karapantazis & Pavlidou, 2005) —a

general HAPS' prototype architecture is in Figure 2.4. In addition, the airship base location should be treated: the decisions of having hangars should be considered by easy to construct, blast resistant, inexpensive, wind-resistant, and operationally convenient for tie-down (Tozer & Grace, 2001), (Grace & Mohorčič, 2010).

Furthermore, it must be recognised that disadvantages exist using HAPS. There are a number of technical and technological challenges to be met before they are likely to be widely accepted for communications services, *e.g.*, reliability-service availability, network-configuration interoperability, and practical deployment in materials (lightweight fabrics) plus low-cost flexible solar cells energy storage.

2.1.2. HAPS-based projects

2.1.2.1. An overview for market issues

There are a number of challenges to be met before HAPS are totally accepted for deploying communication services; one of them is the important consideration of the conditions in costs.

At this overview of HAPS-market assessment, it should be said that there could not be opportunistic volume production of HAPS to bring large cost benefits in terms of initial procurement. However, it is the overall cost of the ownership and operation that needs to be considered. In particular, a single HAPS may be rapidly deployed to provide communication services, with relatively little infrastructure, and at lower overall cost than alternative solutions. And, as the HAPS industry matures, together with the development of a parallel commercial market, initial costs can fall sharply for a clearer HAPS performance.

The prospective economical issues of how HAPS-based systems can be put into practice are within the two major directions of employment: being a supplementary wireless communication system and being a by-air reconnaissance support —latter options are being examined under the point of view of specialised organisations and research groups, *e.g.*, Department of Homeland Security (Stephen & Makrinos, 2005), and CAPANINA (Capanina.org).

A growing commercial interest in airships is been noted worldwide (Jamison *et al.*, 2005), (Bolkcom, 2006). At least 32 companies are being involved in the design or manufacture of commercially available airships and aerostats: Canada, China, Czech Republic, France, Germany, India, Japan, The Netherlands, The Republic of South Korea, Russian Federation, United Kingdom, and the United States of America.

Furthermore, a specific vehicle system budget comprising or interacting with vehicle-based flight systems will be concerned for licensing matters, related to other additional sectors such as command and control link, command and control software, flight control systems, structure, guidance and navigation, propulsion and fuel, thermal protection/thermal control, vehicle recovery system, and so forth. Other features to be considered for a specific finance of HAPS test and construction are given by the overall length, diameter, fitness ratio, height, width, hull volume, payload, net mass, and propulsion variables.

Another economical aspect of HAPS can be analysed by estimating the revenue and costs incurred by the provisioned service in order to evaluate the profitability of HAPS employment, the number of subscribers should be estimated and then the net value, payback period, and the rate of return on investment can be calculated under various scenarios.

After all, as HAPS is used more often and an increase flight experience is gained, costs can be lowered by reducing field personnel, by spreading fixed costs over more flight hours, and by allowing agencies to develop and improve the needed technologies and investigation.

Even more, as a large airship can be considered for implementation, other numerous possible markets are being allowed for intervening with the HAPS service. On the commercial side, potential HAPS-based system markets can include:

- Natural Resources and Scientific Exploration. Airships provide a stable, relatively vibration free platform for any number of sensors and equipment, such as ground penetrating radar. Oil and precious metals prospectors, loggers, fisheries and other entities will be able to make use of HAPS in their operations. With their long endurance, airships could provide ideal platforms for many forms of exploration.
- Air tourism. HAPS could offer a more tranquil environment capable of a slow speed flight and hover over areas of interest, enhancing a peculiar viewing experience; a larger window to a panoramic view can be offered. For instance, European operators are experiencing high demands for airship tourism.
- Eco-tourism. Airships equipped with electric motors are quiet and virtually pollution free, presenting a unique opportunity in and around sensitive ecosystems. Certain areas that are now off-limits to vehicles under environmental laws may become accessible by HAPS. HAPS, equipped with renewable solar power and quiet electric motors, is an ideal candidate for these markets.

On the government and military market side, potential applications for larger airships can include:

- Surveillance/Reconnaissance. HAPS could allow military and law enforcement agencies to go higher and farther, remain aloft longer, and increase the opportunity for surveillance and security. Surveillance opportunities can include fire spotting, border patrol, anti-terrorism activities and even early warnings of assaults. Interest also can be extended to mine detection, submarine counter measures and offensive weaponry.
- Emergency and humanitarian manoeuvre. In the wake of natural or man-made disasters, exists the need for reconnaissance, communication and intervention. HAPS can serve all of mentioned functions, from an airship command and control platform to a station for humanitarian aid. With lower operating costs and minimal infrastructure requirements, HAPS-based systems may be particularly suited to disaster management roles in developing nations.

2.1.2.2. Relevant applications

For our interest, HAPS applications are aiming broadband access for the telecommunication payload, which can include: narrowband access, direct broadcast, Internet access, entertainment video and audio, videoconferencing, cellular telephony, broadband LMDS access, and assistance to supply digital networks (i.e., ISDN), and also including the applications to disaster services, remote sensing (earth observation, pollution monitoring, meteorological measurements, real-time monitoring of seismic or coastal regions and terrestrial structures, traffic monitoring and control, surveillance missions, and agriculture support), intelligent transportation systems, homeland security, and emergency communications.

Two service scenarios can be conceived for HAPS. The first one employs HAPS as a backup base station covering a wide area partially served by terrestrial base stations acting as an "umbrella," and the second scenario can have the HAPS providing a full-service coverage into a wide area where no terrestrial network is active.

Hence, HAPS may be deployed in a number of ways to provide a range of tactical communications: broadcast radio services (including multimedia), stand-alone two-way tactical data links (with potential for high capacity for multimedia), surrogate/complementary services for existing military terrestrial and airborne systems (either by effectively flying a base station or by acting as an additional network node), surrogate/complementary satellite commu-

nications effectively helping to a satellite transponder (possibly using existing satellite communications ground terminals), and overlay of GSM or UMTS system providing civil mobile phone demands.

Getting into the next significant matter, HAPS holds an attractive feature by virtue of its immediate response in time and flexibility, it is well suited for "short-term applications". For instance, HAPS can be used to cover a seasonal or one-time event, for providing temporary services in disaster relieve operations (accidents, search and rescue, evacuations, forest fires).

HAPS are expected to conform a third major infrastructure for communications and broadcasting, after terrestrial and satellite systems. A supplemental proposal, which is maintained by many authors, is the use of HAPS as alternative wireless network provider that can partially replace or add capacity to damaged or overloaded wireless networks during a man-made or large- and small-scale natural disaster (Peha 2005), [Palma-Lázgare & Delgado-Penín, 2010a]. During these critical phenomena, the telecommunications infrastructure and the required coverage for the emergency service operations might be unavailable due to the destroyed area or overloading by the excessive communications demand; along with satellites, HAPS could be completely isolated from the effects of disasters on the ground and can manage the disaster aid deployment assessing communication viability and outlining issues in interoperability with the core networks.

Furthermore, as an important example, key points can be established for discussion in the referenced application to the security aspect working with HAPS:

- It is necessary to define the field of security applications precisely.
- To investigate previous studies for defining these security applications.
- Monitoring of future security threats can be identified as an important permanent task since this may lead to new security mission profiles.
- With respect to the definition of security mission profiles, it was agreed that the separation in short-, mid-, and long-term missions based on the endurance of the platform is useful.
- With respect to the derivation of capability needs and user requirements, it was concluded that the first step is the investigation of previous studies.

- With respect to the system requirements, the following key points can be identified: autonomy, reliability/availability, classification capabilities, geo-location capability, broadband communication capability, and adaptability.
- With respect to the common work with other application groups, the following areas were identified: technology gap, state-of-the-art, critical sub-systems, and growth potential.
- Specifically, main security missions (already outlined by the European Commission) can be discussed into the topics of protection against terrorism and crime, security of infrastructure and utilities, border security, supporting crisis management, and environmental hazard.

2.1.2.3. Related advances

Studies on high altitude aircrafts and airships are being deployed to produce a prospective aeronautical research agenda and mission/applications.

The objectives of the European Union in deploying high altitude airship/aircraft were carried through the completion of, chiefly, the HeliNet project (Grace et al., 2003) and continued in November 2003 by the EC in a new research project named CAPANINA (Capanina.org) and COST297-HAPCOS (high altitude platforms for communications and other services), which was partially funded by the 6th European Union's Framework initiative. Built on the HeliNet project, Capanina was aiming the development of low cost broadband technology from HAPS to deliver cost effective solutions to users in urban and remote rural areas, or to users traveling inside high-speed public transport vehicles (e.g., trains) with the mnemonic "Broadband to All."

Other advanced projects are also presented. The one with name SOLITAIR (Solar Powered Aircraft for High Altitude Long Endurance) is referenced to an unmanned solar powered platform developed at DLR in Germany with prototypes demonstrating aeronautical aspects. Geoscan (UK) Plc is a British-Russian Technology Partnership that has been developing a network based on the Russian M-55 stratospheric aircraft. Advanced Technologies Group (ATG) in Bedford, UK, was considering developing a range of airships; ATG proposed an airship named StratSat, 200 m in length, supporting a communications payload of up to 800 kg. Lindstrand Balloons, another UK company, has also proposed HAP airships. The University of Stuttgart has developed a novel design of HAPS comprising several smaller air-

ships joined together in an “airworm” configuration; this sausage-like formation aims to provide the lift while avoiding some of the structural and aerodynamic problems associated with very large airships. SkyNet is another major project funded by the Japanese government led by the Science and Technology Agency, the Ministry of Posts and Telecommunications and the Yokosuka Research Centre, and was aiming to produce an inter-connected network of some 15 airships covering Japan designed to provide broadband and broadcasting services about all over Japan territory. In addition, two flight test vehicles have demonstrated and proved key technologies for the SPF airships in cooperation with Japan Aerospace Exploration Agency (JAXA) in association with other funding. Another project was underway in Korea, jointly managed by the Electronics and Telecommunications Research Institute (ETRI) and Korean Aerospace Research Institute (KARI).

General Atomics is a U.S. (San Diego) base manufacturer of UAVs. The Global Hawk project of the Defence Advanced Research Projects Agency (DARPA) is concentrated on the use of UAVs for military applications. Lighter than Air Solar International, LLC (“LTASI”) is an aerospace company based in the State of Nevada, USA, which was developing a proprietary airship concept with private investment funding from its ownership, including European-based companies. SkyStation (U.S. project) was aiming towards a 150 m long airship, operating at 20 km altitude and carrying a payload of up to 1000 kg. Applications including earth science and atmospheric monitoring, plus telecommunications at high-density high capacity services over metropolitan areas were objectives of the main contractors of Lockheed Martin Global Telecommunications as the end-to-end systems integrator, and Alenia Spazio as the payload developer. Angel Technologies (USA) already has an operational (piloted) aircraft called HALO, designed to circle above a metropolitan area and deliver a range of communication services.

Other activities include the ESA ‘HAVE’ (High Altitude Very long Endurance) study programme that involved DASA and Lindstrand Balloons, although this has not proceeded to a working prototype. Sanswire Technologies, Inc., a U.S. company, has entered into a joint venture with Telesphere Communications Inc. to launch a series of high altitude airships called “stratellite” in order to provide high-speed wireless Internet access to the entire continental United States and parts of Canada and Mexico. The NASA ERAST programme (Environmental Research Aircraft and Sensor Technology) covers several areas of research, and has been aiming towards three types of long endurance platforms (Centurion, Alliance I, and Helios). Through funding support from NASA (USA), AeroVironment has developed an unmanned, solar-powered aircraft named Helios; which will provide a telecommunications plat-

form from the stratosphere —hence its SkyTower name. In collaboration with AeroVironment, its subsidiary SkyTower and NASA, the Communications Research Laboratory and Telecommunications Advancement Organisation divisions of Yokosuka Research Centre successfully tested the world's first digital high-definition television (HDTV) broadcast transmission from the stratosphere using Pathfinder Plus, an unmanned, solar-powered vehicle manufactured by AeroVironment (June 2002); the test was followed by an IMT-2000 mobile application demonstrating video telephony.

2.1.3. Advantages and disadvantages of HAPS praxis, limitations and vulnerabilities

In the broad multiform communications, HAPS possesses all the potentialities to be proposed as a novel stratospheric segment in the wireless communications market. They are able to overcome the main drawbacks of satellite technology due to its reduced distance from the ground with respect to satellites, and its quasi-stationary situation in the sky. Additionally, the costs of construction, deployment, launch, and maintenance can be kept in lower orders of magnitudes than those of satellites can, and all these at an environmental sustainable effort because of their solar power supplies. On the other hand, it is evident that HAPS cannot replace satellites or terrestrial radio links, for reasons of coverage, reliability, safety, and cost. In fact, satellites, HAPS, and terrestrial broadband systems have different but complementary characteristics among each other. While satellites are more suited for coverage of very large areas and broadcast applications, HAPS are able to cover remote or sparsely populated areas at reduced costs, and to offer broadband services to fixed/mobile users; terrestrial infrastructures are advantageous for interactive services in densely populated areas. For these reasons the final design goal must be a flexible and synergic integration between satellite, stratospheric, and terrestrial segments, which can lead to a truly evolutionary scenario.

As far as services integration is concerned, the establishment of the stratospheric network is pointed out to be a challenging task, but whose positive benefits should be exploited in the best possible way. Since the weight constraints for HAPS are generally less critical than those for satellites, many different payloads may be carried by the same platform, thus exploiting the transmitting position of HAPS for improving performance and coverage of a variety of services. Hence, HAPS bring the idea of global communications and information infrastructure defining the main objective in which integrates service operations in a cost-

effective way. What is more, from the operational stratospheric altitude, HAPS have a wide coverage area and can provide additional capacity to the existing network or replace the coverage holes left from the terrestrial bases and repeaters. Besides, HAPS has the potential of superior flight endurance relative to airplanes and helicopters, and the results are the diverse uses for HAPS at a specific time necessities.

The coverage region served by HAPS is essentially determined by a line-of-sight (LOS) propagation situation and a minimum elevation angle at the ground terminal; a practical lower elevation limit for broadband wireless access (BWA) services might be 5°, while 15° is more commonly considered to avoid excessive ground clutter problems; from 20 km altitude above smooth terrain, 5° implies an area of 200 km, although for many service applications (city or suburban area), such wide coverage may not be required or appropriate. There is then opportunity to subdivide this area into a large number of smaller coverage zones, or cells, to provide large overall capacity optimised through frequency reuse plans.

The HAPS architecture lends adaptive resource allocation techniques, which can provide efficient usage of bandwidth and capacity. Since the HAPS is at relatively close range, this represents a power advantage of up to about 34 dB compared to a Low Earth Orbit (LEO) satellite, or 66 dB compared to a Geostationary Earth Orbit (GEO) satellite, and compared with terrestrial schemes, a single HAPS can offer a capacity equivalent to that provided by a large number of separate base-stations (Tozer & Grace, 2001), (Grace & Mohorčič, 2010).

Table 2.1 and 2.2 refer to the general comparison of the prospect types of stratospheric vehicles, between HAPS and the stated technologies of satellite and terrestrial wireless systems.

Moreover, some specific areas for HAPS technical risk, shown in Table 2.3, can be based on a review of the supplier design data. As a result, a relevant HAPS terminology and interaction can emerge based on the technical risk and operational utilities. Restricting the use of the airship in adverse conditions, by accepting reduced performance, or by providing extra airships to relieve those on station when environmental conditions are justified, could reduce HAPS risks. Also, there would always be those risks that are unpredictable and that could result in a catastrophic and unexpected system failure. These risks flow from the stochastic nature of the environment in which the vehicle operates: the effects of weather and, particularly (in the case of an airship), wind; weather is the risk factor that could be significant

if airships are not furnished with reliable sensors for on-site meteorological data, from which controllers can predict turbulence, icing, and violent gusts that can jeopardise the platform.

Conclusions about the degree of vulnerability in HAPS to air defences might have to wait knowledge about the ultimate composition of HAP structures and payload equipment (*e.g.*, system level requirements, propagation and diversity, modulation and coding, resource allocation and network protocols, antennas).

TABLE 2.1. COMPARISON OF UNMANNED STRATOSPHERIC PLATFORMS (HORI, 2002)

	Airship	Solar plane	Jet plane
Length, m	200 approx.	70 approx.	30 approx.
Weight, kg	30000	1000	2500
Power source	Solar panel	Solar power	Oil fuel
Flight duration	3 years approx.	6 months	8 hours/pilots
Position keeping error, km	1 approx.	1.5 approx.	10 approx.
Mission payload weight, kg	1000 approx.	100 approx.	1000 approx.
Mission payload power, kW	10 approx.	1 approx.	20 approx.
Example	Japan, Korea, China, development projects	Helios, Pathfinder	Proteus

TABLE 2.2. COMPARISON OF BROADBAND TERRESTRIAL, HAPS, AND SATELLITE SERVICES IN TYPICAL PARAMETERS (TOZER & GRACE, 2001)

	Terrestrial (e.g. BFWA)	HAPS	LEO satellite	GEO satellite
Station coverage (typical diameter)	<1 km	Up to 200 km	>500 km	Up to global
Cell size (diameter)	0,1-1 km	1-10 km	~50 km	400 km minimum
Maximum transmission rate per user	155 Mbps	25-155 Mbps	<2 Mbps up, 64 Mbps down	155 Mbps
System deployment	Several base stations before use	Flexible	Many satellites before use	Flexible but long lead time
Estimated cost of infrastructure	Varies	~$50 million upwards	~$9 billion	>$200 million

TABLE 2.3. A BRIEF OF HAPS ISSUES AND RISKS

Issues	Risk Management Approach
Envelope material (strength and weight)	Restrict ascent/descent conditions
Thermal control (superheat)	Incorporate reflective envelope
Helium leakage	Limit endurance: use hydrogen from fuel cells
Photovoltaic cells	Limit endurance
Fuel cells	Use LI-polymer batteries as fallback
Weatherability	Restrict ascent/descent conditions; Improve weather prediction; provide emergency ballast dump; add sprint engines(s)
Survivability	Operate within own air defense envelope
Airspace access	Restrict ascent/descent locations and times
Launch/recovery	Mechanization; restrict ascent/descent locations/times

2.2. Communication design issues for the civil HAPS-based system evaluation

The HAPS-based system contribution has been considered herein as a stand-alone airship stationed in stratosphere about 21 km above the Earth's surface, whose expectation is to offer an alternative or complement to terrestrial and satellite based communication systems.

A HAPS is expected to take the most advantages of the main wireless technologies, and is being presumed to have the capability of carrying a large variety of wireless communication payloads (Djuknic & Okunev, 1997), (Hase *et al.*, 1998), (Tozer & Grace, 2001), (Widiawan & Tafazolli, 2007), (Aragón-Zavala *et al.*, 2010), (Grace & Mohorčič, 2010); a viable and futuristic framework of the HAPS-based telecommunications network architecture is displayed in Figure 2.5.

Satellite systems possess many attractive features that are moderated by their disadvantages of large propagation delays (MEO and GEO satellite cases) and the unreliability of the satellite channel. Accordingly, HAPS can be employed since they represent a solution preserving most of the advantages of satellites, while avoiding some of their drawbacks (Karapantazis & Pavlidou, 2005). Looking at the terrestrial components, it is difficult and economically inefficient to cover remote and impervious areas with terrestrial wireless, wired, or fibre networks; HAPS can constitute a real asset to less wireless infrastructure and provide telecommunication services over such areas with the two optional operative HAPS positions at the end-to-end path (Karapantazis & Pavlidou, 2005), HAPS can be employed to connect

private networks (*e.g.*, corporate LANs), or to provide trunk connections between core networks.

The HAPS-based system's performance evaluation is being focused in this dissertation, and the signal processing actions has been approached with a reliable and robust modelling through a block diagram operations comprising the transmitter, the channel, and the receiver. As the impairments of the signal are focused on rather than those at the processing in the transceiver, the channel modelling was hold as the principal concern at our work worthwhile for performance evaluation and regulation commitments.

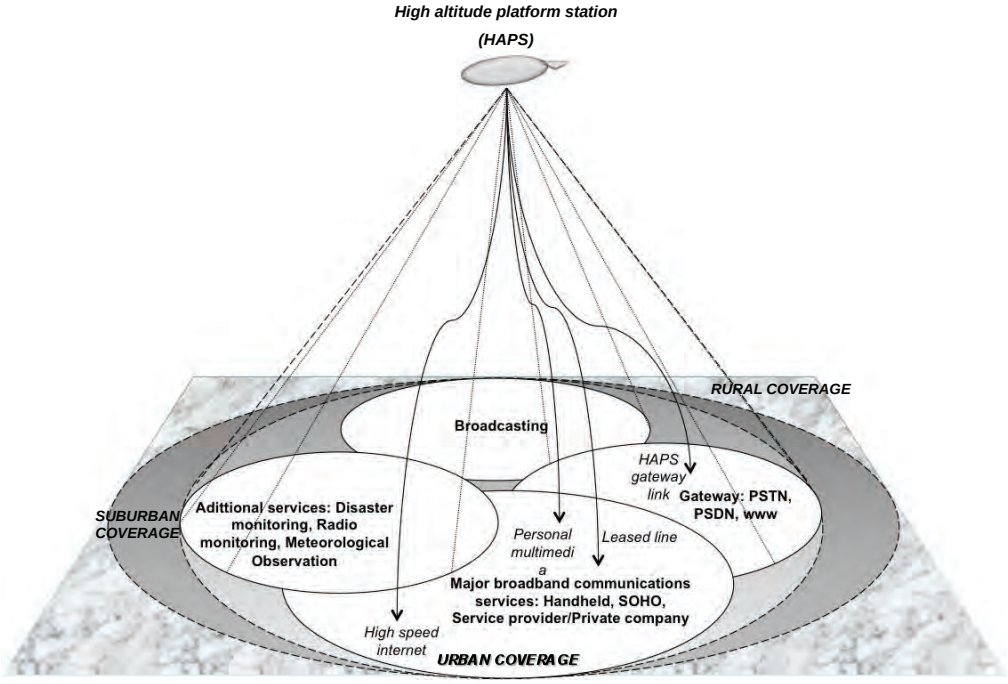

Figure 2.5. The exploratory technology development for commercial wireless communications and other services (Palma-Lázgare & Delgado-Penín, 2010b).

The HAPS analysis is introduced with the stratospheric channel modelling contribution appropriate for a stratospheric communication link approach. At this position, a controlled environment is required in which suitable equipment of techniques may be implemented or be planned for test. Therefore, the design referring to the propagation effects with dependence on the surrounding area for an end-to-end communication link is been considered.

The concentration is realised only on a specific type from the two existing impairment classes for the channel modelling. In our case, the first impairment class considered in this

work is belonging to the channel and service environment that includes propagation effects of noise, fading, and shadowing; atmospheric effects were not considered from the stratospheric altitude and in the operating frequency band. The remaining second class of impairments (i.e., phase noise and offset, channel nonlinearities, adjacent/co-channel interference, and HAPS/terminal-motion) was not regarded in our analysis, so being considered for probable future analytical approaches.

2.2.1. On ITU regulatory issues and frequency allocation

One of the main objectives in this study is the possibility of usage of platforms to provide regulatory International Mobile Telecommunications-2000 (IMT-2000) services with its established (next-generation) wireless technologies through current practical equipment in the bands 1885-1980 MHz, 2010-2025 MHz, and 2110-2170 MHz in Regions 1 and 3, and 1885-1980 MHz and 2110-2160 MHz in Region 2. Nevertheless, the Radio Regulations are not establishing priorities, but rather considerations, nowadays of allocation using such bands for HAPS at IMT-2000 and IMT-Advanced (Aubineau *et al.*, 2010) development. In our particular case, the concern is the use of the IEEE 802.16^{TM}-2009 experimental technology (ITU-R M.1457, 2001-2007) for HAPS-based system communication, and a position of its standardisation is existing in order to address wireless services and could act as a broadband wireless access (BWA) technology.

At a further considered topic, a number of countries were deciding that the allocation for the fixed service (in the mentioned bands) might also be used by HAPS (World Radiocommunication Conference 2000, WRC-2000). The use of these bands by HAPS is being limited to operation in the HAPS-to-ground direction, but also this allocation can be used by HAPS in the ground-to-HAPS direction subjected to further restrictions. Furthermore, other issues for HAPS have appeared on the agenda of WRC in 2003 (Table 2.4 and 2.5), where was resulted in a number of updates to the regulatory provisions, i. e., the “Feasibility of Use of High-Altitude-Platform Stations in the Fixed and Mobile Services in the Frequency Bands Above 3 GHz Allocated Exclusively For Terrestrial Radiocommunication,” (Resolution 734 and Rec. ITU-R F.1764), and the “Use of High-Altitude-Platform Stations Providing IMT-2000 in the Bands 1885-1980 MHz, 2010-2025 MHz, and 2110-2170 MHz in Regions 1 and 3 and 1885-1980 MHz and 2110-2160 MHz in Region 2” was revised.

Recently, at WRC a revision to the issues of services (Figure 2.6) above 3 GHz were undertaken serving for support of study and preparation for the forthcoming WRC (taking

place in Genève in 2012), mainly at the specific decisions of deployment enabling gateway links so the ground stations can maintain communications with the HAPS (Resolution 734) and support operations in the fixed and mobile services; it is desirable to have the adequate provision for the gateway links to serve the HAPS operations (Aubineau, 2010).

TABLE 2.4. FREQUENCY SPECTRUM AVAILABLE FOR HAPS APPLICATION (BASED ON THE WRC-2003)

Frequency band (GHz)	Area/Country	Service	Sharing service (primary allocation)	Reference in RR[1]
47,9-48,2	Global	FS (uplink & downlink)	FS, FSS, MS	5.552A
47,2-47,5	Global	FS (uplink & downlink)	FS, FSS, MS	5.552A
31,0-31,3	20 countries + Region 2	FS (uplink)	FS, MS	5.543A
27,50-28,35	20 countries + Region 2	FS (downlink)	FS, FSS, MS	5.437A
2,16-2,17	Regions 1 & 3	IMT-2000 (base station)	FS, MS	5.388A
2,11-2,16	Global	IMT-2000 (base station)	FS, MS, Space Research	5.388A
2,01-2,025	Regions 1 & 3	IMT-2000 (base station)	FS, MS	5.388A
1,885-1,98	Global	IMT-2000 (base station)	FS, MS	5.388A

[1] Radio Regulations, edition of 2004, ITU-R.

Region 1: Europe, Africa, Russia, and Middle East
Region 2: North and South America
Region 3: Asia and Pacific countries

FSS: Fixed satellite service
FS: Fixed service
MS: Mobile service

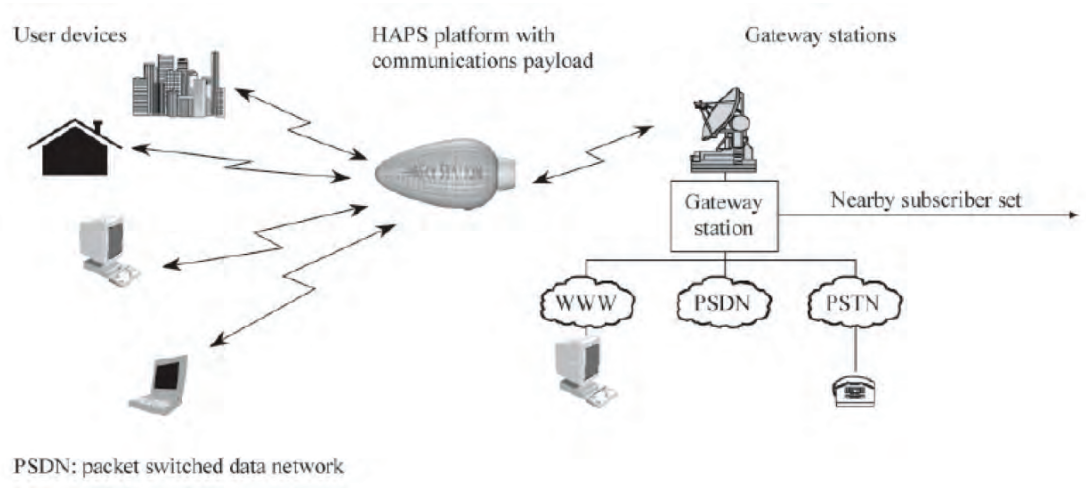

Figure 2.6. The regulation of an optional HAPS-network configuration.

Therefore, from the ideas of enhancing the international spectrum regulatory framework and keeping such current practice for the likely future wireless communication requirements, two principal remarks according to WRC can be reminded for our interests of the HAPS use: systems based on new technologies using HAPS can potentially be used for various applications such as the provision of high capacity services to urban and rural areas, and its provision has been made in the Radio Regulations for the deployment of HAPS in specific bands, including as base stations to serve IMT-2000 networks.

TABLE 2.5. ITU-R RECOMMENDATIONS RELATED TO HAPS

No.	Title
47/48 GHz (FS)	
P.1409	Propagation data and prediction methods required for the design of systems using high altitude platform stations at about 47 GHz
F.1500	Preferred characteristics of the systems in the fixed services using high altitude platforms operating in the bands 47.2-47.5 GHz and 47.9-48.2 GHz
F.1501	Coordination distance for systems in the fixed service (FS) involving high-altitude platform stations (HAPSs) sharing the frequency bands 47.2-47.5 GHz and 47.9-48.2. GHz with other systems in the fixed service
F.1608	Frequency sharing between systems in the fixed service using high altitude platform stations and conventional systems in the fixed service in the bands 47.2-47.5 and 47.9-48.2 GHz
SF.1481-1	Frequency sharing between systems in the fixed service using high-altitude platform stations and satellite systems in the geostationary orbit in the fixed-satellite service in the bands 47.2-47.5 and 47.9-48.2 GHz
28/31 GHz (FS)	
F.1569	Technical and operational characteristics for the fixed service using high altitude platform stations in the bands 27.5-28.35 GHz and 31-31.3 GHz
F.1570-1	Impact of uplink transmission in the fixed service using high altitude platform stations in the Earth exploration-satellite service (passive) in the 31.3-31.8 GHz band
F.1607	Interference mitigation techniques for use by high altitude platform stations in the 27.5-28.35 GHz and 31.0-31.3 GHz bands
F.1609	Interference evaluation from fixed service systems using high altitude platform stations to conventional fixed service systems in the bands 27.5-28.35 GHz and 31-31.3 GHz
F.1612	Interference evaluation of the fixed service using high altitude platform stations to protect the radio astronomy service from uplink transmission in high altitude platform station systems in the 31.3-31.8 GHz band
SF.1601	A methodology for interference evaluation from the downlink of the fixed service using high altitude platform stations to the uplink of the fixed-satellite service using the geostationary satellites within the band 27.5-28.35 GHz
2 GHz (IMT-2000) and others	
M.1456	Minimum performance characteristics and operational conditions for high altitude platform stations providing IMT-2000 in the bands 1885-1980 MHz, 2010-2025 MHz and 2110-2170 MHz in Regions 1 and 3 and 1885-1980 MHz and 2110-2160 MHz in Region 2
M.1641	A methodology for co-channel interference evaluation to determine separation distance from a system using high-altitude platform stations to a cellular system to provide IMT-2000 service within the boundary of an administration
F.[HAPS-RSS]	Methodology to evaluate interference from fixed service system using high altitude platform stations (HAPS) to fixed wireless system in the bands above 3 GHz

2.2.2. The physical layer and communication techniques

At the proposed HAPS operation frequencies, propagation impairments are severely caused by rain, with other lesser effects of ice and water vapour in clouds. Even though rain attenuation effects are predominant at higher frequencies, especially above 20 GHz, these are negligible at the range of 2 GHz; the higher the frequency is, the higher the attenuation and the impact on the quality of service (QoS) can be.

Generally, wireless system availability is defined as the percentage of time for which services are not affected by outage due to shadowing or blocking, and a channel could be available only if there is line-of-sight (LOS) condition. From author's research results can be showed that HAPS can give full availability even in dense urban environments: as coverage increases, performance becomes deficient in urban areas, but one HAPS could be enough for covering a large city.

The HAPS radio channel, or stratospheric channel, is having many common points with satellite and wireless terrestrial channels. The challenges in the stratospheric propagation model are intended for predicting the average received signal power at a given distance from the transmitter (large scale propagation models), as well as the fluctuations of the received power over very short travel distances of a few wavelengths or short time durations in the order of seconds (small-scale propagation or fading models). Therefore, in addition to the expected power decay due to HAPS-to-ground distance, remaining chief propagation effects are considered with the shadowing and multipath.

Some HAPS channel models have been analysed, one of them is based on a semi-Markov process giving two-state and three-state channel modelling contributions (Cuevas-Ruiz & Delgado-Penin, 2004a), (Cuevas-Ruiz & Delgado-Penin, 2004b). For instance, in Pérez Fontán & Mariño Espiñeira (2008) the identification of three levels in the rate of change of the received signal (as a function of the *Tx-Rx* separated distance) can be identified for HAPS with the very slow variations (for the range-dependent loss, and free-space loss), slow or long-term variations due to shadowing, and fast or short-term variations due to multipath. A more complete channel model would include the Doppler effect and consideration of the directivity or adaptive MIMO at the on-board antenna; the Doppler effects (absolute shift as well as spreading) can exist when communicating to moving vehicles.

The modelling techniques involving the HAPS-based system are also having a comparison to those used in the broadcasting coverage area systems at urban services. Hence, remarkable similarities over the frequency bands of our interest are including the mechanisms

giving rise to the path-loss subjected to shadowing and multipath effects but much milder, and megacell-coverage can be created with such higher HAPS “access point height” use. Nevertheless, man-made structures (buildings, small houses), with sizes from a few meters to tens of meters, are dramatically influencing the propagation channel. Latter features are similar or greater in size than the transmitted wavelength (metric, decimetric, centimetric waves) and might block and scatter the signal causing specular and diffuse reflections. Such contributions might reach the end-terminal by way of multiple paths in addition to the often-present direct signal, and a sufficient amount of energy can reach the receiver and the communication link could be feasible, specifically when the direct signal is being blocked.

Further key objectives are referring to the establishment of modulation/coding and suchlike schemes suitable to serve the broadband telecommunication services with specified QoS and BER requirements; *e.g.*, linear or non-linear modulation schemes, QPSK, QAM, *M*-APSK/star QAM, CPM, GMSK, orthogonal frequency division multiplexing (OFDM), and concatenated coding, and the prospective turbo coding and antenna diversity features could be reviewed. Regarding synchronisation, this should include both carrier and symbol timing correction, and also a case can be contemplated in which fast fading does not impose a serious problem due to coherent demodulation applied. One of the main issues in defining the HAPS communication system is also represented by the effect of the non-linear amplifiers (NLAs) on the high-order modulation schemes. In the presence of adjacent channels, two effects impair the signal detection at the receiver: symbol constellation distortion and adjacent channel interference; co-channel interference can be generated in the presence of cross-polarisation losses at the receiver antenna. Thus, the aforementioned impairments can differently affect the modulation formats due to their dissimilar spectral and envelope behaviour.

Presently, cutting edge technologies are being explored and considered to be attached to HAPS, including the use of MIMO as a platform diversity technique. In addition, antenna patterns have been used to quantify the carrier-to-interference (C/I) behaviour for a system of aperture-based antennas, extending the work for simple models to antenna beam patterns (smart antennas) to improve efficiency, flexibility, and cost effectiveness, a complete provision of re-configuration is opened; furthermore, a range of solutions that combine both electronic and mechatronic steering are being investigated to contribute to higher benefits.

In the HAPS-based system, interference can be caused by antennas serving cells on the same channels and be arisen from overlapping main lobes or sidelobes. Two kinds of interference are differentiated: interference originating from users of the HAPS-based network and interference from/to terrestrial or satellite systems sharing the same or adjacent fre-

quency bands. Terrestrial systems are generally interference limited, but it is difficult to predict the interference levels from place to place as they strongly depend on terrain and building patterns. In contrast, propagation in HAPS-based systems is achieved mainly through free space, thus the interference levels can be predicted quite successfully. And regarding interference from/to other systems, specifically, interference paths can be distinguished between HAPS ground stations, terrestrial stations or satellite earth stations, space stations, and HAPS on-board stations. In cellular HAPS architectures, with frequency re-use planning, this can give rise to the problem in which signals intended for one cell are scattered above that cell into another co-channel cell, and constitute the interference.

In advance, HAPS could achieve a substantial indoor coverage with the probabilities of having a good quality of service at low cost. The possibility of such improvement at the indoor case-study has been managed by determining an appropriate diversity technique (space, time, and frequency) for each traffic type and carrying out the aims of the required data rate, i.e., a specification defined by the feasibility of the multiple antennas use, or steerable or fixed antennas —a useful operation is restricted to high elevation angles (and short distances) due to the fact that the angle changes less significantly, and to overcome such boundary narrower beamwidth antennas could be used as distance increases leading to a gain increase.

2.2.3. Propagation Impairments and Modelling

For relatively short transmission paths, propagation over the 2–11 GHz frequency range is relatively non-dispersive. Rain attenuation is negligible at the lower end of the band. Attenuation of emissions by terrain, foliage, and human-generated structures can be significant. Diffraction loss is finite. This allows consideration of both LOS and NLOS transmission links.

LOS-link at such lower frequency bands may be a combination of thermal and interference noise-limited. Dispersive multipath is not significant until path lengths become greater than 10 km, which last should be the case for HAPS implementation. For NLOS radio systems, consideration must also be given to the excess path loss experienced from diffraction and the fading experienced from reflective facets that could be fixed or in motion. Measurement data indicates that this form of fading might follow a Ricean distribution with parameters set by the characteristics of a specific direct-path transmission. For severely attenuated links, the fading distribution characteristics can approach to a Rayleigh. Hence, a variety of channel

models can be developed to classify the existing different terrain types of communication scenarios.

Some conclusions can be given having a high availability unobstructed radio link, and subsequently, HAPS case coexistence considerations are based on a LOS primary transmission path (Perez-Fontan *et al.*, 2006). Other simplified channel models, possible related to the HAPS frequency operation for the purpose of coexistence calculations, have been developed from other authors at standardisation levels. For instance, channels for 3.5 GHz system parameters with a PMP and mesh architectures, the diffraction loss calculations used methods described in ITU-R Recommendation P.526-7, in the proposed statistical models (IEEE 802.16.3c-01/29r4) for delay spread, *K*-factor, and others were used in the 1-4 GHz range with appropriate frequency correction factors together with path loss models in an extended frequency range —the Doppler spectrum was reviewed as a function of the centre frequency but with a more work being required.

On the other concerned subject, the propagation models are derived to be in the narrowband and wideband (or broadband) categories.

If the signal bandwidth is less than the channel's coherence bandwidth, the channel modelling is described as being narrowband (a limiting case of the wideband situation), not leading to frequency selective effects. At this narrowband channel family is corresponding the sub-classification: (1) single-mode models, where the channel modelling is described by a single statistical process, generally describing the channel as a stationary process, (2) multi-mode models (or channel state oriented, typically helped by the Markov chain model), where the channel modelling is described by a small finite temporarily number of states that can present different statistical models for each of the states along with the transmitted information time and with their corresponding state transitions —last mode can concern to the non-stationary process which is determined by a set of distribution parameters defined by pdf's of the received signal depending on the environment and can be derived from a sample of measured received signals for each state—, and (3) empirical models, in which channel response measurements can be used continuously to produce the channel modelling.

Therefore, the model of the stratospheric channel can be taken by the possibilities of measured channel responses, sampling appropriately and then utilise the results (via linearity) to the appropriate channel modelling; the HAPS channel modelling can exist where specific details featuring a specific environment are determining the radio link state prediction, and

given such information some sort of explicit solution for the electromagnetic wave equations can be applied.

At the remaining case of broadband channel implementation, a common used fading model exhibiting a frequency selective behaviour can be described by a multiplicative bandlimited noise with differential delay (Figure 2.7).

For small time durations the received multipath or faded signal is highly correlated, and with a similar result for the level of signal's correlation over small physical distances (of the order of 10's of wavelengths). Thus, the waveform can be divided into *windows*, in which the data in each one can be considered highly correlated and treated as the output of a stationary random process: a wideband channel modelling based on a linear, tapped-delayed, transversal filter mimicking the physical processes.

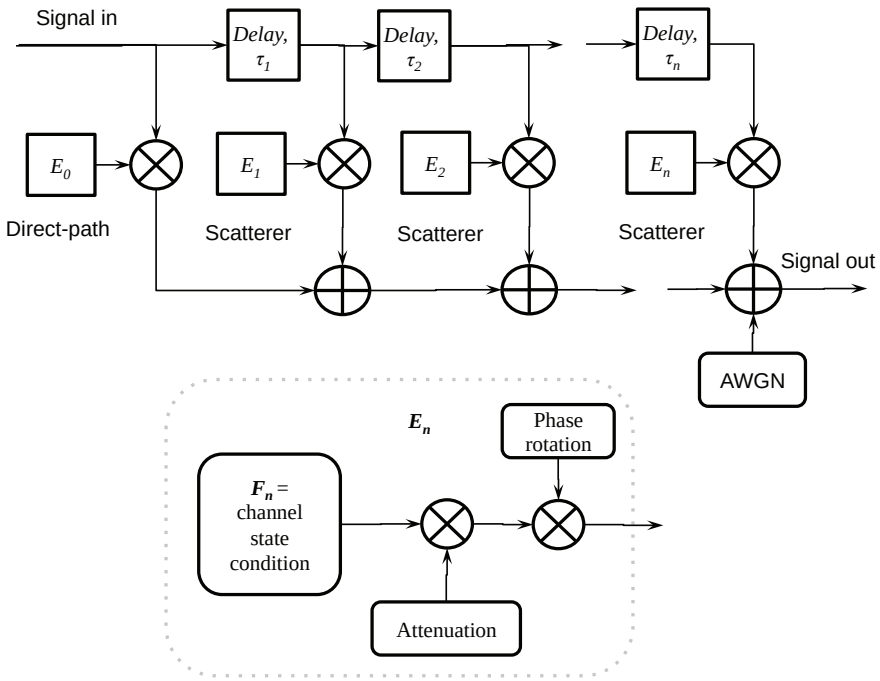

Figure 2.7. An example of the broadband channel modelling.

For instance, modelling the linear wide sense stationary uncorrelated scattering (WSSUS) channel of Bello (1993) has the meaning of being WSS with the time-invariant autocorrelations of the delay-spread functions characterising the channel (or, the gains on the time varying taps for a given delay be chosen from a fixed probability distribution), and US is corresponding to have the description of the channel by a time varying TDL whose coeffi-

cients on distinct taps are not correlated (or, the chosen fixed pdf's are corresponding to the independence among them). Under later assumptions, the channel are completely characterised by a two-dimensional scattering function in terms of its echo-delays and Doppler spread; the model can have an irregular-spaced TDL or a constant one for implementation with the indication of the number of scatterers to be modelled.

The given taps can be thought associated with a physical scatterer. The scatterers are not typically points and the delayed signal can correspond to one of such scatterers faded in the same fashion at the narrowband signal —an implementation by passing to the frequency domain multiplied by the appropriate phasor (a random phase shift uniformly over [0,2π)) and associated to an attenuation—. The signal from the scatterer is to be subjected to the same stated-oriented channel conditions where in each one the number of scatterers is inconsistent.

Also, a further complex delay design can be generated: when a given number of scatterers is created and processed each one of their sections, throughout time existing scatterers can die with a fixed probability and new ones can be created with a fixed probability, determining a mean number of scatterers at long-term statistics; a birth/death random process can be defined: a death probability can be determined by the environment, the user type, and the channel sampling rate, and a birth probability is a function of the mean number of scatterers and the death probability of a scatterer. The parameters associated to an individual scatterer can be derived when its creation occurs and remain constant over its lifetime —it is remarkable that the input to the system has the delays given in microseconds, so that the simulation can convert to samples and the number of samples per second can be also a parameter into the simulation.

4

The HAPS-based Communication System Performance Estimation

4.1. Performance evaluation: Downlink examination and simulation

Herein, a synthetic model of the HAPS broadband channel was part of a radio system design, and its optimisation was supported by means of simulations that might be implemented into software channel simulators in order to approximate the physical radio channel for experimental investigations.

Latter goal is dealing with attaining the demonstrative approach to the performance evaluation perspective of the HAPS-based communication system. Involving these bases, terms of performance evaluation were achieved using the denominated 802.16™-2009 HAPS-based system embracing the Matlab®-based simulation tool. This software-aided approach was achieved by the miscellaneous configurations from the applied model; the examination involving the simulation used is now for discussion.

The treated block diagram of the radio communication system is comprising the transmitter, channel, and receiver stages (Figure 4.1). On the simulated system, the transmitter is including the coding and modulation, and at the receiver the inverse operations to those in the transmitter are carried out; the actions simulated into the last widespread blocks belong to the system signal processing. The channel model, the remaining essential task of the

simulation work, is focused on the impairments of the signal but not regarding the signal processing essentially. Through this work, the distinction made is concerning that the signal processing is not regarded in deep but useful.

From the considered general model in Figure 4.2, the proper blocks dealt in this work are primarily the signal impairments not produced by the deliberate signal processing; the fundamental signal impairments including the propagation effects of fading, shadowing and coloured noise are determining the downlink (DL) mode implementation, and not involving the uplink (UL) case.

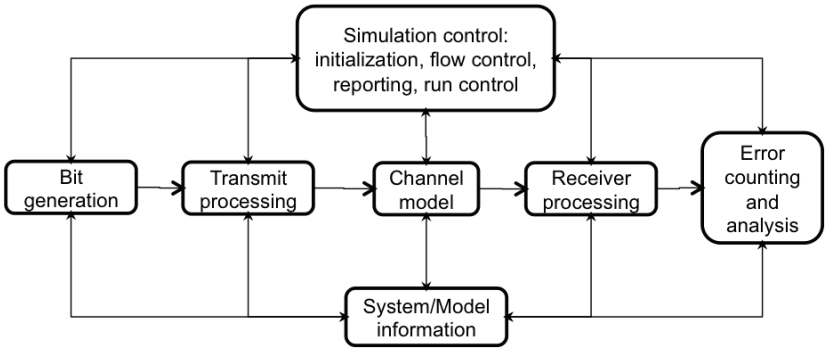

Figure 4.1. The mainstream block diagram for the HAPS-based communication system realisation.

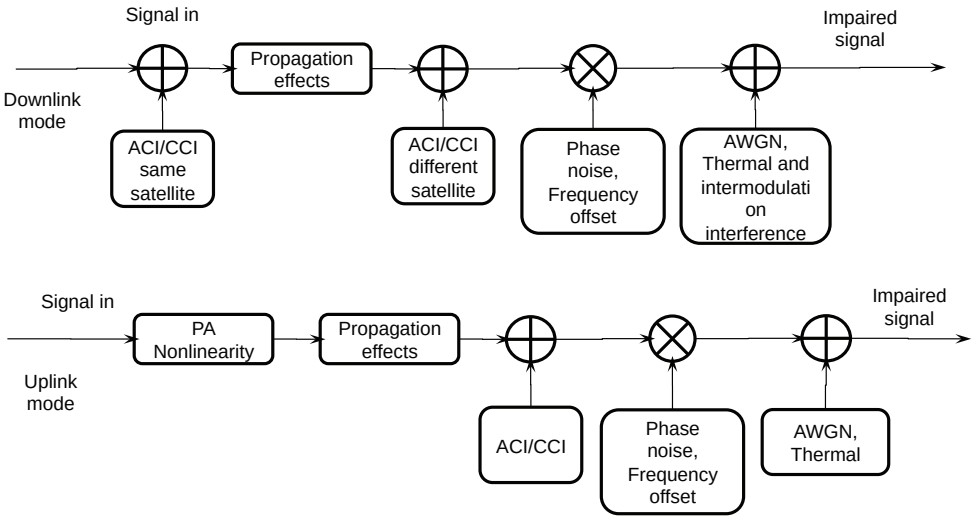

Figure 4.2. The familiar overall radio channel description.

The simulation was focused on the carrier frequency of 1.820 GHz, and the overall modelling (Figure 4.3) plus signalling waveforms were particularly implemented into the simulator by means of Matlab® m-files. Hence, such forming analysis was chosen for the performance test of the system by means of the bit error rate (BER) versus energy bit noise power density ratio (E_b/N_0) (see Subchapter 4.2).

Firstly, it is referred to make headway for some essential details of the IEEE Std 802.16™-2009 PHY-layer specifications and simulations (Batlles, 2008). Most of the OFDM symbol parameters are already defined by the standard: the nominal channel bandwidth, number of used subcarrier, sampling factor, ratio of guard time to useful symbol time (CP), number of total OFDM subcarriers, subcarrier spacing, useful symbol time, and OFDM symbol time. The structure of the implemented baseband transceiver is shown in Figure 4.4; at this setup, the mandatory features were implemented while letting the implementation of optional advanced features out.

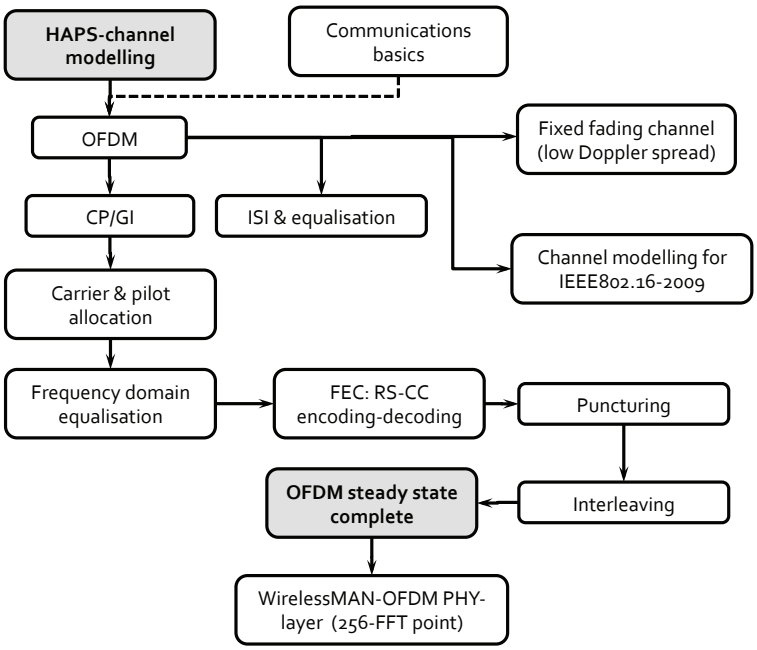

Figure 4.3. The outline simulation work, the block diagram ordering for the HAPS-based communication system implementation.

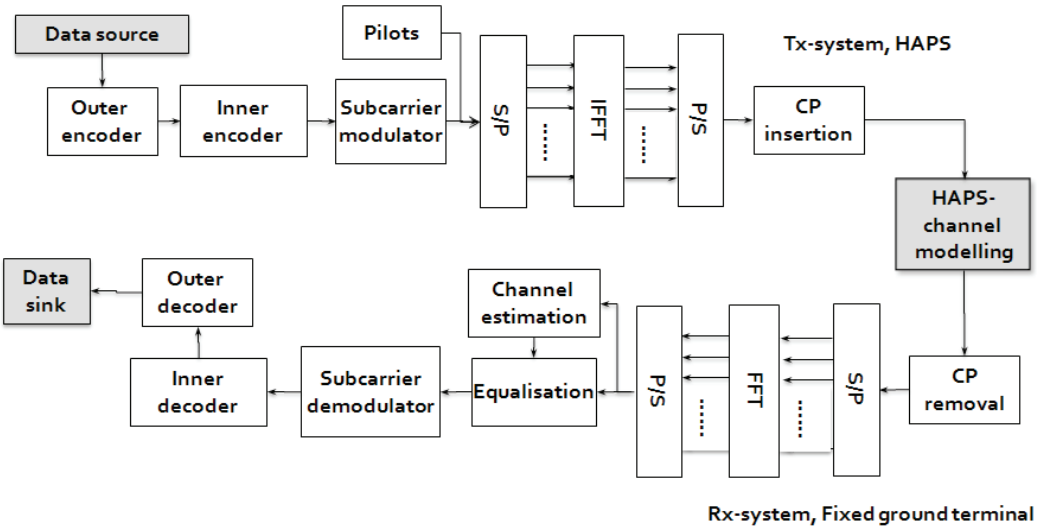

Figure 4.4. The use of WirelessMAN-OFDM PHY-layer block diagram.

And secondly, the HAPS-analysis was built up from narrowband model states accommodated to the broadband capabilities at the HAPS channel modelling proposal in the DL case (Figure 4.5). It is recalled that as most of the models already designed for the terrestrial and satellite communications are having some relationships with the recently developed HAPS-technology, and was established that both resources for the relevant HAPS system's performance evaluation can support the stratospheric channel modelling.

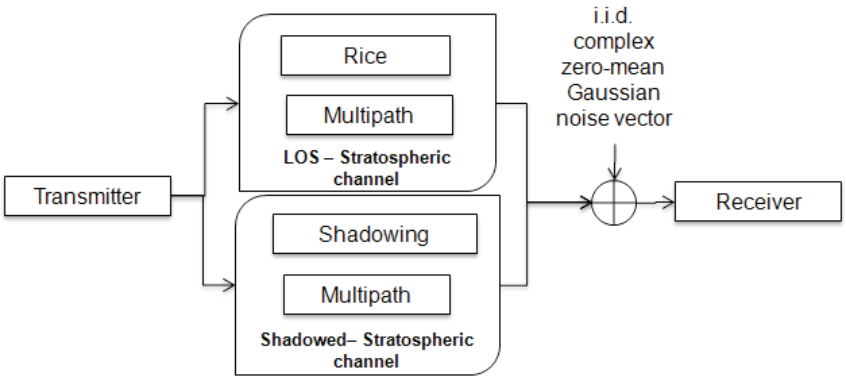

Figure 4.5. The narrowband states plus multipath presented for the HAPS channel modelling approach.

The HAPS-wireless channel was characterised by path loss (including shadowing), multipath delay spread, fading characteristics, and Doppler spread; all model parameters were dependent upon the urban terrain type, HAPS-height, and surrounding scatterers' motion. Other parameters of interference were not considered.

The simplest channel modelling was corresponding to the fading modelled by multiplying the transmitted signal and the bandlimited noise. The remaining complex fading was assumed mostly dominated by tall buildings and obstructions; blocking and reflecting the direct-signal path was assumed to occur between the transmitter and the receiver. A couple of channel states were distinguished for the radio link situation of the HAPS-based communication system: the received signal power at the ground terminal can be interpreted at the LOS and shadowing cases. And, at this point the received signal power at simulations was properly combined with a total independency between these two states; the direct-path signal modelling needed to be combined with the "alive" shadowing one, but without having higher complexities putting both states into a nonsingle channel simulation. Henceforth, a noncomplex channel approach was assumed to be for each of the states and run in separated simulations employing the appropriate channel model situation; results then were combined consistent with the assumptions of the time percentage spent in each of the shadowed and no shadowed state, ignoring the transition effects changing from one state to another and without fading countermeasure techniques sensitive to such transitions —for instance, the effects of interleaving could be dependent to the mean length of time in the given state, not only on the channel state's time percentage.

The HAPS-based system simulation approach was prepared for normalisation and evaluation: a normalisation with respect to the signal level from an undisturbed received waveform —normalisation to LOS corresponds to that where the received signal strength is divided by the LOS level hence the power was corresponding to the time domain channel characteristics—. The LOS reference was corresponding to the signal level received by the terminal with no channel effects (multipath interference or shadowing) and the CTF equals to 1; the received power level was expected to fluctuate in an interval of dB's from the LOS reference due to the multipath transmission and fading impairments.

The simulated PDP model was based among the references for a satellite-to-ground situation extended to our stratospheric platform case for urban coverage with supplemental assumptions regarding the scattering model structure (Figure 4.6).

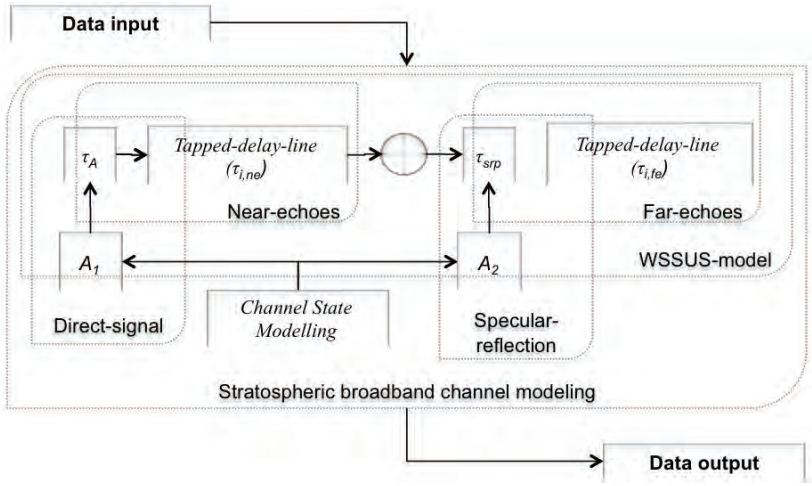

(a)

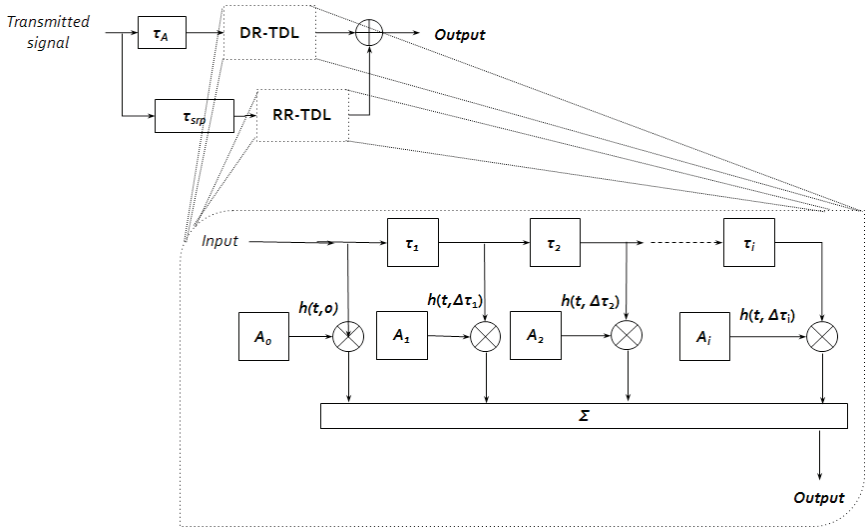

(b)

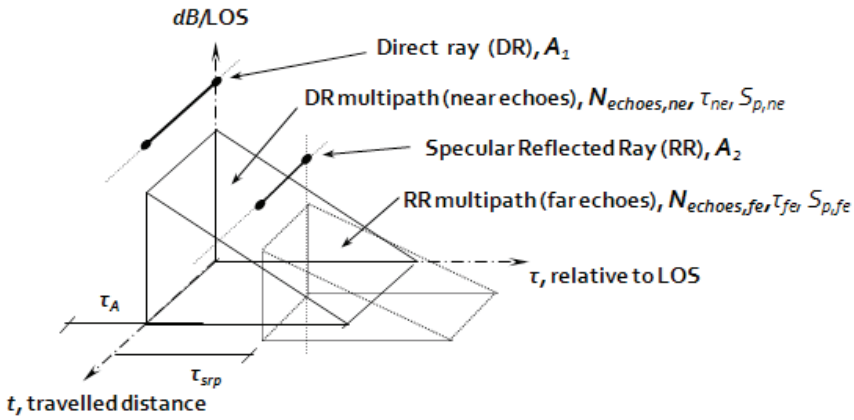

(c)

Figure 4.6. The PDP model for the stratospheric channel simulator (Palma-Lázgare and Delgado-Penín, 2010b): (a) the broadband channel into the overall system approach, and (b)-(c) the multipath fading with its main divisions and elements.

A statistical channel modelling and the representation of WSSUS model were used to conform into the two-state channel situation with a discrete and finite numbers of scatterers around the receiver. With the tapped-delay-line (TDL) design, paths were simulated as an equal-spaced array from τ=0 to $\tau = \tau_{max}$; the term i=0 represents the echo-numbering of multipath, A_i stands for the amplitude corresponding to the i-th echo, and τ_i is the delay-time. The simulated fading process estimation was conducted as a Gaussian distributed array, which was bandlimited by a FIR filter with a bandwidth that corresponds to the maximum Doppler spread. Next, the latest was multiplied by the delayed and fading input with the corresponding gain factor. The outputs from all the i-taps were then summed together.

An utmost point was determined at the communications channel, which is to be carried by the process of transmission ensuring that inaccuracies caused by improper length of vectors and sampling were not leading to system degradation (higher error rates); instead of generating the envelope of the channel output, the simulator has generated complex-valued channel output to preserve the phase distortion on the channel.

Adequate simulation parameters were chosen to provide the framework (Figure 4.7) of developing and testing the proposed HAPS channel model. Figure 4.8 is leading the simulation to the outcome of the overall HAPS-based communication system.

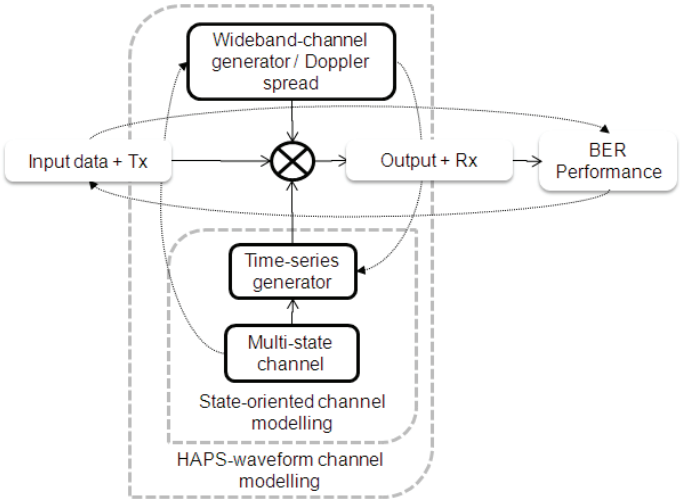

Figure 4.7. The simulation-framework for developing and testing the proposed stratospheric channel model.

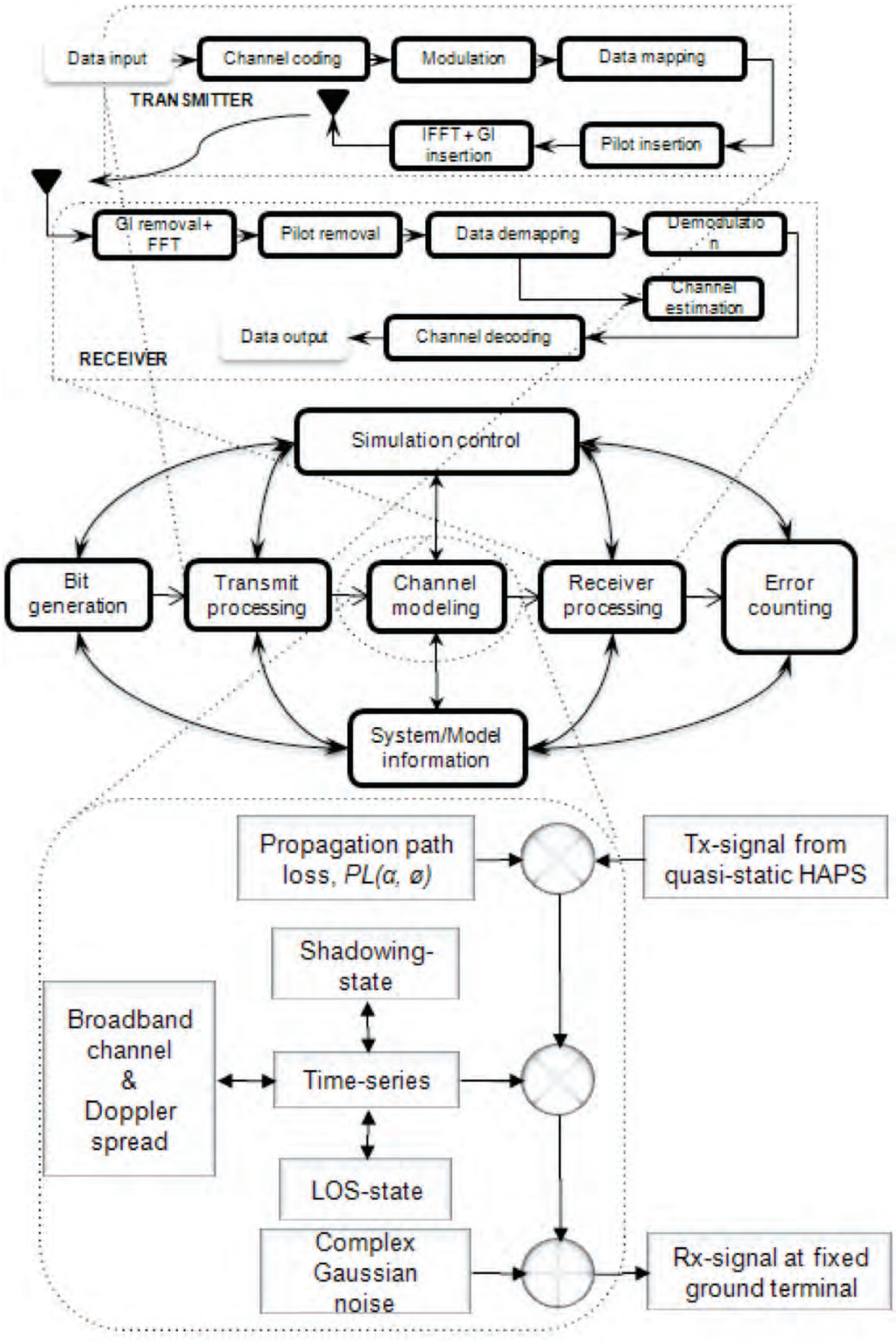

Figure 4.8. The overall HAPS-based communication system simulation control.

The time-series (Pérez Fontán & Mariño Espiñeira, 2008) were produced presenting very simple analysis techniques and covering the fast variations (due to the multipath) combined with the channel conditions of either the shadowing or direct path. The latest was implemented by a narrowband generator producing the channel's complex envelope, which is represented by the complex Lognormal/Rice/Rayleigh series with their appropriate Gaussians in quadrature and Butterworth filter (Doppler spread shaping).

The interpretations of the channel signal modelling via simulations are shown in the corresponding plotting tests, through Figure 4.9 to Figure 4.13.

Respectively, Tables 4.1 to 4.4 set the remaining parameters held and acquired for usage at the transceiver and the channel propagation approach.

Table 4.1 is making reference to some relevant thresholds that could be utilised in the transceiver under the standardisation circumstances, not in our circumstances, and could be applied essentially for having a more robust and power-spectral efficient communication outcome aiming to the adaptive modulation coding (AMC) suggestion. As a general implied idea, there can be defined mainly two types of AMC techniques for possible employment in the overall system: maximum throughput AMC to achieve the best overall throughput without any constraint on the data reliability (i.e. bit error probability), and minimum bit error probability AMC to meet specific data reliability constraints (e.g., 10^{-4} BER). And, such defined methods can be referred to assign equal power across all OFDM subcarriers according to plausible slow and fast adaptations (propagation conditions of the radio link, or channel state, known at the transmitting end), but not incrementing the complexity of the system compared with AMC with dynamic power allocation. For latter reasons, correct AMC decisions must be made to find alternative potential thresholds (at another probable future work) and, to maintain an efficient link adaptation mechanism of the system according to its conditions of application and performance.

At Table 4.2 through Table 4.4 are referred to the Std 802.16 and channel parameters and values for simulation model accomplishments: the performance outcome of the HAPS-proposal. The respective parameter variations for the performance results are used, different conditions of modulation, coding, and channel characteristics.

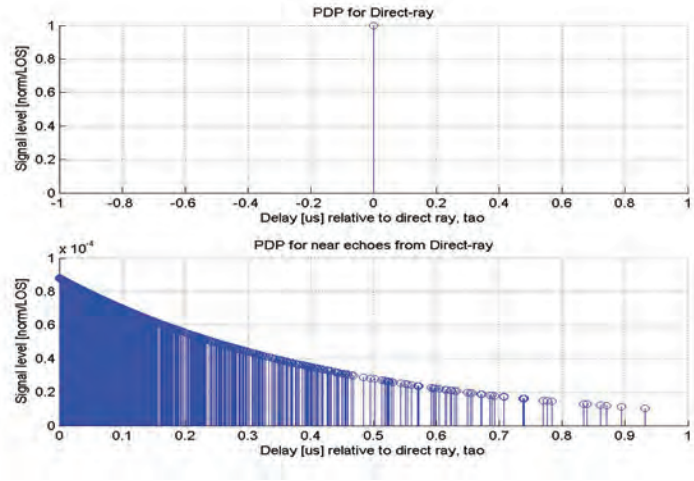

Figure 4.9. An example: PDP for direct ray (LOS) and near-echo multipath normalised.

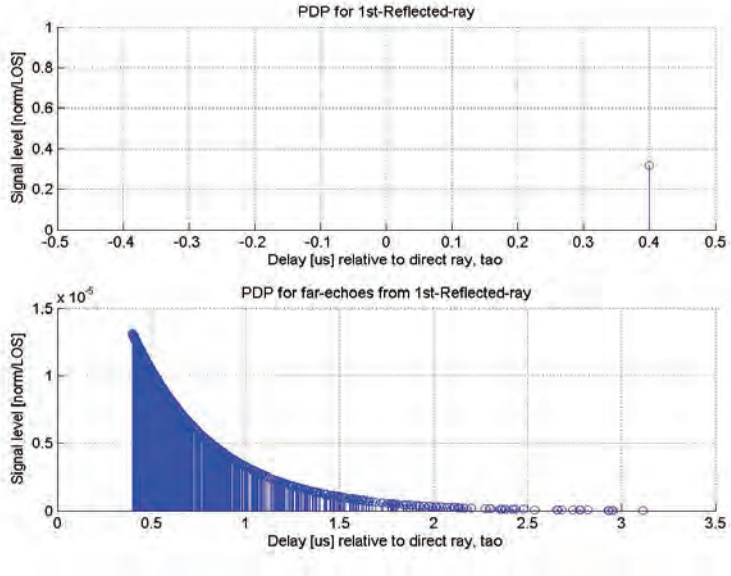

Figure 4.10. An example: PDP for the specular ray (1RR) and far-echo multipath normalised.

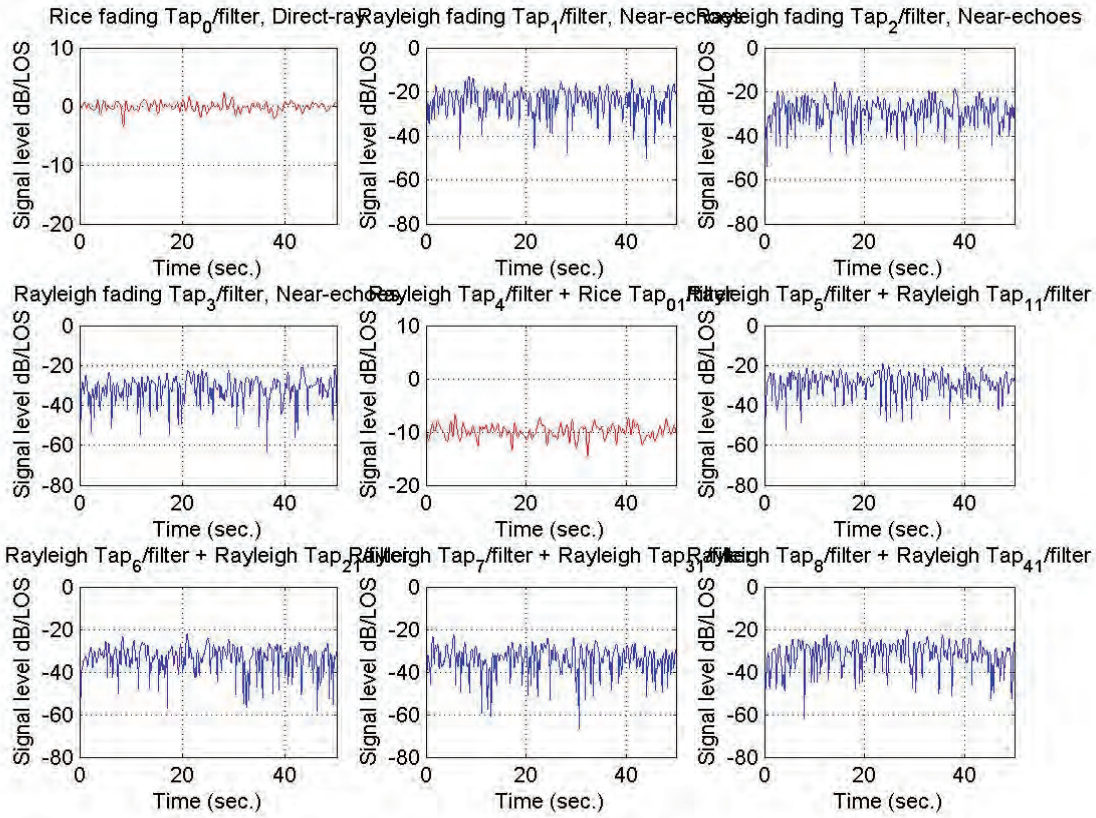

Figure 4.11. An example: The time-series representations for the WSSUS-TDL model, LOS-near-echoes plus 1RR-far-echoes.

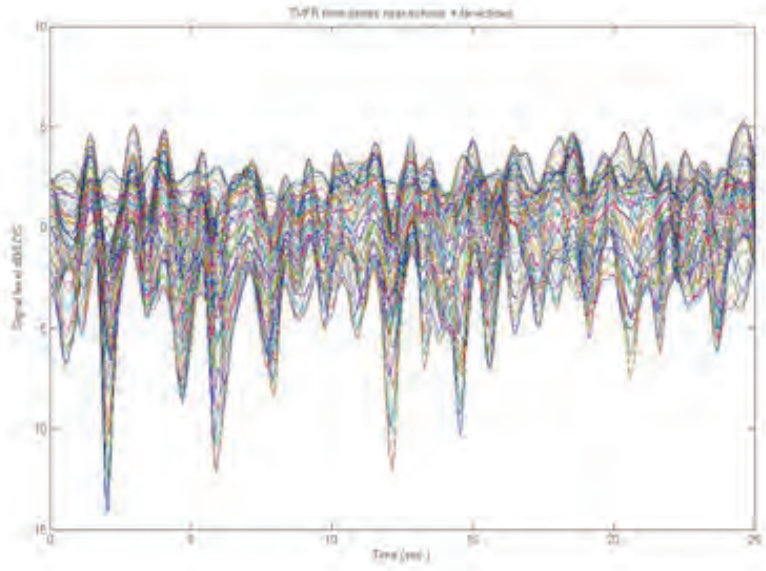

Figure 4.12. An example: Time-series representation for LOS-near-echoes plus 1RR-far-echoes.

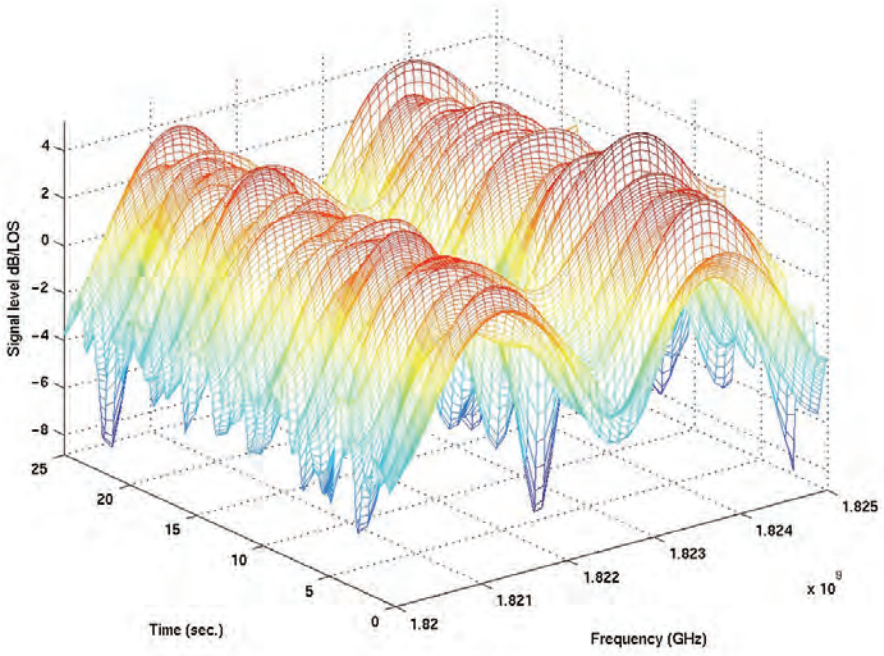

Figure 4.13. An example: Time-variant frequency (power in dB's) of LOS-near-echoes plus 1RR-far-echoes —frequency-selective fading effect in the stratospheric propagation channel with bandwidth of 5MHz at L-band.

TABLE 4.1. RELEVANT THRESHOLDS OF ADAPTIVE MODULATION CODING DEPENDING ON SNR

Lower-bound	Upper-bound	Map constellation & Coding rate
≥6.4 dB	<9.4 dB	BPSK ½
≥9.4 dB	<11.2 dB	QAM ½
≥11.2 dB	<16.4 dB	QAM ¾
≥16.4 dB	<18.2 dB	16QAM ½
≥18.2 dB	<22.7 dB	16QAM ¾
≥22.7 dB	<24.4 dB	64QAM ⅔
≥24.4 dB	NA	64QAM ¾

TABLE 4.2. PARAMETERS FOR THE PHY-LAYER IEEE 802.16™-2004/2009 PROVISION IN DOWNLINK MODE

Parameter	Value
FFT size	256
Channel bandwidth, BW [MHz]	5, 10, 20
Sampling frequency, F_s [MHz] = n·BW·8000/8000; with sampling factor of n = 8/7 (5 MHz) at licensed-band, n = 57/50 (10 & 20 MHz) at licensed-band; n = 144/125 (BW = 1.25MHz)	5.71 for 5 MHz, 11.4, 22.8 for 10 MHz and 20 MHz
Sampling period, $1/F_s$ [μs]	0.175, 0.087, 0.043
Subcarrier frequency spacing, $\Delta F = F_s/N_{FFT}$ [kHz]	22.31, 44.5, 89.03
Useful symbol period, $T_b = 1/\Delta F$ [μs]	44.81, 22.47, 11.23
Guard time, $T_g = T_b \cdot CP$ [μs]; CP = 1/4 and CP = 1/32 (cyclic prefix ratio)	11.2, 5.61, 2.8; 1.4, 0.7, 0.35
OFDM symbol duration, $T_s = T_b + T_g$ [μs]; CP = 1/4 and CP = 1/32	56.14, 28.07, 14.04; 46.32, 23.16, 11.58
No. of used subcarriers	200
No. of pilot subcarriers	8
No. of data subcarriers	192
No. of null subcarriers, and DC subcarriers	55, 1

TABLE 4.3. RADIO PROPAGATION AND CHANNEL FADING CHARACTERISTICS AT OUTDOOR SITUATION.

General parameters			
f_c = 1820 MHz, λ = 0.1647 m	r_{HAPS} = 21 km, r_{Earth} = 8504 km	R_{HAPS} = 0-36.15 km (at urban area with α = 90°-30°)	α = 43°, R_{HAPS} = 22.43 km, ξ = 47°
d_{HAPS} = 30.727 km (at α = 43°)	h_{mbh} = 25 m	$h_{terminal}$ = 1.5 m	$x_{TB1,LOS}$ = 5 m, $x_{TB2,LOS}$ = 20 m
$x_{BB} = x_{building}$ = 25 m	$h_{building}$ = 23.5 m	ζ = 0.9468	$f_{D,max} \approx$ 2.4 Hz
$T_{coherence} \approx$ 0.1 s	$BW_{coherence} \approx$ 833.33 kHz	$\Delta\tau_i$ = 0.1 μs (equally WSSUS spaced-TDL model)	i = 11 taps
$n_{i,ne}$ = 6 (taps), $n_{i,fe}$ = 5 (taps)	$\tau_{echoes,ne}$ = [0 0.6) μs, $\tau_{echoes,fe}$ = [0.6-1.2) μs	$N_{echoes,ne}$ > 50, $N_{echoes,fe}$ > 50	$\tau_{e,ne}$ = 0.069 μs, $\tau_{e,fe}$ = 0.091 μs
$\tau_{m,ne}$ = 0.6 μs, $\tau_{m,fe}$ = 1.2 μs	$S_{p,ne}$ = 10 dB/μs, $S_{p,fe}$ = 10 dB/μs	A_1 = 0 dB (level power of the direct-signal)	A_2 = -10 dB (level power of the specular reflected signal)
MP_{ne} = -23.6 dB, MP_{fe} = -26.8 dB	Average multipath power at *i*-th tap [dB]: $MP_{1,ne}$ = -24.49, $MP_{2,ne}$ = -31.67, $MP_{3,ne}$ = -39.21, $MP_{4,ne}$ = -49.03, $MP_{5,ne}$ = -59.40, $MP_{6,ne}$ = -50.40, $MP_{7,fe}$ = -51.66, $MP_{8,fe}$ = -57.71, $MP_{9,fe}$ = -63.49, $MP_{10,fe}$ = -69.11, $MP_{11,fe}$ = -73.47		
Parameters, Direct-path case 1			
$\phi_{LOS} \approx$ 0°	L_{LOS} = 127.4 dB; $PL_{HAPS,FSL}$ = 127.4 dB	$\tau_{A,LOS}$ = 102.5 μs, $\tau_{B,LOS}$ = 102.67 μs, $\tau_{srp,LOS}$ = 0.346 μs, $d_{srp,LOS}$ = 30.78 km	$\Delta\tau_{srp,LOS}$ = 0.173 μs, $\Delta r_{srp,LOS} \leq$ 30 m

Parameters, Direct-path case 2			
$ø_{LOS}$ = 5°	L_{LOS} = 131.5052 dB; $PL_{HAPS,FSL}$ = 127.4 dB, $PL_{Terrestrial,DD}$ = 4.08 dB, $L_{srp,FSL}$ = 0.0231 dB	h_{LOS} = 55m, h_{SR} = 707.47m	d_{LOS} = 78.44 m, d_{SR} = 705.97 m
$\tau_{A,LOS}$ = 102.5 µs, $\tau_{B,LOS}$ = 102.67 µs, $\tau_{srp,LOS}$ = 0.346 µs, $d_{srp,LOS}$ = 30.78 km	$\Delta\tau_{srp,LOS}$ = 0.173 µs, $\Delta r_{srp,LOS}$ = ≤ 30 m		
Parameters, Shadowing case 1			
A_{tss} = 54% (shadowing time percentage)	µ = -13.6 dB (Mean power relative to LOS under shadowing condition)	σ = 2.9 dB (standard deviation of log-normal fading)	$ø_{shadowing}$ ≥ 75°
$x_{TB1,shadowingV1}$ = 12.5 m, h_{LOS} = 13.56m, $h_{threshold}$ = 12.37m, $x_{TB2,shadowing}$ = 12.5 m	$L_{shadowing}$ = 176.68 dB; $PL_{HAPS,FSL}$ = 127.4 dB, $PL_{Terrestrial,RSL}$ = 48.28 dB, N_{RB} = 1, PL_{EPLMRB} = 10 dB, $PL_{Terrestrial,MSDL}$ ≈ 0 dB	τ_A = 102.5 µs, $\tau_{B,shadowing}$ = 102.58 µs, $\tau_{srp,shadowing}$ = 0.166 µs, $d_{srp,shadowing}$ = 30.75 km	$\Delta\tau_{srp,shadowing}$ = 0.086 µs, $\Delta r_{srp,shadowing}$ ≤ 15 m
Parameters, Shadowing case 2			
A_{tss} = 54%	μ_{LN} = -13.6 dB	σ_{LN} = 2.9 dB	$ø_{shadowing}$ ≥ 75°
$L_{shadowing}$ = 238.98 dB: $PL_{HAPS,FSL}$ = 127.4 dB, $PL_{Terrestrial,foliage}$ = 5 dB (g = 0.2 dB/m, l = 5m , n = 5), $PL_{Terrestrial,DS}$ = 106.53 dB, $L_{srp,FSL}$ = 0.0116 dB	τ_A = 102.5 µs, $\tau_{B,shadowing}$ = 102.58 µs, $\tau_{srp,shadowing}$ = 0.173 µs, $d_{srp,shadowing}$ = 30.75 km	$\Delta\tau_{srp,shadowing}$ = 0.086 µs, $\Delta r_{srp,shadowing}$ ≤ 15 m	$x_{TB1,shadowingV2}$ = 5 m; with $x_{TB1,\ shadowingV1}$ ≤ 12.5m, h_{LOS} = 13.56m, $h_{threshold}$ = 12.37m, $x_{TB2,shadowing}$ = 20 m

TABLE 4.4. RADIO PROPAGATION AND CHANNEL FADING CHARACTERISTICS AT OUTDOOR-INDOOR SITUATION.

General parameters			
f_c = 1820 MHz, λ = 0.1647 m	r_{HAPS} = 21 km	R_{HAPS} = 0-36.15 km (at urban area with α = 90°-30°)	α = 43°, R_{HAPS} = 22.43 km, ξ = 47°
r_{Earth} = 8504 km	d_{HAPS} = 30.691 km (at α = 43°)	x_{BB} = 10 m, $x_{indoorL}$ = 5 m, $x_{indoorR}$ = 15 m, x_{indoor} = 20 m	h_{mbh} = 30 m
n_{floor} = 6, $n_{floor,total}$ = 10, h_{floor} = 18 m,	$x_{TB1,LOS}$ = 15 m	$h_{building}$ = 10.5 m, $h_{terminal}$ = 1.5 m	ζ = 0.9468
$f_{D,max}$ ≈ 2.4 Hz	$T_{coherence}$ ≈ 0.1 s	$BW_{coherence}$ ≈ 833.33 kHz	$\Delta\tau_i$ = 0.1 µs (equally WSSUS spaced-TDL model), i = 11 taps
$n_{i,ne}$ = 6 (taps), $n_{i,fe}$ = 5 (taps)	$\tau_{echoes,ne}$ = [0 0.6) µs, $\tau_{echoes,fe}$ = [0.6-1.2) µs	$N_{echoes,ne}$ > 50, $N_{echoes,fe}$ > 50	$\tau_{e,ne}$ = 0.069 µs, $\tau_{e,fe}$ = 0.091 µs
$\tau_{m,ne}$ = 0.6 µs, $\tau_{m,fe}$ = 1.2 µs	$S_{p,ne}$ = 10 dB/µs, $S_{p,fe}$ = 10 dB/µs	A_1 = 0 dB (level power of the direct-signal)	A_2 = -10 dB (level power of the specular reflected signal)
MP_{ne} = -23.6 dB, MP_{fe} = -26.8 dB	Average multipath power at *i*-th tap [dB]: $MP_{1,ne}$ = -24.49, $MP_{2,ne}$ = -31.67, $MP_{3,ne}$ = -39.21, $MP_{4,ne}$ = -49.03, $MP_{5,ne}$ = -59.40, $MP_{6,ne}$ = -50.40, $MP_{7,fe}$ = -51.66, $MP_{8,fe}$ = -57.71, $MP_{9,fe}$ = -63.49, $MP_{10,fe}$ = -69.11, $MP_{11,fe}$ = -73.47		

Parameters, Direct-path			
$ø_{LOS} \approx 5°$	$L_{LOS,outdoor}$ = 130.40 dB; $PL_{HAPS,FSL}$ = 127.4 dB, $PL_{D,Terrestrial}$ = 3.01 dB	$L_{I,NI}$ = 10 dB, $L_{I,GI}$ = 15 dB, $L_{I,VW}$ = 7.8 dB, $n_{I,VW}$ = 4, t_{loss} = 2 dB/floor height	L_{BLv1} = 65.23 dB, L_{BLv2} = 23.34 dB, L_{BPL} = 26.23 dB
$L_{LOS,total}$ = 195.64 dB	$\tau_{A,LOS}$ = 102.4 μs	$\tau_{B,LOS}$ = 102.49 μs, $d_{srp,LOS}$ = 30.72 km	$\Delta\tau_{srp,LOS}$ = 0.086 μs, $\tau_{srp,LOS}$ = 0.173 μs
$h_{LOS} = h_{SR}$ = 180 m	$d_{LOS} = d_{SR}$ = 235.32 m		
Parameters, Shadowing			
A_{tss} = 54% (shadowing time percentage)	μ = -13.6 dB (Mean power relative to LOS under shadowing condition)	σ = 2.9 dB (standard deviation of log-normal fading)	$ø_{shadowing} \geq 75°$
$x_{TB1,shadowing}$ = 15 m, $h_{threshold}$ = 14.67m	τ_A = 102.5 μs, $\tau_{B,shadowing}$ = 102.49 μs, $\tau_{srp,shadowing}$ = 0.173 μs, $d_{srp,shadowing}$ = 30.72 km	$\Delta\tau_{srp,shadowing,indoor}$ = 0.086 μs, $\Delta r_{srp,shadowing} \leq x_{indoorR}$	$L_{shadowing,outdoor}$ = 289.26 dB; $PL_{HAPS,FSL}$ = 127.4 dB, $PL_{S,Terrestrial}$ = 156.87 dB, $PL_{Terrestrial,foliage}$ = 5 dB (g = 0.2 dB/m, l = 5m , n = 5)
$L_{I,NI}$ = 10 dB, $L'_{I,GI}$ = 6 dB, $L_{I,VW}$ = 7.8 dB, $n_{I,VW}$ = 4	L_{indoor} = 47.20 dB, L_{BPL} = 16 dB	$L_{shadowing,total}$ = 336.46 dB	
Parameters, Indoors (multipath case 1)			
$A_{tss,indoor}$ = 100% (shadowing time percentage)	$\mu_{LN,indoor}$ = -(6.1 dB/floor * n_{floor}) / ($n_{floor,total}$-n_{floor})) (Mean power relative to LOS under shadowing condition)	$\sigma_{LN,indoor}$ = 9 dB (standard deviation of log-normal fading)	flag_indoor = (1) two-paths (multipath) coefficient fading
$MP_{1,indoor}$ = -25 dB ($f_{D,max} \approx 0.2$ Hz), $MP_{2,indoor}$ = -39 dB ($f_{D,max} \approx 0.5$ Hz), i = 2 taps,	flag_room = (1) with an exponential function, 19.3 ns in average rms delay spread, standard deviation of 3.4 dB, small rooms; (2) with an exponential function, 27.7 ns in average rms delay spread, standard deviation of 4.1 dB, open environment; (3) with an exponential function, 67.4 ns in average rms delay spread, standard deviation of 4.3 dB, large environment.		
Parameters, Indoors (multipath case 2)			
$A_{tss,indoor}$ = 100% (shadowing time percentage)	$\mu_{LN,indoor}$ = -(6.1 dB/floor * n_{floor}) / ($n_{floor,total}$-n_{floor})) (Mean power relative to LOS under shadowing condition)	$\sigma_{LN,indoor}$ = 9 dB (standard deviation of log-normal fading)	flag_indoor = (2) multipath clustering >2 WSSUS TDL FPF fading model
PDc = 20 ns, PDr = 60 ns, $Sp_{c,indoor}$ = 23.90 dB/μs, $Sp_{r,indoor}$ = 71 dB/μs	$\Delta\tau_{i,indoor}$ = 0.05 μs (equally WSSUS spaced-TDL model), $\Delta\tau_{specular,indoor}$ = 0.1 μs (arrival time delay of the specular ray with diffuse component)	$MP_{cluster1}$ = -45 dB (room type 1), $MP_{cluster1}$ = -65 dB (room type 2 & 3), $MP_{cluster2}$ = -60 dB (room type 1), $MP_{cluster2}$ = -80 dB (room type 2 & 3),	$MP_{TDL,1}$ = -42.87 dB (room type 1), $MP_{TDL,2}$ = -38.95 dB (room type 1), $MP_{TDL,3}$ = -34.23 dB (room type 1), $MP_{TDL,4}$ = -98.94 dB (room type 1)
A_0 = -22.5 dB (level power of the direct-signal room type 1), A_0 = -32.5 dB (level power of the direct-signal room type 2 & 3)	A_1 = -30 dB (level power of the direct-signal room type 1), A_1 = -40 dB (level power of the direct-signal room type 2 & 3)	flag_room = (1) with an exponential function, 19.3 ns in average rms delay spread, standard deviation of 3.4 dB, small rooms; (2) with an exponential function, 27.7 ns in average rms delay spread, standard deviation of 4.1 dB, open environment; (3) with an exponential function, 67.4 ns in average rms delay spread, standard deviation of 4.3 dB, large environment	

The channel characteristic cases in Table 4.3 and Table 4.4 are having in importance the following considerations.

The parameters used in simulations were divided into the correct cases at their specific environment radio transmission. Concerning the long-term fading at the direct-path situation, this was related to the usage of a direct-ray and a reflected ray (possible diffracted ray), with the case of having an azimuthal angle approximated to zero. At the shadowing channel state, a first case was standing for the use of a direct plus diffracted plus probable multiple side-reflections (discarding the multiple screen-diffraction rays) and, a second case was referred to the diffracted ray plus the diffracted reflected ray. All latter cases are referring to the outdoors block; at indoors, the building loss path was available and regarded in addition to the outdoors loss.

At the short-term outdoor fading, the rays of multipath were concerning to the direct-ray and specular ray (not diffracted) for the diffuse components; at indoors were contemplated the two possible cases presented at the building interiors corresponding to the two-tapped delay case and the clustering multipath occurrence.

The elevation angle was always considered at 43º and referenced to the predominant ray.

4.2. Performance evaluation: Results

The established goal of having the HAPS-based system evaluation, according to the IEEE 802.16-2009 OFDM PHY-layer, is presented with its proper outcome and discussion. The adequate simulation preparation was chosen in the last subchapter for providing the framework of such system testing. The HAPS-based communication system's functionality supported by the software-aided operations is performed, and the goal for this performance evaluation is accomplished by the BER vs. E_b/N_0 plot line.

At the first point, the PHY-layer setup for the OFDM-based transmission has concerned with the WirelessMAN 256-OFDM parameters (Figure 4.4).

Next, for the fixed terminal case, the Doppler PSD was mainly distributed around 0 Hz.

The coherence bandwidth $BW_{coherence}$ and coherence time $T_{coherence}$ of the channel were evaluated to allow the prediction of fading affecting the transmission link, being frequency selective ($BW_{coherence}<BW$), and flat ($BW_{coherence}>\Delta F$) on each subcarrier. The evaluation of $T_{coherence}$ was compared to the OFDM symbol duration and long enough in the order of

microseconds; the HAPS-to-user link was experiencing slow fading ($T_{coherence}>T$). The HAPS-channel was established frequency nonselective at each subcarrier when proper minimum $BW_{coherence}$ approximation equalled the inverse of the maximum delay spread τ_m at least 10 times higher than the bandwidth of a single subcarrier ($BW_{coherence} \geq 10 \cdot \Delta F$); i.e., $BW_{coherence}$ = 833.33 kHz was greater than ΔF using BW = 1.25, 5, and 10 MHz, but becoming selective in frequency for the BW = 20 MHz case.

The maximum transmission bit rate R_b, or link speed, was corresponding as showed in Table 4.5 for the values of BW = 5, 10, 20 MHz —at other higher bandwidth, the system was experiencing a plausible ISI phenomena—. The approximation to the quality values from the bandwidth efficiency parameter η was obtained and showed in Table 4.6.

TABLE 4.5. TRANSMISSION DATA RATES

M-QAM and R_C	*Data rate, R_b [Mbps]*	*M-QAM and R_C*	*Data rate, R_b [Mbps]*
BW=5 MHz	***T_s = 56.14 µs (CP = 1/4)***	16QAM ¾	20.52 *(CP=1/4)*
	T_s = 46.32 µs (CP = 1/32)		24.87 *(CP=1/32)*
QAM ½	3.42 *(CP=1/4)*	64QAM ⅔	27.36 *(CP=1/4)*
	4.14 *(CP=1/32)*		33.16 *(CP=1/32)*
QAM ¾	5.13 *(CP=1/4)*	64QAM ¾	30.78 *(CP=1/4)*
	6.21 *(CP=1/32)*		37.30 *(CP=1/32)*
16QAM ½	6.84 *(CP=1/4)*	***BW=20 MHz***	***T_s = 14.04 µs (CP = 1/4)***
	8.29 *(CP=1/32)*		***T_s = 11.58 µs (CP=1/32)***
16QAM ¾	10.26 *(CP=1/4)*	QAM ½	18.23 *(CP=1/4)*
	12.43 *(CP=1/32)*		22.10 *(CP=1/32)*
64QAM ⅔	13.68 *(CP=1/4)*	QAM ¾	20.51 *(CP=1/4)*
	16.58 *(CP=1/32)*		24.87 *(CP=1/32)*
64QAM ¾	15.39 *(CP=1/4)*	16QAM ½	36.46 *(CP=1/4)*
	18.65 *(CP=1/32)*		44.21 *(CP=1/32)*
BW=10 MHz	***T_s = 28.07 µs (CP = 1/4)***	16QAM ¾	41.02 *(CP=1/4)*
	T_s = 23.16 µs (CP = 1/32)		49.74 *(CP=1/32)*
QAM ½	9.12 *(CP=1/4)*	64QAM ⅔	54.70 *(CP=1/4)*
	11.05 *(CP=1/32)*		66.32 *(CP=1/32)*
QAM ¾	10.26 *(CP=1/4)*	64QAM ¾	61.53 *(CP=1/4)*
	12.43 *(CP=1/32)*		74.61 *(CP=1/32)*
16QAM ½	18.24 *(CP=1/4)*		
	22.10 *(CP=1/32)*		

And, the system's performance evaluation was fulfilled by the execution of the Matlab®-based programming tool (Heiskala & Terry, 2002), (Aragón-Zavala *et al.*, 2008), (Pérez Fontán & Mariño Espiñeira, 2008), (Batlles, 2008). Results are presented through Figure 4.14 to Figure 4.21.

TABLE 4.6. SPECTRAL EFFICIENCIES

M-QAM and R_C	*Spectral efficiency, η*	*M-QAM and R_C*	*Spectral efficiency, η*
5 MHz	***T_s = 56.14 (CP = 1/4)*** ***T_s = 46.32 (CP = 1/32)***	16QAM ¾	2.05 *(CP=1/4)* 2.48 *(CP=1/32)*
QAM ½	0.68 *(CP=1/4)* 0.82 *(CP=1/32)*	64QAM ⅔	2.73 *(CP=1/4)* 3.31 *(CP=1/32)*
QAM ¾	1.02 *(CP=1/4)* 1.24 *(CP=1/32)*	64QAM ¾	3.07 *(CP=1/4)* 3.73 *(CP=1/32)*
16QAM ½	1.36 *(CP=1/4)* 1.65 *(CP=1/32)*	***20 MHz***	***T_s = 14.04 (CP = 1/4)*** ***T_s = 11.58 (CP=1/32)***
16QAM ¾	2.05 *(CP=1/4)* 2.48 *(CP=1/32)*	QAM ½	0.91 *(CP=1/4)* 1.10 *(CP=1/32)*
64QAM ⅔	2.73 *(CP=1/4)* 3.31 *(CP=1/32)*	QAM ¾	1.02 *(CP=1/4)* 1.24 *(CP=1/32)*
64QAM ¾	3.07 *(CP=1/4)* 3.73 *(CP=1/32)*	16QAM ½	1.82 *(CP=1/4)* 2.21 *(CP=1/32)*
10 MHz	***T_s = 28.07 (CP = 1/4)*** ***T_s = 23.16 (CP = 1/32)***	16QAM ¾	2.05 *(CP=1/4)* 2.48 *(CP=1/32)*
QAM ½	0.91 *(CP=1/4)* 1.10 *(CP=1/32)*	64QAM ⅔	2.73 *(CP=1/4)* 3.31 *(CP=1/32)*
QAM ¾	1.02 *(CP=1/4)* 1.24 *(CP=1/32)*	64QAM ¾	3.07 *(CP=1/4)* 3.73 *(CP=1/32)*
16QAM ½	1.82 *(CP=1/4)* 2.27 *(CP=1/32)*		

Subsequently, it was considered the bit error rate (BER) as the number of bit errors occurred when accessing the radiocommunication system transmitting data from HAPS and being received at ground terminal; *e.g.*, if the radio link medium was good in a particular time and with high E_b/N_0, the BER would be very low. Hence, at the simulation-level the values of BER were deduced from the error number divided by the total number of bits sent. The energy per bit to noise power spectral density ratio was the other important parameter, with an essential role at the comparisons of the BER performance simulations for specific coding and modulation (*M*-QAM) variabilities.

Chiefly, plots are showing the comparisons of the two proposed channel states (and their channel modelling sub-cases) in which the radio communication system was carried out, with their mandatory parameter variations validated, i.e., channel bandwidth, cyclic prefix length, modulation and coding profiles.

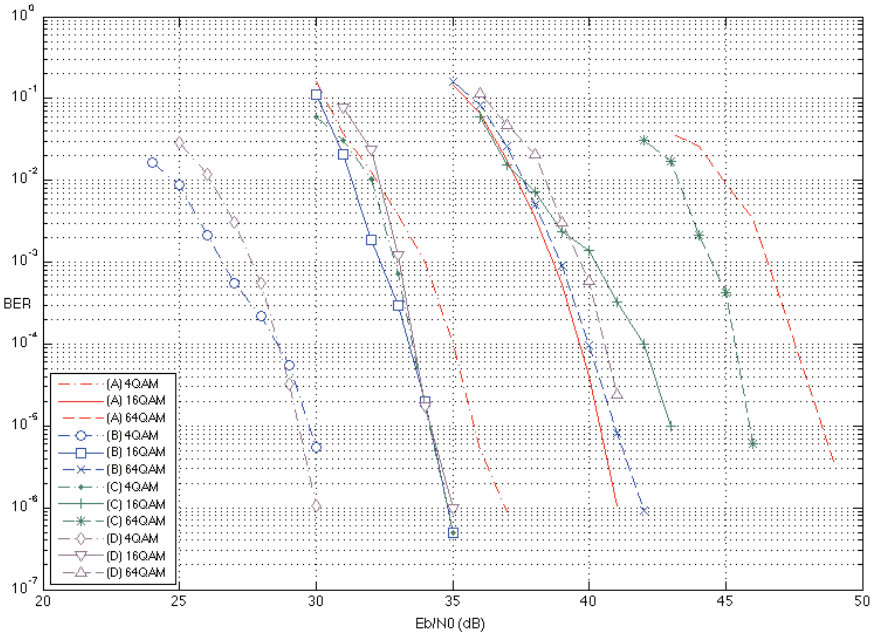

Figure 4.14. The HAPS-based system's performance evaluation at outdoor communications: (A) BW=10 MHz, CP=¼, shadowing version 2, R_c=½ & ⅔, (B) BW=10 MHz, CP=1/32, shadowing version 2, R_c=½ & ⅔, (C) BW=10 MHz, CP=¼, shadowing version 2, Rc=¾, (D) BW=10MHz, CP=1/32, shadowing version 2, R_c=¾.

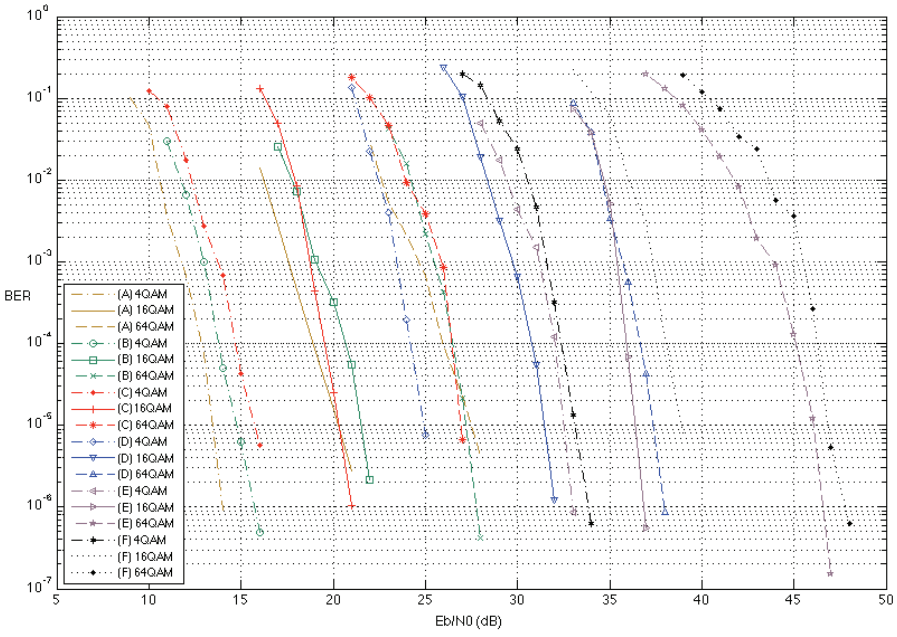

Figure 4.15. The HAPS-based system's performance evaluation at outdoor communications: (A) BW=5 MHz, CP=⅛, LOS version 2, R_c=½ & ⅔, (B) BW=10 MHz, CP=⅛, LOS version 2, R_c=½ & ⅔, (C) BW=20 MHz, CP=⅛, LOS version 2, R_c=½ & ⅔, (D) BW=5 MHz, CP=⅛, shadowing version 1, R_c=½ & ⅔, (E) BW=10 MHz, CP=⅛, shadowing version 1, R_c=½ & ⅔, (F) BW=20 MHz, CP=⅛, shadowing version 1, Rc=½ & ⅔.

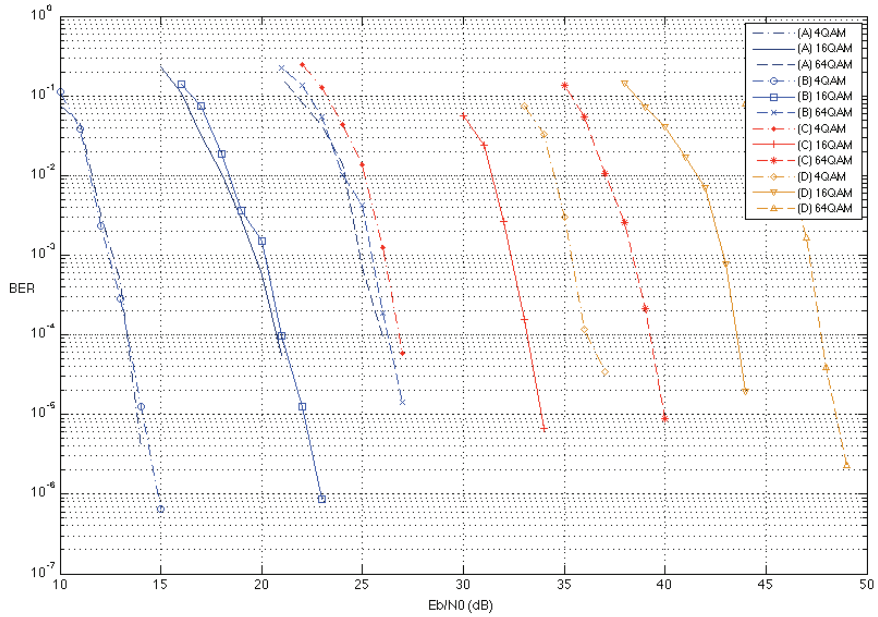

Figure 4.16. The HAPS-based system's performance evaluation at outdoor communications: (A) BW=10 MHz, CP=⅛, LOS version 1, R_c=¾, (B) BW=10 MHz, CP=⅛, LOS version 2, R_c=¾, (C) BW=10 MHz, CP=⅛, shadowing version 1, R_c=¾, (D) BW=10 MHz, CP=⅛, shadowing version 2, Rc=¾.

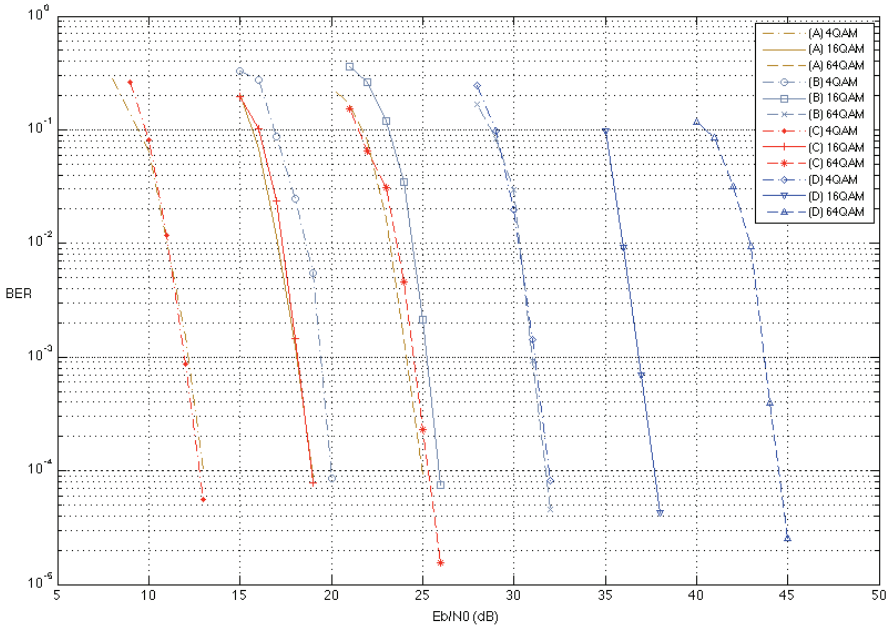

Figure 4.17. The HAPS-based system's performance evaluation at outdoor communications: (A) BW=1.25 MHz, CP=¼, LOS version 2, R_c=½ & ⅔, (B) BW=1.25 MHz, CP=¼, shadowing version 2, R_c=½ & ⅔, (C) BW=28 MHz, CP=¼, LOS version 2, R_c=½ & ⅔, (D) BW=28 MHz, CP=¼, shadowing version 2, R_c=½ & ⅔.

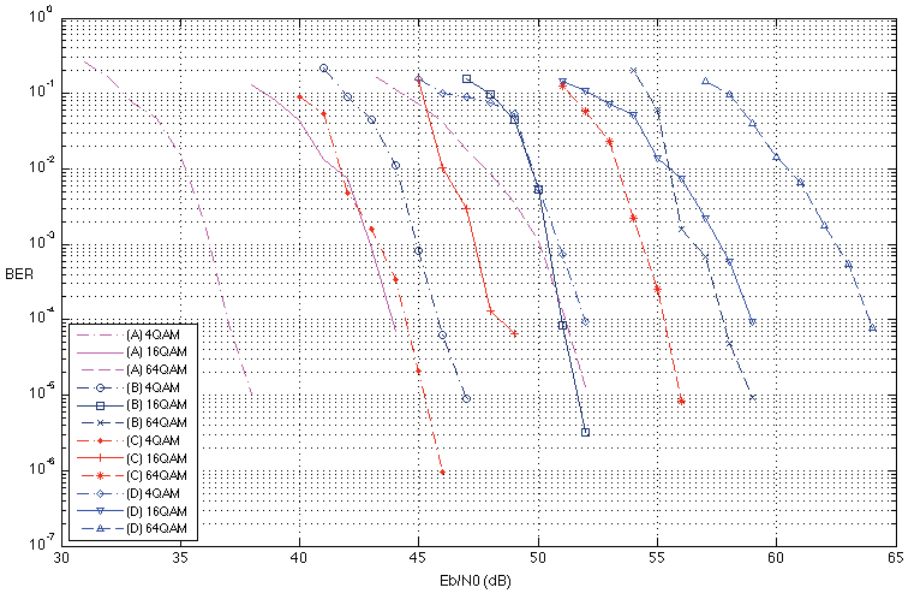

Figure 4.18. The HAPS-based system's performance evaluation at outdoor-to-indoor communications: (A) BW=10 MHz, CP=¼, shadowing path, R_c=½ & ⅔, (B) BW=10 MHz, CP=1/32, shadowing path, R_c=½ & ⅔, (C) BW=10 MHz, CP=¼, shadowing path, R_c=¾, (D) BW=10 MHz, CP=1/32, shadowing path, R_c=¾.

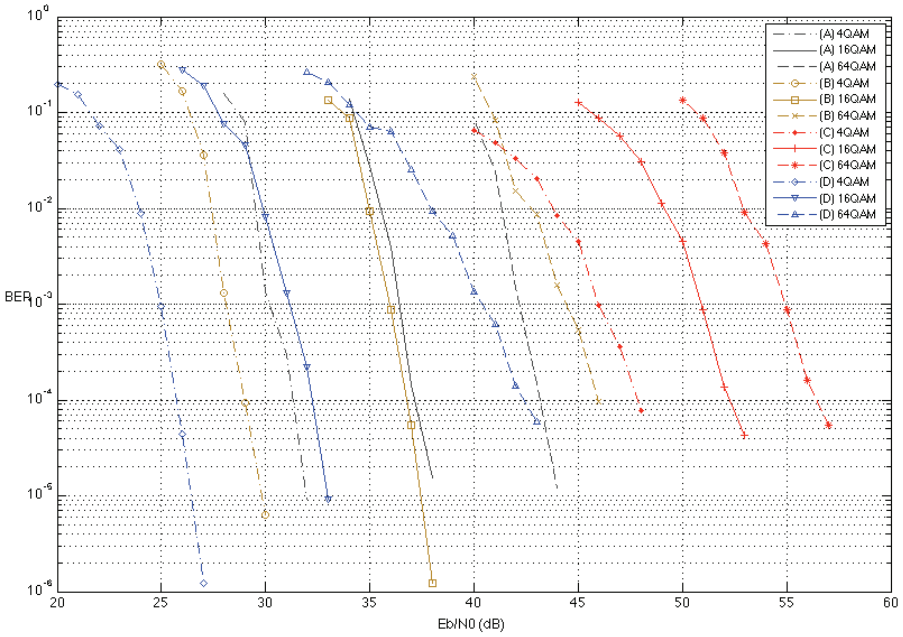

Figure 4.19. The HAPS-based system's performance evaluation at outdoor-to-indoor communications: (A) BW=20 MHz, CP=¼, LOS path, R_c=½ & ⅔, (B) BW=20 MHz, CP=1/32, LOS path, R_c=½ & ⅔, (C) BW=20 MHz, CP=¼, LOS path, R_c=¾, (D) BW=20 MHz, CP=1/32, LOS path, R_c=¾.

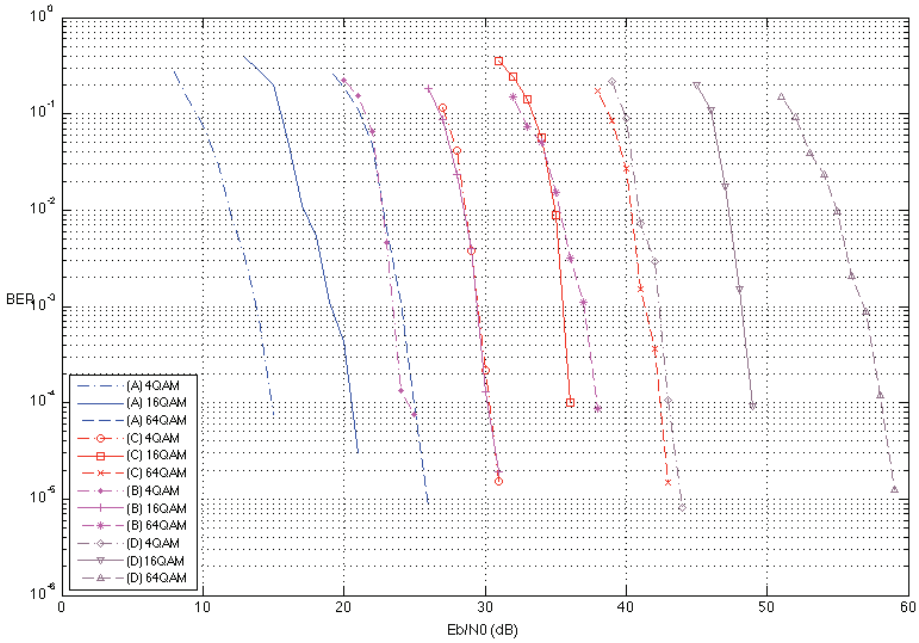

Figure 4.20. The HAPS-based system's performance evaluation at outdoor-to-indoor communications: (A) BW=1.25 MHz, CP=¼, LOS path, R_c=½ & ⅔, (B) BW=1.25 MHz, CP=¼, shadowing path, R_c=½ & ⅔, (C) BW=28 MHz, CP=¼, LOS path, R_c=¾, (D) BW=28 MHz, CP=¼, shadowing path, R_c=¾.

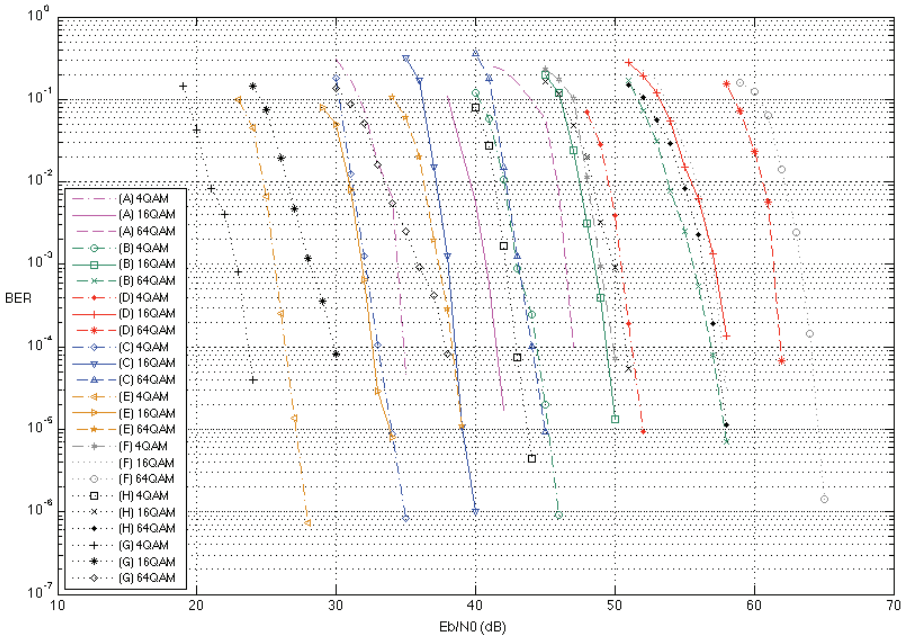

Figure 4.21. The HAPS-based system's performance evaluation at outdoor-to-indoor communications with alternative simulation values: x_{BB}=25 m, n_{floor}=8 m, h_{floor}=24 m, $x_{indoorL}$=5 m, $x_{indoorR}$=15 m, flag_room=1, flag_indoor=2, BW=10 MHz, (A) CP=¼, LOS path, R_c=½ & ⅔, (B) CP=¼, shadowing path, R_c=½ & ⅔, (C) CP=¼, LOS path, R_c=¾, (D) CP=¼, shadowing path, R_c=¾, (E) CP=1/32, LOS path, R_c=¾, (F) CP=1/32, shadowing path, R_c=¾, (G) CP=1/32, LOS path, R_c=½ & ⅔, (H) CP=1/32, shadowing path, R_c=½ & ⅔.

The results through simulation plots for the stratospheric channel approximation are exposed, and the trends of the received signal quality can be given as the different parameters were varying.

Observing at a glance the variations of the system's performance, the system can be defined operable to offer broadband communication access. Simulations can show that long- and short-term fading were behaving as the described hypotheses and expectations for such channel conditions; the supposition of a better system performance outcome for the HAPS-based broadband transmission scheme was confirmed since the OFDM multicarrier technique helped conveniently for the studied case of a time-variant channel, *e.g.*, in Figure 4.17 (outdoor case) and Figure 4.20 (outdoor-indoor case).

The time-variations of the established HAPS communication scenario were originated from two main channel variations and were influencing the performance outcome. As a reminder, firstly, the variations of the local mean due to shadowing effects of the surrounding environment, and secondly, the short-term variations due to multipath was superimposed to the first ones; thus, concerning such effects for the wireless propagation transmission no only direct-path appeared but also shadowing/blockage conditions were exhibited for the worse case at the system's performance.

The environmental situations (state-oriented channel modelling) have been applied to predict the median field strength and fading over the received signal with enough accuracy, the prevention from and counteracting against the signal variations were founded convenient to settle the performance behaviour of the overall HAPS-based system.

Therefore, Rice fading characterisation has dominated the direct signal (mainly in Figure 4.19), and the shadowing conditions caused fairly shallow fades (mainly in Figure 4.14, Figure 4.18): the severity of corruption was smaller at the LOS-state channel modelling than in the shadowing one. The level of fading (LOS or shadowing signal power) was attributed to the overall variations of parameters used in the system, not to the Doppler effect merely, which was reasonably small for the fixed terminals' deployment.

Referring to the outdoor-indoor transmission issue, the built-up environment was concerning of great influence on performance due to the new impairment issues of visibility, building height, vegetation, and structure material, originating lower performance (Figure 4.18 to Figure 4.21) and with a lowest one if specified parameters such as low code rate, low cyclic prefix ratio, and high nominal bandwidth were used (Figure 4.19 and Figure 4.20). Hence,

complete calculations for the outdoor-indoor case are showing that the performance was better at the direct (or QLOS-path) due to less impact from the building structure (Figure 4.19 to Figure 4.21). The experience of having a worse performance outcome than in outdoors for the shadowing case was assured, where even more the received signal was worse influenced by the floor height (the worst situation if closer to the first floor) plus the remaining variable issues at the indoor transmission situation (the worst situation if larger and deeper room from the illuminated wall) (Figure 19 to Figure 21, and specific case at Figure 18).

Generally, when the direct path channel situation was absent, the decreasing of performance was visibly related to a higher E_b/N_0 for obtaining less errors, and an irreducible error floor was presented due to the conditions at the transmitted signal strongly distorted by those from Rayleigh fading and shadowing.

The Doppler effect did not distort the orthogonality between subcarriers in the frequency-domain, although the nature of wind speed and traffic density have produced some Doppler spread over the transmitted signal spectrum —with no motion at both ends of communication—. The robustness performance at the HAPS system governed adequately due to the spectral efficiency and due to the resistance to the small Doppler shifts experienced in the fixed terrestrial end-users. The latest has been assured due to the fact that all multipath coming from the HAPS can demonstrate same Doppler shift at such relatively high altitude of 21 km above ground. In addition, the quasi-static HAPS assumption made the multipath to be assumed with small Doppler shifts.

At the time-domain, the received signal envelope was fluctuating along with the phase rotations, which could create additional errors in the multicarrier demodulation process, but the interleaver/deinterleaver have provided frequency-diversity improving the system performance at the possibilities of time-selective fading channel situation.

Additionally, the severity order of the corrupted channel can be understood by considering the tap-power and delays of the assumed broadband channel model. The assumed model had arrivals at receiver no longer than 1.2 μs (referring to the outdoor case, at indoors the values were becoming less severe), which corresponded to the last received random echo at its respective tap and so dominating and determining the order of corruption severity.

The performance influence from the nominal bandwidth *BW* was further applied (Figure 4.15, Figure 4.17, Figure 4.19, and Figure 4.20): most of the higher values (*BW*>10 MHz) take less improvement on the system performance than having fewer values (1.25 or 5 MHz) where also a major delay-spread or channel condition was supported; the worst performance

case has corresponded to have BW=28 MHz (T_b=8.02 μs, ΔF=124.68 kHz) in which the system was able to present a no confident operational system dependent on the variables presented in the overall system, *e.g.*, CP or coding rate value use.

In the next topic, the COFDM system was stating to combat the ISI, and so has reduced the ICI in the system. Besides, some drawbacks from the COFDM implementation could be about appeared in the system. This is described by the situation where the timing and frequency offsets can cause the system to be sensitive if incorrect demodulation of the OFDM signal at reception appeared and so presenting high offset issues.

The guard interval added to the transmitted signal was revealing that can help against frequency selectivity, however not really useful saving frequency spectrum at other times when waste of system's resources were highly noticed (Figure 4.14, Figure 4.18, and Figure 4.19).

Further observations are made concerning the FEC coding effects. The size of the FEC coding was selected in order to counteract the effects of multipath fading and with the possibilities of no wasting great part of the system resources. Hence, concerning the values being low at the nominal bandwidth and at the modulation-coding scheme, not only a better performance was obtained (less errors with low E_b/N_0) but also with some unsatisfactory outcome; comparisons can be seen in Figure 4.14, Figure 4.18, Figure 4.19, and Figure 4.21.

The statistical channel coding variations in the HAPS channel model have had a clear improvement keeping up a correspondence to the FEC coding and OFDM. Plots for the mandatory modulation and coding profiles were presented gaining approximately 5 dB between each modulation scheme of 4QAM, 16QAM, and 64QAM. Each modulation case had its own dissimilarities and performs in different manner. For instance, the higher modulation scheme (64QAM) was not presenting high robustness but carrying high data rate, and on the opposite side the lower modulation scheme (QPSK) was more robust but carried lower data rate. As expected, BER performance using 64QAM was having the worst outcome under worst channel conditions, but handling with the highest spectral efficiency. At less levels of constellation mapping, we had the opposite effects, i.e., with QPSK we had fewer errors but less save of spectrum (a situation recommended for a larger link or coverage distance from HAPS to receiver). On the other hand, plots showed performance improvements with higher code rates undergoing shadowing situation and with no improvements for smaller code rate values, but in an opposite effect if the direct-path situation was presented. Hence, the variabil-

ity of size for the FEC coding, as already mentioned previously, was appropriate to counteract the effects of multipath fading and/or not with a great part of the system resources.

As a reminder, in this work the variable values in the simulation realised for *M*-QAM and RS-CC coding were manually varied, but possibly extended to the theory of a switching process depending on the channel estimation tasks. The selection of the appropriate modulation-coding scheme was applied to all subcarriers at the multicarrier scheme, and the adaptive modulator/demodulator synchronised via a return signalling link (for AMC) was not considered.

Using the IEEE Std 802.16^{TM}-2009 is instructing that a data preamble might be sent before each data transmission. Hence, a block-estimation type was regarded and two-pilot-symbols could exploit the fact of having a slow varying channel and only limited by noise. At receiver, perfect channel estimation and synchronisation were implemented in order to avoid the effect of any particular estimation method on the simulation results; even though, the insertion of pilot subcarriers in the transmitted OFDM symbols could make the HAPS system to use a possible comb-type estimator and develop a part of the simulator to implement such new feature; i.e., considering an OFDM symbol with BW = 5 MHz, the minimum frequency domain pilot tone period was equal to (48/256)*5x10^6 = 0.9375 MHz, and such frequency period corresponded to 1.06 μs which was the τ_m that this type of estimation could correct —with other bandwidth value of 10 MHz, the maximum correctable time-delay would be of 0.53 μs, and so forth.

Last but not least, the scheme used in the urban environment DL case has only concerned the 43º of elevation angle; specifically, the elevation angle has concerned to that angle formed by the signal coming from the HAPS to the ground terminal at *x*-axis (see Figure 3.3 or 3.4). If changes are had in the elevation angle lower or greater than 43º, the system surely undergo a worse performance (at lower angles) and better operations (at higher angles). Thus, the HAPS-based communication coverage zone is behaving different for each area case, and the system's performance must be evaluated for each one of their particular conditions related to a particular elevation angle; the latest particularities were not able to be performed in the present work.

5

Concluding Statements

5.1. A précis of the contributions

Nowadays, the tendency of networks converging to IP-based structures is being a main characterisation, hence last relationship can concern to the HAPS updating, influencing, and working together with the standardisations and regulatory bodies for broadband communications.

The main objective herein was the use of a profitable HAPS-based communication system integrated to the existing wireless broadband technologies, with a high performance and flexible communications payload.

Therefore, our acceptance to the IEEE 802.16 interface implementation in HAPS was established. The potential of the 802.16-HAPS architecture has been verified suggesting such analyses as a proficient broadband wireless communication system with prevision of providing LOS and NLOS coverage within the IMT-2000 and IMT-Advanced radio-technology assistance. Specifically, the HAPS-based system was based on the multicarrier technology proposed in the IEEE Std 802.16-2009 being at lower frequencies of L-band (1-2 GHz), chiefly, and possibly extended to S-band (2-4 GHz); the overall system was following a standardised functional limit for pragmatic applications.

A summary and conclusions of the fulfilled simulation-based system's results and optimisation are following expressed:

- The demands of high-data rates were affordable and the expectation of use of civil broadband wireless communications to outdoors/indoors via HAPS-network was assessed. A proper real HAPS-model approximation was thought for expecting a technology to address a suitable complement to the “last mile” issue in terrestrial network deployment.
- The contributions to the stratospheric channel modelling and performance estimations of the HAPS-based system to a regulatory tendency in the IEEE and ITU-R were collected.
- The full stratospheric channel model process for performance analysis was described by the cascade sequence of HAPS, terrestrial and indoor blocks. At the outdoor stage, the statistical-physical channel was derived from geometrical operating urban scenario presented with diffraction and reflection ray theory. The built-up outdoor and indoor structures were determined with estimates from satellite-based empirical models (LMSS) experiencing similar angle of arrivals, and mid- and short-term characterisations.
- The improvement of HAPS’ PHY-layer performance at elevation angles of 43º into a wide-distance (metropolitan) coverage was accessible. The representation of the stratospheric propagation channel design was defined essentially by the conditions of path-loss and multipath, and certainly adequate. The impairments at carrier frequency of 1.820GHz were determined by the propagation conditions where large-scale effect had the main influence from issues of the urban environments; the degree of shadowing was dependent on the elevation angle and, if the elevation angle were smaller than the considered one, it could cause higher order of shadowing in the time of connection. On the other matter, for the spatial characteristics counting for the fading process (in such dense urban scenario), the specular reflections and scattering were in high presence due to building surfaces smooth enough to generate multipath fading effect.
- The environmental situations encountered for the HAPS-to-ground transmission were described by a first channel state referring to the line-of-sight (LOS) path existence, and a second state following the shadowing condition. The received signal was stated with a significant portion of the total signal energy received as a direct or diffracted wave, and the remaining power was determined by a specular wave, plus randomly scattered rays that constituted the diffuse wave. The indoor transmission block op-

eration was additionally based on the practical fact that indoors had the predominant parameters of building penetration, wall material, angle of incidence, floor height, position in the room, and indoor fading; all last denoting additional loss and delay spread impairments undergoing different link states such as obscured-LOS, non-LOS, and hard-NLOS cases.

- The research purposes were produced in order to have a channel modelling via simulations from specific urban scenarios and using frequencies near to the regulations of IMT-2000's 2 GHz. The feasibility of this variable establishments was to have an adaptable channel to new scenarios or the reaction to an expected link situation and transitions between them, all predicted without the need of extensive measurement campaigns and with very limited laboratory tools.
- Performance results fulfilled the evaluation suit (BER vs. E_b/N_0 outcome) to show the possibilities of overcoming the presented urban propagation impairment effects. The simulated variances at the IEEE standard and outdoor/indoor facts, plus the channel state conditions, were confronting the fine representation of the total transmission variations and loss considerations.
- The plots were used to accomplish the viability with standardisation for a comprehensive performance evaluation of the next-generation wireless technology use: the HAPS-based system for (fixed) broadband access communications under specific environmental conditions estimated and modelled by the stratospheric channel approach.
- According to our simulation results, estimating and alleviating the propagation impairments suffered at the transmitted information signal in the urban conditions, it was able to improve and complement the wireless capacities with the HAPS-capabilities. Such requirements for HAPS-utilisation counted into a variable bandwidth, coding and modulation, among other variables, intending for a direct candidate of a flexible HAPS-based system at real environment-based channel conditions. Hence, the simulated implementation of two state-oriented channel modelling was accepted: long- and short-term approaches were well compared to each other demonstrating their 'good' and 'bad' channel situations. However, the range of coverage for indoor terminals were definitively lower than those in the outdoor case, where as high as 50% performance reduction could be obtained.

- The on-board HAPS payload and adaptive-to-environment concatenated coding and modulation solution, all suggested the offer of flexibility required by the transmission system for a broadband communication service deployment. In our case, the adaptive coded modulation techniques used were dependent on the low or high population, building structures, and/or tree obstacles.
- The reliability to the spectral-efficiency and system robustness was obtained. The IEEE's radio-interface for the HAPS approach has supported modulation and coding established for management and abled to significantly improve system's performance with respect to standard solutions. Regarding to simulation results, the design of a suitable coverage area was carefully operative to the requirement in HAPS of adaptive high-gain coding and modulation schemes. The potential of suitable adaptive schemes, targeting the fixed operating scenarios, were representing a close counterpart of requirements for delivering efficiently high-data rate services from HAPS.
- Despite the fact that a strict level of refinement for the implemented HAPS-simulation model was regarded, it would be necessary further technology implementations but simply have not yet been matured enough and if existed would be a longer time development for a full technological demonstrator in a single step. The way ahead can demonstrate even more applications and deep maturity of HAPS for civil telecommunications, among other services; the HAPS-array will surely play a key complementary role in the future of fixed/mobile system networks in developed countries and also in ground infrastructure where is lacking or prohibited due to expensive implementation. In addition, studies of an improvement in indoor (hard) NLOS environments with feasible multiple antennas is needed for coming work, an analysis to compensate such moderate high mentioned degradation with diversity-space gains.
- Some disadvantages and practicalities to design the simulation-based model can be found on the choice of parameters from empirical data, which tend to arise approaches to the actual physical mechanisms; also, in the absence of enough good estimations and connections to such physical mechanisms, it would be difficult to regulate to the appropriate manner the parameters to the communication link scenarios for which measured data cannot be in hand.

5.2. Extensions of current work, future research

In the interim, the utilisation of standardisation together with the OFDM technique have accomplished for our research the enough requirements to realise a palpable, reliable, and robust communications, which has been based on a stratospheric platform for the metropolitan coverage area.

Regardless, other challenges involved in such deployment of HAPS-system solution can be inferred. A future work and further challenges should be overcome facing on fields of the HAPS-based broadband network with optional and more complex algorithms. Other advanced key challenges would involve the HAPS-system on the field of broadband wireless networks, *e.g.*, the use of optional features of the IEEE 802.16 specifications in order to face the enhancement of mobility in terrestrial terminals.

5.2.1. Broadband communications requirements

Today, upgrading a legacy of infrastructures and having the dynamism of new networks are primarily tasks on the telecommunications market. It is recognised the importance of broadband to unroll the next generation for on-line services and social potential from multi-platform access.

Broadband deployment must be facilitated in remote and rural areas, apart from the urban/suburban instances. The wide supply of broadband wireless services can be facilitated by a more efficient use of spectrum and an increase in its availability. Currently, with a rapid growth of interests on civil communications, market are being fuelled by the phenomenal growth in demand for Internet and multimedia traffics, which could be accompanied by progress in diverse platform developments, *e.g.*, stored and distributed from airships and unmanned aircraft vehicles. Hence, it is the time to look at the specific benefits of the HAPS-based technology exploring its synergy with the civil communications scenario.

As a BWA technology employment, a modified version of the IEEE 802.16 standards/ WiMAX (Worldwide Interoperability of Microwave Access), and the new possible standard technology IEEE 802.20 - Mobile Broadband Wireless Access (MBWA), could be studied for the HAPS-based communication system. Also, DVB (Digital Video Broadcasting with the DVB-S/S2, DVB-RCS, DVB-RCT, DVB-H, DVB-T formats, among others, might be used. Additionally, the choice of network protocols (such as TCP/IP, Wireless ATM, Wireless IP, and

HIPERACCESS protocols) should be made for the basis of network topologies and the integration with terrestrial and satellite networks.

In more details at HAPS implementations (WHAPS'05, 2005), IEEE 802.16 has been suggested and widely accepted to provide future broadband services and to operate in both licensed and unlicensed frequency bands, where substantial 802.16™ (WiMAX) systems will face coexistence with other systems.

For instance, a determined work has been carried out to illustrate the coexistence performance when HAPS and terrestrial WiMAX system coexist within the same coverage area (Bon-Jun *et al.*, 2008), (Jong-Min *et al.*, 2003), (Likitthanasate *et al.*, 2005), (Yang *et al.*, 2005). A low rate modulation scheme could be used and users could have a relatively narrow beamwidth receive antenna under 30º of the arrival angle: the coexistence capability degrades when the user antenna beamwidth increases or higher order modulation schemes are used. Respectively, the combination of high-speed mobility and platform movement can present a significant challenge in maintaining adequate communication links with high-speed vehicles (Capanina.org) making to require rapid and frequent handover between cells on the platform.

Routing in IP-based hybrid systems is another issue to deal with. For example, IP routing can pose new challenges over hybrid HAPS-satellite systems but many other problems can be simpler, outstanding the low propagation delay and reduced delay jitter. Multi-Protocol Label Switching (MPLS) has been designed to enable IP routing based on hard performance guarantees and may facilitate seamless integration of terrestrial, HAPS, and satellite systems (Karapantazis & Pavlidou, 2005). Also, transmission Control Protocol (TCP) can be designed to provide and assess a reliable end-to-end byte stream over an unreliable network.

Multicasting is also a deterministic application that HAPS-based systems are called to support. This could be supported via the widely used Internet Group Management Protocol; the main challenge is to develop efficient multicast protocols for adaptive systems rather than static links, which may be the case of HAPS-satellite crosslinks.

A new channel access technology for HAPS communication networks was studied (Karapantazis & Pavlidou, 2005) and called Space Division Multiple Access (SDMA); a novel Dynamic Broadband Multiple Access (DBMA) scheme, was developed at York University based on Packet Reservation Multiple Access (PRMA) schemes, which is intended for use in both terrestrial and high altitude platform networks and split the access channel into several virtual regions (VRs) for a particular service category.

5.2.2. Fixed broadband wireless access and backhauling

A working towards the HAPS modelling is being required to know deeply the facilities on sharing the introduction of HAPS as a support technology (*e.g.*, at WRC's agenda).

The operating at lower bands (L, S, C, X) is being deployed globally, in various regions in very dense deployments. Such frequency bands are important due to their low atmospheric absorption characteristics enabling implementation of communication links with a high degree of reliability, particularly in rainy geographic areas that count for severe fade conditions.

Hence, the right applications are becoming the provision of systems operating in the satellite services and have data backhauling, private communication networks, video broadcasting, disaster relief, telephony, communication links (local and national government agencies), etc. Particular deployment scenarios are needed when considering the HAPS-satellite (FSS, MSS) sharing operating characteristics (non and geostationary), and where also feeder downlinks/uplinks for such services should be protected. The use of feeder links can be considered part of regulated radio connections offered from HAPS complementary technology, and depending on their location, HAPS-based gateway stations can require wide coverage of the sky around the station location starting at low elevation angles. The support for user application can include duplex voice, simplex and duplex data and disaster relief, and first response of communications (telemetry, tracking, command and control information are related to HAPS-based gateway link). The support of backhaul connections could be deployed at environment requirements and sorted for all types of real-time multimode global-basis cellular networks and complex wireless multiprotocol networks, with great impact to the gateway data link.

Accordingly, the fixed broadband wireless access and backhauling for applications from HAPS can contemplate further essential advanced design of interference mitigation techniques, platform stabilities, onboard steerable beamforming antenna usage (or power flux density, pattern and boresight aspects), in order to add directivity, selectivity, and effectiveness for the gateway links. High link availability (99.999%), high bit rates (from 66 Mbps, for instance, with a minimum total system gateway bit rate capacity of 8 Gbps for high user traffic load), considerable frequency reuse, high spectral efficiency, and bit error rates of 10^{-9} are imperative for a gateway link and follow a high grade of service for the end user application and services provided.

Therefore, at fixed terminologies, many types of important social organisations, such as schools, hospitals, small-medium size businesses around the world, can be benefitted from the broadband services provided by the HAPS-based network. The gateway to the HAPS network can provide access to terrestrial telephony and to the Internet backbone for diverse services (i.e., world wide web and electronic commerce), providing the information content of a wide-access network to a large population of subscribers. The remarkable features can include a seamless ubiquitous multimedia service, adaptability to the end-user requirements in changeable environments, rapidly deployable to sites of opportunity, and bandwidth on demand from the available spectrum for efficient usage.

5.2.3. Mobile broadband wireless access

A direct perspective on next-generation mobile communications and services can be presented with the use of novel wireless communication technologies, including the HAPS employment. Herein, a vision for the convergence of fixed-mobile on next-generation communications can be exploited, where the HAPS-based communications can be incorporated.

Therefore, as a summary execution and referring to the next-generation mobile service definitions, the scenario-based analysis hierarchy of services is consisting of three main different service levels: the service areas, the service functionalities, and the service technologies (Ryu *et al.*, 2005). And, a conceptual reference network architecture (standing with characteristics of information and service flows) is being proposed focusing on the realisation of the service technologies where the HAPS-based system can be comprised: the network is divided into four different parts such as the user equipment and access part, the network service provisioning layer part, the network control layer part, and the non-mobile network operator service part. At this network architecture reference, the service elements, such as servers, processors, gateways, wireless technologies, can be placed in each network part to support the derived next-generation mobile services for a ubiquitous mobile life.

The mobile communications were evolving from the first-generation analogue systems to the second-generation systems. Now the third-generation (3G) IMT-2000 is providing a variety of services with almost the same quality as integrated service digital network (ISDN) services provided in the wired-network; and following, the next-generation mobile communications and services are being watched with keen interest.

ITU-R is proposing the concept of a mobile communication system beyond 3G with basic requirements of high data rate, multimode air interface, low cost, the use of IPv6, number portability, and the integration of wired and wireless communications. Accordingly, ITU-R is proposing the concepts of new radio interfaces and new usages of spectrum and bandwidth for systems beyond 3G that can support up to approximately 100 Mbps of data transmission speed for mobile access and approximately 1 Gbps for nomadic and local wireless access.

Therefore, next-generation mobile communication (or fourth generation, 4G) is a system able to provide a variety of multimedia services with high speed and high quality via the converged network of wireless and wired infrastructures. In order to support these newly introduced characteristics of next-generation services, several core technologies could be developed, including: OFDM (considered the strongest candidate for radio access), multi-input-multi-output (MIMO), and software defined radio (SDR), other related technologies, such as ad hoc networking, session initiation protocol (SIP)-based multimedia services, and all-IP-based networking, are also been required.

Nevertheless, next-generation mobile services have not yet been deeply actively studied, since there are no neat definitions of how next-generation mobile communications and its services will be developed.

5.2.4. MIMO and OFDMA concepts

An additional feature to the communication system can contain the adaptive arrays & space-time coding (STC), and STC may be used on the DL to provide second order (space) transmit diversity. There can be two transmit (Tx) antennas and two reception (Rx) antenna (Alamouti STC). This scheme requires Multiple Input Multiple Output (MIMO) channel estimation, and decoding is very similar to maximum ratio combining (MRC). For the STC insertion into the OFDM chain, each Tx antenna has its own OFDM chain and they should have the same local oscillator for synchronisation purposes. The benefits of adaptive arrays can be realised for both the upstream and downstream signals using retro directive beamforming concepts in TDD systems, and to some extent in FDD systems using channel estimation concepts.

The spatial diversity, or the employment of multiple antennas, can reduce the time-variations of wireless communication channels, i.e., for M_r antennas (at receiver) the distribu-

tion of the received power can migrate from an exponential (Rayleigh fading) to a χ^2 distribution with $2M_r$ degrees of freedom (Hutter, 2002). Hence, the antenna reception can be twofold: first, the mean signal can be increased by a factor M_r, and second, the variance of the amplitude variations can be decreased, representing the referred terms of antenna and diversity gains, respectively. Due to the mentioned actions, the required SNR for a specific QoS can be reduced with respect to the single antenna utilisation.

The reduction of time-variations is seeing as the reduction of the effective maximum Doppler frequency, and a longer OFDM symbol duration could be tolerated. With an increase number of antennas must be achieved any desired level of robustness against time-variations; however, the increase of antennas can saturate the communication system and is established that the first additional antennas are the most advantageous, whereas the benefit from further antennas will have lesser significant impact; a same performance gain can be achieved through transmit diversity as well as through the receive one. The transmit diversity implementation is advantageous in the asymmetric data traffic systems, where high-data rate has to be offered to the fixed/mobile terminal.

For the last-mentioned scenarios can be economically beneficial to implement multiple antenna arrays at the transmitter base side rather than at the numerous receiver devices, but with a penalty in training-overhead to estimate the channel association.

List of Appendices

Appendix A. The IEEE Std 802.16™ network scenario

This appendix serves as a guide to the steps towards the analysis of the HAPS communication system based on the operation in bands below 10 GHz. The operation in these bands has the expectations of implementing the multicarrier modulation, OFDM specifically, for data transmission, such as that proposed in the IEEE Std 802.16™ standard; in addition, the Worldwide Interoperability for Microwave Access (WiMAX) Forum, an industry-led non-profit corporation, promote and certify the compatibility and interoperability of broadband wireless products using the IEEE 802.16™ and ETSI HiperMAN specifications.

The 2-11 GHz bands provide a physical environment where due to the longer wavelength LOS is not necessary but multipath may be significant. While many technologies currently available for fixed broadband wireless can only provide line of sight (LOS) coverage, the technology behind the standard has been optimised to provide excellent non-line-of-sight (NLOS) coverage; some technologies may solve or mitigate the problems resulting from NLOS conditions: OFDM technology, sub-channellisation, directional antennas, transmit and receive diversity, adaptive modulation, error correction techniques, and power control.

For our concern, the IEEE Std 802.16™-2009 is an extension of the 802.16™ standard specifying the physical layer (PHY) of the air interface with interoperable point-to-multipoint (PMP) and optional mesh topology FBWA systems (access to data, video and voice services with a specified quality of service) in licensed and unlicensed spectrum from 2-11 GHz. This standard is suited to a particular operational environment, both in licensed bands, 3.5 GHz (non-US) and 2/2.5 GHz for public network access, and in license-exempt bands, 5.8 GHz. The nomenclature used in the various air-interface specifications and PHY compliance is summarised into the single-carrier (SC) modulation, 256-point transform OFDM, and 2048-point transform OFDMA. In our contribution, it is referred to the WirelessMAN-OFDM specification, or the so-called 256-point transform OFDM PHY air-interface, concerning an approximation to the lower licensed bands of 2/2.5 GHz.

Now, examining that high-data rate communications are limited not only by noise but also (especially at increasing symbol rates) more significantly by the intersymbol interference

(ISI) due to the memory of the dispersive wireless communications channel. The effects of de facto time-variant and time-dispersive channels on the transmitted subcarrier data symbols can be diverse. And, if the impulse response of the channel is longer than the duration of the OFDM guard interval, then energy might spill over between consecutive OFDM symbols, leading to inter-OFDM-symbol interference; hence, the length of the CP is generally chosen to be longer than the longest anticipated channel impulse response (CIR).

Analogously to the case of serial modems in narrowband fading channels, the amplitude and phase variations inflicted by the channel transfer function (CTF) upon the received symbols can severely affect the bit error probabilities, in which different modulation schemes are suffering different extents from the CTF effects, *e.g.*, coherent modulation schemes rely on the knowledge of the symbols' reference phase. Therefore, if specific modulation scheme is to be employed, then distortion has to be estimated and corrected. For multilevel modulation schemes (i.e., *M*-PSK or *M*-QAM) used within the standard (where the magnitude of the received symbol is bearing the information), the magnitude of the CTF is affecting at the demodulation; the performance of this system is depending on the quality of the channel estimation.

As long as the OFDM system was presenting a parallel transmission without ISI, the average BER performance plot of an OFDM system can have the same average BER performance of a single carrier modulation system over an AWGN channel; the evaluation of the propagation effects on the system at any other channel state condition can present an irreducible error floor in the *BER* vs. E_b/N_0 plot (our case study).

Since the stratospheric channel can be frequency selective within the whole bandwidth *BW*, by appropriately choosing N_{FFT} each subcarrier can be made frequency non-selective. The HAPS channel modelling is frequency non-selective at each subcarrier when *M*-QAM is chosen so that the minimum coherence bandwidth $BW_{coherence}$, which approximately equals the inverse of the maximum delay spread τ_m, at least 10 times higher than the bandwidth of a single subcarrier.

Appendix B. The OFDM utility alongside 802.16™ Evolution

The future trend in wireless communications is recalled that clearly have to satisfy the demands of high-data rates. Such vision is greatly of our interest for future wireless genera-

tion systems, in which the physical layer (PHY-layer) performance is dependent on the reliability of spectral efficiency and the variability of the scenarios.

It is well-known that establishing the required high-capacity wireless link will represent a variety of challenges, ranging from the variable propagation conditions (i.e., the presence of Doppler and multipath fading, the power efficiency of nonlinear amplifiers, and the synchronisation aspects) to the radio resource management issues (coping with the limited spectrum availability and the interference with other existing or foreseen services). Herein, examining some of those PHY-layer main challenges, and the signal transmission via wideband frequency-selective radio channel is foremost considered. At this requirement, the multicarrier modulation scheme is required for mitigating the frequency-selective effect and lessening the multipath fading, that is, to have the coherence bandwidth greater than the channel or subcarrier bandwidth.

The OFDM technology is a promising technique for achieving high-data rate and combating multipath fading in wireless communications. Using OFDM all the orthogonal carriers are transmitted simultaneously, and the entire allocated channel can be occupied by the aggregated sum of the narrow orthogonal subbands. By transmitting several symbols in parallel, the symbol duration can be increased proportionately, which can reduce the effects of ISI caused by the dispersive fading environment (Heiskala & Terry, 2002).

The principle of functionality in the multicarrier transmission is given by the computationally efficient fast Fourier transform (FFT) algorithm and its inverse (FFT^{-1}, or IFFT). At the transmitter, the FFT^{-1} converts the complex amplitudes of the individual subcarriers from frequency to time domain, whereas at the receiver the inverse operation is made. The input data are distributed into equidistant subcarriers (FFT-size), and the individual subcarriers are modulated with adaptive modulations. Each subcarrier is modulated with a smaller data rate compared to the input transforming the wideband frequency selective channel into narrowband flat channels. The output signals from the OFDM modulator conform to a multiplexed signal ready to be transmitted over the channel conditions; the multipath propagation presented in the HAPS channel impulse response (CIR) model may cause interblock interference (IBI), or intersymbol interference (ISI) that could lead to interference between the subcarriers —a cyclic prefix (CP) can be inserted prior to transmission to intend the mitigation of IBI, where the duration of the CP is chosen so that the delay-spread duration can occur before the selection of all samples of the FFT-window in the receiver.

At the receiver, therefore, the multicarrier signal is demodulated with respect to all subcarriers, the CP is removed before using the FFT modulation —the pilot-aided tones and block pilot-symbols can be considered in the transmitted signal to estimate the channel propagation effects and the channel effect can be undone by a frequency domain equaliser.

As a concise statement, the IEEE Std 802.16 has been designed to meet today's most promising challenges, such as the NLOS operation capability, the safe of high costs of the intensive labour deployment of cables, and the large coverage radii for a rapid deployable infrastructure network, that in our case could be able under the HAPS coverage area term.

Whence the use of the OFDM technique is a significant technology of implementation for the HAPS-based system performance. Our considered whole system contribution is including the COFDM scheme extended to the fixed wireless application into the HAPS-channel modelling scheme; as further research and details, other analyses and measurements based on this standard and on HAPS-structures were also studied (Ku *et al.*, 2003), (Yang *et al.*, 2005), (Likitthanasate *et al.*, 2005), (Yang *et al.*, 2007b), (Bon-Jun *et al.*, 2008), from which the respective consensus for HAPS regarding interoperability and spectrum harmonisation were considered.

The employment of multicarrier in HAPS-based system, moreover, can gather certain pros and cons:

❖ *Pros:* Can fight much better against multipath with less computational complexity and more robustness than other techniques, can permit portions of spectrum to be used to transmit data by different specifications, can divide the channels into narrow band flat fading sub-channels, a more resistance to frequency selective flat fading exists, easy to filter out noise, CP helps to overcome ISI and IBI, channel equalisation is simpler than in the single carrier channel, computational efficiency using FFT and IFFT, the system's performance degrade gracefully when the system delay reaches a highest limit, provides benefit of transmitting low power for low data rate users, narrowband interference can be reduced through spectral efficiency, suitable for coherent demodulation, accepts simultaneous low or high data rates for multiple users, provides different channel quality depending on the requirement and condition of the channel, frequency diversity gives efficient use of spectrum, time diversity for group-carrier is of interest, receiver simplicity can be provided by eliminating intra-cell interference, in fading environment BER performance tends to be lower, time and frequency synchronisation can give orthogonality, and a single frequency network coverage is possible.

❖ *Cons:* strong synchronisation is required between users and BS, OFDM technique uses pilot signals and data spectrum can be misspent for synchronisation purposes, very much sensitive to phase noise and frequency offset, delay in co-channel interference is more complex in OFDM, inefficient power consumption as FFT algorithm and FEC are constantly active, if very few data subcarriers are allotted to each symbol the diversity gain of OFDM and frequency selective fading might be vanished, much complex adaptive subcarrier channel assignment, complicate obtainment of fast power control system, prone to inter-channel interference, and requires high peak to average ration RF power amplifiers to avoid amplitude noise.

Appendix C. The 802.16™ embedment to the stratospheric propagation channel approach

According to the substantial evaluation of the downlink performance using the HAPS-communications channel, it must be required a fading mitigation technique to ensure the channel quality of being above a minimum level performance, i.e., in this present work is proposed the use of coded orthogonal frequency division multiplexing (COFDM) (Czylwik, 1998), (Falletti *et al.*, 2006) aiming the standardisation at ITU administration under the IMT-2000 and IEEE framework. In our case, the performance evaluation is being expressed in terms of the achievable bit error rate (BER) and able to carry broadband and other communications services at different information bit rates —adaptability of the system to on-demand circumstances.

The transceiver components for our system were built on the principles of COFDM (Czylwik, 1998), (Heiskala & Terry, 2002), and together with the IEEE standardisation (IEEE 802.16™, 2009), (Grønsund *et al.*, 2007), (Pedro-Eira & Rodrigues, 2009) are supporting us with a wide range of operating bandwidths to flexibly address the need of diverse spectrum allocation and application requirements.

Next points shortly describe the main endeavours of the main IEEE Std 802.16™-2009 blocks implemented:

❖ *Channel coding:* The channel coding stage included randomisation, coding and puncturing. The input data was randomised in order to avoid long runs of ones and zeros. The output of the data randomiser was encoded with a block of Reed-Solomon-Convolutional Coder (RS-CC); CC constraint length was 7, and its native code rate was ½.

The puncturing block punctured the output of the concatenated encoder to produce variable higher code rates.

❖ *Interleaving:* This block mapped adjacent encoded bits into separated subcarriers, thus minimising the impact of burst errors caused by spectral nulls.

❖ *Modulation:* The modulation block converted the sequence of interleaved bits into the sequence of complex symbols depending on the chosen modulation scheme *M*-QAM (BPSK, 4-QAM, 16-QAM, and 64-QAM).

❖ *Data mapping:* The data were mapped into blocks/frames.

❖ *Pilot insertion:* Pilots were inserted at this point. Moreover, at this stage all data symbols were mapped to the data region and their corresponding logical subcarriers.

❖ *IFFT:* The final stage converted the data into time domain for use at the radio front-end; a guard interval (*GI*) was inserted after this step.

Based on the supposed standard for channel bandwidth, the properties of the stratospheric channel contribution can be advantageously exploited to design a highly efficient OFDM system.

The OFDM-based structure can be mainly characterised by the FFT-size and guard intervals of variable duration being the inherent features of the multicarrier system. Hence, for the OFDM engineering the total available channel bandwidth *BW* was divided into a number of subcarriers. The data of a specific user was used to modulate all the subcarriers by considering quadrature modulations in our case. Afterwards, first applying IFFT to the modulated subcarriers and extending the IFFT output by a precursor signal of samples, which equals the last samples of the IFFT output plus the CP, produced the transmitted signal.

The language used in OFDM was very important, so it must be identified that the basic resource allocation quantum was a subcarrier or subchannel, which contained data carriers N_{used}. For all *FFT* sizes, each OFDM symbol carried an integer number of subchannels. The amount of data, which fitted into a subchannel, depends on the constellation and the coding method used within this subchannel. A two dimensional map, in which one dimension denotes subchannel within OFDM symbol (frequency domain) can visualise the available resource, and the other denoted the consecutive OFDM symbols (time domain) —herein, the data carriers together with the pilot, null, and DC carriers were considered and named subcarriers (belonging to the concept of N_{FFT}), otherwise it will be specified.

Therefore, four primitive parameters can characterise the OFDM symbol, some of them were already mentioned:

BW = nominal channel bandwidth

N_{used} = number of information carriers in the OFDM frame/symbol; it is obtained by subtracting guard and pilot subcarriers from N_{FFT} (including the DC subcarrier N_{DC})

n = sampling factor; this parameter, in conjunction with *BW* and N_{used} determines the subcarrier spacing and the useful symbol time

CP = the ratio of the cyclic prefix time to useful time, $CP = \frac{T_g}{T_b}$

From the last parameters, the following additional parameters can be derived:

N_{FFT} = number of allocated subcarriers. The smallest power of two greater than N_{used}

F_s = sampling frequency or rate, $F_s = \left(n \cdot BW / 8000 \right) \cdot 8000$

ΔF = subcarrier spacing, $\Delta F = \frac{1}{T_b} = \frac{F_s}{N_{FFT}}$

T_b = OFDM (useful) symbol time or FFT interval duration, $T_b = \frac{1}{\Delta F} = \frac{N_{FFT}}{F_s} = N_{FFT} \cdot T$

T_g = CP time with N_g samples, $T_g = CP \cdot T_b = N_g \cdot T$

T_s = (total) OFDM symbol time, $T_s = T_b + T_g = \left(1 + CP\right) \cdot T_b = \left(N_{FFT} + N_g\right) \cdot T$

T = sampling time or period (at multiples of *T*) of *m*-th OFDM symbol, $T = \frac{1}{F_s} = \frac{T_b}{N_{FFT}}$

M_{QAM} = number of bits for each symbol in the QAM constellation used to modulate the OFDM symbol

R_c = rate of the code used for the channel coding; in absence of code $R_c = 1$

$R_{b,raw}$ = raw bit rate, $R_{b,raw} = N_{used} \cdot M_{QAM} \cdot \frac{R_c}{T_b}$

where N_{data}, b, R_C, and T_s denote the number of assigned data subcarriers, the modulated bits per sub-carrier, the FEC coding rate, and the total OFDM symbol duration, respectively.

The spectral efficiency η (bps/Hz) can be evaluated by the following expression —the norm IEEE 802.16™ states to increase the spectral efficiency by avoiding some zero-carriers at the two sides of OFDM frame in the frequency domain

η = spectral efficiency (bps/Hz), $\eta = \frac{R_b}{BW}$,

and, $\eta = n \cdot \frac{\left(N_{used}+1\right)}{N_{FFT}} = \frac{F_s}{BW} \cdot \frac{\left(N_{used}+1\right)}{N_{FFT}} = \frac{\Delta F \cdot \left(N_{used}+1\right)}{BW}$

R_b = bit rate, $R_b = \frac{N_{bit}}{T_s}$

N_{bit} = number of bits transmitted per OFDM symbol, $N_{bit} = N_{used} \cdot M_{QAM}$

The bandwidth efficiency η is designed in (IEEE 802.16™, 2009) to be in the range of 83.95%, depending mainly on the FFT size, in order to occupy the maximum usable bandwidth and to allow an adequate RF filtering.

At next, the pseudo random binary sequence (PRBS) generator in usage was a 15-stage shift register with a generator polynomial $1+ X^{14}+X^{15}$. In the downlink mode (DL), the scrambler was re-initialised at the start of each frame with the sequence: 1 0 0 1 0 1 0 1 0 0 0 0 0 0 0.

The encoding was performed by first passing the data in block format through the RS encoder and then passing it through a zero-terminating convolutional encoder. The Reed-Solomon/Convolutional code (RS-CC) concatenation was described as in Table C.1.

A block interleaver interleaved all encoded data bits with a block size corresponding to the number of coded bits per the specified allocation, N_{cbps}.

The interleaver was defined by a two-step permutation. The first ensures that adjacent coded bits were mapped onto non-adjacent carriers. This ensured that if a deep fade affects a bit, its neighbouring bits were likely to remain unaffected by the fade, and therefore FEC was sufficient to correct the effects of the fade. The second permutation insured that adjacent coded bits were mapped alternately onto less or more significant bits of the constellation, thus avoiding long runs of lowly reliable bits and makes detection accurate.

TABLE C.1. MANDATORY CHANNEL CODING PER MODULATION.

Modulation	Uncoded block size (bytes)	Coded block size (bytes)	Overall coding rate	RS code	CC code rate
QPSK	24	48	1/2	(32,24,4)	2/3
QPSK	36	48	3/4	(40,36,2)	5/6
16-QAM	48	96	1/2	(64,48,8)	2/3
16-QAM	72	96	3/4	(80,72,4)	5/6
64-QAM	96	144	2/3	(108,96,6)	3/4
64-QAM	108	144	3/4	(120,108,6)	5/6

The modulation formats available for the OFDM system were BPSK, Gray-mapped QPSK, 16-QAM, and 64-QAM. The last constellations were normalised by multiplying the constellation point with the indicated factor κ to achieve equal average power.

The Gray-mapped data were then sent to IFFT for time-domain mapping, and this block delivered a vector of 256 elements, where each complex number represented one sample of the OFDM symbol; the FFT block was applied at receiver having the frequency representation of the *i*-th multipath as $A_i\delta\left(\tau-\tau_i\right)\rightarrow A_i e^{-j\omega\tau_i}$.

Now, the channel estimator was related to insert pilot tones in each of the OFDM symbols (comb-type channel estimation) at frequency-domain period of 48 (samples) and with minimum period of $N_{pilot\cdot per\cdot cylce}\cdot BW/N_{FFT}$, whose inverse stood for the maximum delay that this type of estimation could correct. Hence, the possibility of using LS (least square) estimation could be had; nevertheless, perfect channel estimation was considered. After estimating the channel, the received signal needed to be equalised. The CP was longer than the maximum delay, and the model referred to the effect of the channel as a complex multiplication in the frequency-domain; thus, the equalisation simplified to a complex division of the received signal by the perfect estimated channel. As a disadvantage, the use of such oversimplified model could be resulting in a considerably low performance.

Moreover, a data preamble was sent before each data transmission. This data preamble was constant and could be used at receiver as a pilot-OFDM-symbol —this block pattern led to excellent frequency resolution, but poor time resolution, however, time resolution was unimportant when our channel coherence time had high value.

If a frequency-subcarrier coincided with a channel null, then all the information carried by that subcarrier was lost. Hence, channel coding together with interleaving (and/or frequency hopping) was used to cope with the “bad subcarriers” in OFDM, or the so-called

coded OFDM (COFDM), which was variable for adaptive environment conditions at the price of a reduced bandwidth efficiency —*e.g.*, in a worst case, to correct L errors induced by channel zeros, a linear block code must have a minimum Hamming distance $d_{min} \geq 2L+1$, but for a block code with an input block of size k and an output block of size n, the Singleton bound can assert that $d_{min} \leq n-k+1$ and at least $n-k=2L$ redundant symbols must be transmitted, and if the length-L CP was inserted at the transmitter, a redundancy of at least $3L$ symbols was indispensable.

Now, the channel can be classified as rapidly time-varying due to CIR changing significantly over the duration of an OFDM symbol. At this situation, the frequency-domain transfer function is time-variant during the transmission of an OFDM symbol, and this time-varying frequency-domain transfer function is leading to the loss of orthogonality between the OFDM symbol's subcarriers. The amount of this inter-subcarrier interference is depending on the rate of change in the impulse response. The simplest environment to study the effects of rapidly time-varying channels can be the narrow-band channel, whose impulse response can consist of only one fading path: as the amplitude of this path is varying in time, then the received OFDM symbol's spectrum will be the original OFDM spectrum convolved with the spectrum of the channel variation during the transmission of the OFDM symbol; since this short-term channel spectrum is varying between different OFDM-transmission bursts, the effects of the time-varying narrowband channel have to be averaged over a high number of transmission bursts for the purpose of arriving at reliable performance estimates.

OFDM was the elective promising candidate for having the realisation of broadband wireless systems that by definition can transmit over frequency-selective and time-variant channels (Hutter, 2002). And, the design criterion of the OFDM symbol duration was related to the basic channel variables of maximum excess delay time and maximum Doppler frequency, reflecting the bandwidth efficiency and the robustness of the system.

Therefore, the time-domain convolution of the transmitted time-domain signal from HAPS with the CIR was corresponding simply to the multiplication of the spectrum of the signal with the channel's frequency-domain transfer function $H(f)$

$$e(t) * h(t) \leftrightarrow E(f) \cdot H(f), \tag{C.1}$$

where $H(f)$ is the Fourier transform of the impulse response $h(t)$.

And, the OFDM signal packet (Macedo & Sousa, 1997) being transmitted was represented by

$$e_k(t) = \sum_{m=0}^{M-1} e_m(t - mT_s) \tag{C.2}$$

where M is the number of symbols per packet with T_s being the total symbol duration composed by T_b plus time of the guard interval T_g; for instance, considering 256 subcarriers and transmitting four bits per symbol period (or per subcarrier), and if M = 64 thus the packet can be defined with 256x4x64 = 65536 bits. $e_m(t)$ is the baseband complex signal associated to the k-th OFDM frame (symbol) in the continuous-time domain, and also expressed as

$$\begin{aligned} e_m(t) &= \frac{1}{\sqrt{N_{FFT}}} \cdot \sum_{i=0}^{N_{FFT}-1} \beta_{m,i} \cdot \Phi_{m,i}(t) = \frac{1}{\sqrt{N_{FFT}}} \cdot \sum_{i=0}^{N_{FFT}-1} \beta_{m,i} e^{j2\pi f_i t}, \\ e_m(t_m) &= \frac{1}{\sqrt{N_{FFT}}} \cdot \sum_{i=0}^{N_{FFT}-1} \beta_{m,i} e^{\frac{j2\pi i \cdot t_m}{T_b}}, \end{aligned} \tag{C.3}$$

where

$$\begin{aligned} &f_i = i \cdot \Delta F = \tfrac{i}{T_b}, i = 0, ..., N_{FFT} - 1, \\ &(m-1)T_b \le t_m < mT_b, \end{aligned} \tag{C.4}$$

N_{FFT} is the number of subcarriers, $e^{j2\pi f_i t}$ is representing the complex-valued orthogonal subcarriers, f_i is the i-th subcarrier, T_b is the actual duration of each OFDM symbol, and $\beta_{m,i} = a_{m,i} + jb_{m,i}$ is the information sequence (complex numbers taken from a set of constellation points M-QAM symbol).

In the discrete-time domain $e_m(t)$ became

$$e_m(n\Delta_s) = \frac{1}{\sqrt{N_{FFT}}} \cdot \sum_{i=0}^{N_{FFT}-1} \beta_{m,i} e^{\frac{j2\pi i \cdot n\Delta_s}{T_b}}. \tag{C.5}$$

The FFT algorithm generated the complex samples of an ideal OFDM signal $e_m(t)$ and, in order to generate such sampling, the IDFT was taken for the sequence $\beta_{m,i}$. However, a computation disadvantage with the N_{FFT}-point IDFT of $\beta_{m,i}$ was obtained by the complex-valued time series that was not equivalent to the N_{FFT} modulated subcarriers. Instead, an LN_{FFT}-point IDFT ($L \ge 2$) can be used to generate LN_{FFT} samples of $e_m(t)$, and the samples taken at $e_m(t)$ can be defined by $t = \frac{nT_b}{LN_{FFT}}, n = 0, ..., LN_{FFT} - 1$; thus, the opportune substitutions were

$$e_m\left(\frac{nT_b}{LN_{FFT}}\right) = e_{m,n} = \sum_{i=0}^{N_{FFT}-1} \beta_{m,i} e^{j2\pi f_i \frac{nT_b}{LN_{FFT}}}$$
$$= \sum_{i=0}^{N_{FFT}-1} \beta_{m,i} e^{j2\pi \frac{ni}{LN_{FFT}}} = \sum_{i=0}^{LN_{FFT}-1} \beta'_{m,i} e^{j2\pi \frac{ni}{LN_{FFT}}}, \quad \text{(C.6)}$$
$$\beta'_{m,i} = \theta\left\{\begin{matrix}\beta_{m,i}, 0 \le i \le N_{FFT}-1 \\ 0, N_{FFT} \le i \le LN_{FFT}-1\end{matrix}\right\}.$$

Afterwards, the cyclic prefix was added to the OFDM signal so that successive symbols $\beta_{m,i}$ and $\beta_{m+1,i}$ of the information sequence did not interfere. The cyclic prefix [Wang, 2000] consisting of the last N_{CP} $\left(N_{CP} \ll N_{FFT}\right)$ samples of the IFFT output was used defining a new expression

$$e(t) = \sum_{m=-\infty}^{\infty} e(t_m) = \sum_{m=-\infty}^{\infty} \sum_{i=0}^{N_{FFT}+N_g-1} e'_{m,i},$$
$$e'_{m,i} = \left\{\begin{matrix}e_{m,i+N_{FFT}-N_g}, 0 \le i \le N_g - 1 \\ e_{m,i-N_g}, N_g \le i \le N_{FFT}+N_g-1\end{matrix}\right\}. \quad \text{(C.7)}$$

And, after the parallel to serial conversion step, the discrete time *m*-th OFDM symbol *e(t)* to be transmitted was sampled at multiples of *T* with duration of T_s (Simeone *et al.*, 2004), and within the support of having $t \in (mT_s,(m+1)T_s)$

$$e_m(t) = \sum_{k=0}^{N_{used}-1} \sum_{i=0}^{N_{FFT}+N_g-1} \underline{e}_m[k] \cdot e^{j2\pi\left(k-\frac{N_{used}}{2}\right)\frac{i-N_g}{N_{FFT}}} \cdot \delta(t - iT - mT_s). \quad \text{(C.8)}$$

At this time, looking into the whole transmission scheme (Figure C.1), it was inferred the mathematical representation of the transmitted OFDM complex signal that was associated to the *k*-th OFDM packet experiencing the effect of the wireless channel and noise (Falletti *et al.*, 2006), (Czylwik, 1998), (Palma-Lazgare *et al.*, 2008), (Palma-Lázgare & Delgado-Penín, 2008a):

$$y_k(t) = e_k(t) \cdot h_k(t,\tau) + n_k(t). \quad \text{(C.9)}$$

To carry out the PHY-layer modelling for multicarrier systems, the wideband channel model presented by the CIR time-delay representation was transformed to the domain particularised for all carriers. Multiple narrowband channels showing very slow variations were produced, and the time varying frequency response of the channel (baseband equivalent form) was given by

$$T\left(t,f\right)=\sum_i \beta_i e^{-j\omega\tau_i(t)}, \tag{C.10}$$

which can be particularised for a given subcarrier frequency

$$r\left(t,f_c\right)=T(t,f_c)=\sum_i \beta_i e^{-j\omega_c\tau_i(t)}. \tag{C.11}$$

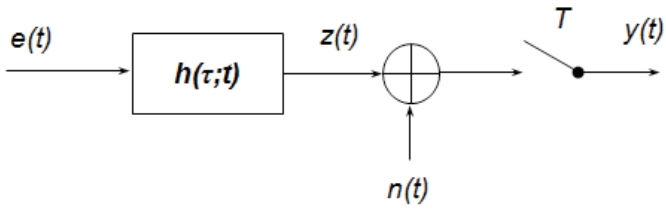

Figure C.1. The radio signal transmission and its representation through the channel.

The latter channel representation was obtained after post processing the channel's scattering matrix

$$s\left(\nu,\tau\right)=\sum_i a_i\cdot\delta\left(\nu-\nu_i,\tau-\tau_i\right), \tag{C.12}$$

where ν can either be a direction of arrival or a Doppler shift.

The small-area (small-scale fading) description was representing the effects inside the limited area where wide-sense stationarity was assumed. The general convolution relationship between the input signal *e(t)* and the output signal *z(t)* can be

$$z(t)=e(t)*h(t,\tau)=\int_{-\infty}^{\infty} e(t-\tau)\cdot h(t,\tau)\,d\tau. \tag{C.13}$$

Describing the response of the channel to cissoidal excitations (time-variant CTF) in the frequency band of interest by characterising the function *T*(*f;t*)

$$z(t)=\int_{-\infty}^{\infty} E(f)\cdot T(f;t)\cdot e^{j2\pi ft}\,df, \tag{C.14}$$

where *T(f;t)* is defined as the simply Fourier transform in τ of *h(t,*τ*)*, so equivalently *h(*τ*;t)* was defined by the mentioned frequency domain representation

$$T(f;t)=\sum_{i=1}^{N} A_i(t)\cdot e^{-j2\pi f\tau_i(t)}. \tag{C.15}$$

Additionally, the Doppler spectra was observed and embedded in the time-varying complex envelope of $h(\tau;t)$ by defining its spectrum $S(\tau,\nu)$

$$z(t) = \int_{-\infty}^{\infty}\int_{-\infty}^{\infty} e(t-\tau)S(\tau,\nu)\cdot e^{j2\pi\nu t}\,d\nu\,d\tau, \tag{C.16}$$

$$S(\tau,\nu) = \int_{-\infty}^{\infty} h(t,\tau)\cdot e^{-j2\pi\nu\tau}d\tau, \tag{C.17}$$

or in terms of the complex spectra by the superposition in frequency-shifts (Doppler-shifts) ν domain

$$Z(f) = \int_{-\infty}^{\infty} E(f-\nu)H(f-\nu,\nu)\,d\nu, \tag{C.18}$$

where $H(f,\nu)$ suitably characterised the channel with wide frequency range in order to study the frequency-selective effects caused by paths of varying lengths.

The output signal $z(t)$ determined that the channel was completely characterised when the time-varying impulse response (small-scale fading) of the propagation channel function $h(\tau;t)$ was known. It was assumed that the signal was composed by Dirac delta function (impulses): the model was assumed in the ideal transmission conditions (no band-limiting effects due to transmit and receive filter inclusions) so the different paths were treated as ideal deltas affected by attenuations, phase shifts, and delays which were time-varying. Thus, the complex impulse response of the multipath propagation channel (stratospheric wideband channel model) was expressed as a sum of N-echoes having delays $\tau_i(t)$ and $\tau_i(t) = \tau_i(t)+\Delta\tau_i(t)$ replicas of the transmitting signal, where $i=2\ldots N$. For the complex low-pass CIR representation

$$h(\tau;t) = \sum_{i=1}^{N} A_i(t)\cdot\delta(\tau-\tau_i(t)), \tag{C.19}$$

where the various echo amplitudes $A_i(t)$ were complex i-tapped-gains expressed by

$$A_i(t) = a_i(t)\cdot e^{j\phi_i(t)}, \tag{C.20}$$

and their phases $\Phi_i(t) = 2\pi f_0\tau_i(t)$ were assumed as uniformly distributed in [0, 2π); f_0 is the centre frequency of the channel.

A further band-pass representation was given by

$$h(\tau;t) = \mathrm{Re}\left[\sum_{i=1}^{N} a_i(t)\cdot e^{j\phi_i(t)}\cdot e^{j\omega_c t}\cdot \delta\left(\tau-\tau_i(t)\right)\right] = \sum_{i=1}^{N}\left[I_i(t)\cos\omega_c t - Q_i(t)\sin\omega_c t\right]\delta\left(\tau-\tau_i(t)\right); \quad \text{(C.21)}$$

the in-phase and quadrature components, attenuation, and phase, were defined respectively as following

$$I_i(t) = a_i(t)\cos\left\{\phi_i(t)\right\}, \quad \text{(C.22)}$$

$$Q_i(t) = a_i(t)\sin\left\{\phi_i(t)\right\}, \quad \text{(C.23)}$$

$$a_i(t) = \sqrt{I_i^2(t)+Q_i^2(t)}, \quad \text{(C.24)}$$

$$\phi_i(t) = \tan^{-1}\left\{\frac{Q_i(t)}{I_i(t)}\right\}. \quad \text{(C.25)}$$

Finally, the overall receiver input signal was referred to the superposition of the scattered impulses

$$y(t) = z(t) + n(t) = \int_0^{\tau_m} h(t,\tau)\cdot e(t-\tau)\,d\tau + n(t), \quad \text{(C.26)}$$

n(t) was the complex valued coloured/white noise process with spectral density height of $N_0/2$.

Such actual OFDM modulation was performed by means of IDFT, where for simplicity FFT algorithms were used putting constraints on the DFT-size N_{FFT}, and for this reason the actual number of subchannels was likely exceeding the number of the modulated carriers $N_{FFT} \geq N_{used}$. The OFDM modulation technique was dividing the total available bandwidth *BW* into the N_{used} subchannels, with each individual subchannel occupying the bandwidth ΔF and exhibiting $\Delta F << BW_{coherence}$ —by using the approximation of $BW_{coherence}$ the condition to obtain frequency-flat subchannels was also translated to $T_b >> \tau_{max}$.— And, the individual subchannels were considered to show frequency-flat transmission characteristic, which could greatly simplify the channel equalisation process.

Following last parameterisation, in order to eliminate interference due to the excess delay components, a guard interval $T_G \geq \tau_{max}$ was prefixed to each OFDM symbol; the reduc-

tion of bandwidth efficiency was clearly determined by the number of guard samples $CP = G = T_G / T_b$. And, the corresponded spectral efficiency for a constellation size of $M_{QAM} = 2^b$ was given by

$$\eta = \frac{N_{used}}{N_{FFT} + G} \cdot \frac{b}{BW \cdot T}. \tag{C.27}$$

The bandwidth coefficient corresponding to $\alpha_B = N_{used} \cdot \Delta F / BW$ was introduced (Hutter, 2002), which relates the actual modulated bandwidth to the total available bandwidth —α_B is an important system design parameter determining the complexity of the selected filters at the input of the receiver (baseband), where high-performance systems can exhibit bandwidth coefficients close to one (α_B = 0.95 for DVB-T) whereas low-cost systems operate with smaller values (α_B = 0.8125 for HiperLAN/2). An additional system design parameter α_C can be defined by $\alpha_C = G/N_{FFT} = T_G/T_b$, and the spectral efficiency's expression can be rewritten to

$$\eta = \frac{\alpha_B}{1 + \alpha_C} \cdot b. \tag{C.28}$$

The new parameter α_C can be deduced to be small to obtain a high spectral efficiency's system, and by setting $T_G = \tau_m$ is guaranteeing the searched high spectral efficiency for the OFDM symbol duration with $T_b = \frac{\tau_m}{\alpha_C}$; moreover, the boundary of α_C smaller than *0.25* can satisfy the frequency-flat equation $T_b >> \tau_{max}$ assuring frequency-flat subchannels.

If the CTF can be not anymore constant and vary during the OFDM symbol period T_b (mobile transmission channel case), the subcarriers would not longer be orthogonal resulting in the so-called inter-carrier frequency (ICI, $I_i = \sum_{i \neq j} \beta_j \mathrm{B}_j \left(f_i + \delta f \right)$, with *i*-th subcarrier and *j*-th subcarrier data) at the output of the OFDM demodulator; the signal power of this additional interference is depending on the Doppler PSD as well as the ratio of the maximum Doppler frequency $f_{D,max}$ to the OFDM carrier spacing ΔF. A further design parameter $\alpha_D = f_{D,\max} \cdot T_b = \frac{f_{D,\max}}{\Delta F}$ can be introduced reflecting the extent of time-variations.

Hence, an added universal upper bound by $P_{ICI} < \frac{\pi^2}{3} \cdot \alpha_D$ can exist, and can be useful when knowledge of the actual Doppler PSD is absent: if such ICI power exceeds the noise power, the appearance of an error floor in the BER curves is imperative, and in order to guarantee a quality of service within a particular BER performance it is to assure P_{ICI} much smaller than the noise power; the last-mentioned parameter is especially important for the quality of channel estimation that is deteriorated by incrementing P_{ICI}.

On the one hand, a long OFDM symbol duration T_b is desired to achieve high spectral efficiency. On the other hand, the ratio of Δf_c and $f_{D,max}$ should be kept small. Henceforward, at design of the OFDM system for frequency-selective and time-variant channels, a moderate short T_b value is desired in order to keep the impact of the time-variations small, and time-variance and frequency-selectivity put such adverse design constraints. Mathematically, by using the definitions of the system design parameters α_C and α_D, the boundaries are represented as

$$\frac{\tau_{\max}}{\alpha_D} < T_b < \frac{\alpha_D}{f_{D,\max}}. \tag{C.29}$$

Thereafter, the demodulation stage (Saeed *et al.*, 2003) for the subcarriers via FFT yield to the received data symbols with the i-th subcarrier of the m-th OFDM symbol

$$y_{m,i} = \beta_{m,i} H_{m,i} + n_{m,i}, \tag{C.30}$$

where $\{y_{m,i}\}$ is the output of the FFT demodulator, $n_{m,i}$ is the bandlimited complex-valued AWGN corrupting the signal, and $H_{m,i}$ is the CTF at the subcarrier frequency f_i (the size of the FFT used to demodulate the OFDM symbol).

The applications of OFDM to wireless and mobile communications are continued to be under exhaustive study. Even though multicarrier transmission has several considerable drawbacks (*e.g.*, high peak to average ratio and strict requirements on carrier synchronisation), the attractive OFDM advantages can consist in lessening the severe effects of frequency selective fading without complex equalisation. And, in order to obtain high spectral efficiencies required by future data wireless systems, the multilevel modulation with non-constant amplitude (*e.g.*, 16-QAM) is necessary to be employed implying the need for coherent receivers that are capable to track the variations of the fading channel. For the fast-varying channel cases, nonnegligible fluctuations at the channel gains can be expected between consecutive (or within each) OFDM symbols. So that, to ensure the adequate tracking

accuracy, pilot subcarriers are placed in each OFDM symbol (comb-pilot pilot pattern arrangement)

The time synchronisation at receiver can be based on the strong autocorrelation properties of the OFDM waveform, where the CP part has a very supportive role: the longer the CP relative to the channel delay spread, the autocorrelation relates to an increase due to CP can collect somehow different multipath than the original instance of the symbol; the timing errors can be sorted in the timing errors towards CP (phase offset of $\underline{\mathrm{B}} = FFT\left(\underline{\beta}\right)$ with $\mathrm{B}_i^{'} = \mathrm{B}_i \cdot e^{-j\frac{2\pi}{N_{FFT}} i \cdot d}$, $i = 1, 2, \ldots, N_{FFT}$) and away from CP (phase offset plus ISI).

Moreover, the carrier frequency synchronisation is another essential component in the coherent receiver. Frequency synchronisation in the OFDM receiver can be based on the stage that handles a fractional frequency offset (the part that is not an integer multiple of the subcarrier spacing) using usually the OFDM waveform autocorrelation (as mentioned in the time synchronisation the OFDM waveform can display autocorrelation even in severe multipath conditions because of the great exceeding from the CP against the channel delay spread), and on the stage that utilise the pilot tones to correct the integer frequency offset (pilot-PN series autocorrelation peak) —frequency synchronisation in a mobile receiver represents more challenge due to wider Doppler frequency shifts and fast fading effects damaging the subcarriers and introducing ICI.

To extract the transmitted signal constellation $\beta_{m,i}$ from the received signal, the OFDM system is assumed with perfect synchronisation and coherent detection having known the time-instants mT_b at which the OFDM symbols start, thus the correlation between the received signal and (each of) the subcarriers was performed over the symbol duration T_b; the *GI* was removed next at each of the *m*-th received OFDM symbol.

The channel estimation at receiver can be based on the pilot subcarriers being in a constant location. The constant location pilots are arranged such that one of every 24 subcarriers is a pilot. This means that by using the pilots from one symbol, a channel estimate with length of up to $1/24$ of the symbol can be done; last capability combined with the length of the OFDM symbols can enable a robust, per symbol, estimation of the channel (Zhang *et al.*, 2009) —the OFDM could not require a downlink preamble, but requires the transmission burst to be shorter than the channel coherence time. In this case, the channel coefficients are known and the estimation of the transmitted symbols are used at the equaliser stage —if the

transmitted symbol were known, the estimation of the channel coefficients has had through a channel estimation method (data-aided, blind, or decision-based) (Simeone *et al.*, 2004).

The SNR per subcarrier after the FFT can be defined as

$$SNR_{m,i} = \frac{E\left\{\left|\beta_{m,i}\right|^2\right\} \cdot \left|H_{m,i}\right|^2}{\sigma_N^2}, \qquad \text{(C.31)}$$

where $\sigma_N^2 = E\left\{\left|n_{m,i}\right|^2\right\}$ is the noise variance for the *n*-th received OFDM symbol represented by *N* signal-size samples.

References

Akalestos, K. (2005), 'Emergency Communications from High Altitude Platforms', *Proceedings of The International Workshop on High Altitude Platforms Systems (WHAPS'2005)* (Athens, Greece).

Aragón-Zavala, A., Cuevas-Ruíz, and Delgado-Penín, J. A. (2008), *High-Altitude Platform Systems for Wireless Communications*, ed. Ltd. John Wiley & Sons, Wiley-Blackwell (1st edn.; England) 256.

Aubineau, Ph., Buonomo, S., Frank, W., and Hughes, K. A. (2010), 'ITU's Regulatory Framework, Technical Studies in ITU-R, and Future Activities in Relation to High-Altitude Platform Stations (HAPS)', *Radio Science Bulletin URSI - Special Issue on High-Altitude Platforms*, (332), 67-74.

Bello, P. A. (1993), 'Characterization of randomly time-variant linear channels', *IEEE Transactions on Communications Systems*, 11 (4), 360-93.

Belloul, B., Saunders, S. R., Parks, M. A. N., and Evans, B. G. (2000), 'Measurement and modeling of wideband propagation at L- and S-bands applicable to the LMS channel', *IEE Proceedings - Microwaves, Antennas and Propagation*, 147 (2).

Berg, J. E. (1999), 'Building Penetration', in European Commission-COST Telecom Secretariat (ed.), *Digital Mobile Radio Toward Future Generation Systems* (Brussels, Belgium: COST Action 231).

Bolkcom, C. (2006), 'Potential Military Use of Airships and Aerostats', in The Library of Congress Congressional Research Service (ed.), *CRS Report for Congress* (CRS Report for Congress - Specialist in National Defense - Foreign Affairs, Defense, and Trade Division), CRS 1-6.

Bon-Jun, K., Do-Seob, A., Nam, K. (2008), 'An Evaluation of Interference Mitigation Schemes for HAPS Systems', *EURASIP Journal on Wireless Communications and Networking,* 2008 (Article ID 865393), 11.

Batlles, Carlos (2008), 'A 802.16d system, A WiMAX system simulation', File Exchange Matlab® Central, Mathworks®.

Castro, M.A.V.; Fontan, F.P.; Villamarin, A.A.; Buonomo, S.; Baptista, P.; Arbesser, B. (1999), 'L-band land mobile satellite (LMS) amplitude and multipath phase modeling in urban areas', *IEEE Communications Letters*, 3 (1), 12-14.

Communities, EU Commission of the European (2004), 'Connecting Europe at high speed: recent developments in the sector of electronic communications', *Communication from the Commission to the Council, the European Parliament, the Economic and Social Committee and the Committee of the Regions* (COM (2004) 61 final; Brussels).

Copyright © CAPANINA Consortium 2004, Website designed by York Electronics Centre, UK 'http://www.capanina.org, CAPANINA Stratospheric Broadband'.

Copyright © COST297, HAPCOS, Website designed by York Electronics Centre, UK 'http://www.hapcos.org/ COST297 - High Altitude Platforms for Communications and Other Services'. MoU : 258/05, CSO Approval date : 15/03/2005, Entry into force: 21/04/2005, End of Action: 04/09/2009; http://w3.cost.eu/index.php?id=110&action_number=297

Copyright © 2011 AeroVironment, Inc. (2011), 'AV - Aerovironment', <http://www.avinc.com/contacts/>.

Cuevas-Ruiz, J. L., Delgado-Penin, J. A. (2004a), 'Channel Modeling and Simulation in HAPS Systems', *The Fifth European Wireless Conference - Mobile and Wireless Systems beyond 3G* (Barcelona, Spain).

Cuevas-Ruiz, J. L., and Delgado-Penin, J. A. (2004b), 'A statistical switched broadband channel model for HAPS links', *Wireless Communications and Networking Conference (WCNC 2004)* (1; Atlanta, Georgia, USA), 290-94.

Cuevas-Ruíz, J. L., Aragón-Zavala, A., Medina-Acosta, G. A., and Delgado-Penín, J. A. (2009), 'Multipath propagation model for high altitude platform (HAP) based on circular straight cone geometry', *2009 International Workshop on Satellite and Space Communications (IWSSC'09)* (Siena, Italy).

Czylwik, A. (1998), 'OFDM and Related Methods for Broadband Mobile Radio Channels', International Zürich Seminar on Broadband Communications, 1998. Accessing, Transmission, Networking. Proceedings (Zürich, Switzerland), 91-98.

Davarian, F. (1987), 'Channel Simulation to Facilitate Mobile-Satellite Communications Research', *IEEE Transactions on Communications*, 35 (1), 47-56.

Devasirvatham, D. M. J., Krain, M. J., Rappaport, D. A., and Banerjee, C. (1990), 'Radio propagation measurements at 850 MHz, 1.7 GHz and 4 GHz inside two dissimilar office buildings', *Electronics Letters*, 26 (7), 445-47.

Djuknic, G. M., and Okunev, Y. (1997), 'Establishing Wireless Communications Services via High-Altitude Aeronautical Platforms - A Concept Whose Time Has Come?', *IEEE Communications Magazine*, 35 (9), 128-35.

Dossi, L., and Tartara, G. (1996), 'Statistical Analysis of Measured Impulse Response Functions of 2.0 GHz Indoor Radio Channels', *IEEE Journal on Selected Areas in Communications,* 14 (3), 405-10.

Dovis, F., Fantini, R., Mondin, M., Savi, P. (2002), 'Small-scale fading for high altitude platform (HAP) propagation channels', *IEEE Journal on Selected Areas in Communications,* 20 (3), 641-47.

Erceg, V., Michelson, D. G., Ghassemzadeh, S. S., Greenstein, L. J., Rustaki, A. J., Jr., Guerlain, P. B., Dennison, M. K., Roman, R. S., Barnickel, D. J., Wang, S. C., Miller, R. R. (1999), 'A model for the Multipath Delay Profile of Fixed Wireless Channels', *IEEE Journal on Selected Areas in Communications,* 17 (3), 399-410.

Ergen, Mustafa (2009), Mobile broadband : including WiMAX and LTE (New York: Springer) xvi, 513 p.

Evans, B. G., Butt, G., Willis, and M. A. N. Parks (1996), 'Land mobile satellite wideband measurement experiment at L- and S-Bands', (United Kingdom: University of Surrey).

Evans, B.; Werner, M.; Lutz, E.; Bousquet, M.; Corazza, G.E.; Maral, G.; Rumeau, R. (2005), 'Integration of satellite and terrestrial systems in future multimedia communications', *IEEE Wireless Communications*, 12 (5), 72-80.

Falletti, E., Laddomada, M., Mondin, M., and Sellone, F. (2006), 'Integrated Services from High-Altitude Platforms: a Flexible Communication System', *IEEE Communications Magazine*, 44 (2), 85-94.

Fernández, O., Jaramillo, R., Domingo, M., Valle, L., and Torres, R. P. (2007), 'Characterization and modeling of BFWA channels in outdoor-indoor environments', *IEEE Antennas and Wireless Propagation Letters*, 6, 236-39.

Fischer de Toledo, A., Turkmani, A. M. D., and Parsons, J. D. (1998), 'Estimating coverage of radio transmission into and within buildings at 900, 1800, and 2300 MHz', *IEEE Personal Communications*, 5 (2), 40-47.

Fontan, F. P., Vazquez-Castro, M., Cabado, C. E., Garcia, J. P., and Kubista, E. (2001), 'Statistical Modeling Of The LMS Channel', *IEEE Transactions on Vehicular Technology*, 50 (6), 1549-67.

Glazunov, A.A., and Berg, J. E. (2000), 'Building-shielding loss modelling', *2000 IEEE 51st Vehicular Technology Conference Proceedings, 2000 (VTC 2000-Spring Tokyo)* (3; Tokyo, Japan), 1835-39.

Goldsmith, A. (2005), *Wireless Communications* (Cambridge University Press) 672.

Grace, D., Thornton, J., White, G. P., Spillard, C., Pearce, D. A. J., Mohorcic, M., Javornik, T., Falletti, E., Delgado-Penin, J. A., Bertran, E. (2003), 'The European HeliNet Broadband Communications Application – An Update on Progress', *4th Japanese Stratospheric Platform Systems Workshop (SPSW'03)* (Shinagawa, Tokyo, Japan).

Grace, D.; Capstick, M.H.; Mohorcic, M.; Horwath, J.; Pallavicini, M.B.; Fitch, M. (2005), 'Integrating users into the wider broadband network via high altitude platforms', *IEEE Wireless Communications*, 12 (5), 98-105.

Grace, David, and Mohorčič, Mihael (2011), Broadband Communications via High-Altitude Platforms (1st edn.; Chichester, West Sussex, United Kingdom: Wiley-Blackwell, 2011 John Wiley & Sons Ltd.) 398.

Grønsund, P., Engelstad, P., Johnsen, T., and Skeie, T. (2007), 'The Physical Performance and Path Loss in a Fixed WiMAX Deployment', *Proceedings of the 2007 International Conference On Wireless Communications and Mobile Computing (IWCMC 2007)* (Honolulu, Hawaii, USA: ACM (New York, NY, USA)), 439-44.

Hase, Y., Miura, R., and Ohmori, S. (1998), 'A novel broadband all-wireless access network using stratospheric platforms', *The 48th IEEE Semi-annual Vehicular Technology Conference (VTC-1998 Spring)* (2), 1191-94.

Hashemi, H. (2002), 'A Study of Temporal and Spatial Variations of the Indoor Radio Propagation Channel', *5th IEEE International Symposium on Personal, Indoor and Mobile Radio Communications, 1994. Wireless Networks - Catching the Mobile Future* (1; The Hague), 127-34.

Heiskala, J., and Terry, J. (2002), OFDM Wireless LANs: A Theoretical and Practical Guide, ed. SAMS Publishing (USA: SAMS Publishing) 315.

Hoeher, P, Woerz, T., Schmidbauer, A., Jahn, A., and Schweikert, R. (1996), 'On Satellite Emulation by an Airborne Platform', *Global Telecommunications Conference (GLOBECOM 1996). Communications: The Key to Global Prosperity* (2; London, UK), 995-1000.

Hori, Teruhisa (2002), 'Overview of High Altitude Platform Station R&D Project', *Sixth APT Standardization Program Forum*.

Husni, E. M., Razali, R., Said A. M. (2001), 'Broadband Communications based on High Altitude Platform Systems (HAPS) For Tropical Countries', *Sixth International Symposium on Signal Processing and its Applications 2001 (ISSPA'01)* (Kuala Lumpur, Malaysia), 517-20.

Hutter, A. A. (2002), 'Design of OFDM systems for frequency-selective and time-variant channels', *2002 International Zürich Seminar on Broadband Communications. Access, Transmission, Networking* (Zürich, Switzerland), 39-1 - 39-6.

IEEE (2004), '802.16™ – IEEE Standard For Local And Metropolitan Area Networks, Part 16: Air Interface For Fixed Broadband Wireless Access Systems', *IEEE Std 802.16™-2004*.

IEEE (2005), '802.16e™ – IEEE Standard For Local And Metropolitan Area Networks. Part 16: Air Interface For Fixed and Mobile Broadband Wireless Access Systems. Amendment 2: Physical and Medium Access Control Layers for Combined Fixed and Mobile Operation in Licensed Bands. Corrigendum 1', *IEEE Std 802.16™-2005 and 802.16™/COR-1*.

IEEE (2009), '802.16™ – IEEE Standard For Local And Metropolitan Area Networks, Part 16: Air Interface For Broadband Wireless Access Systems', *IEEE Std 802.16™-2009 (Revision of IEEE Std 802.16-2004)*, 2082.

Ikegami, F., Takeuchi, T., and Yoshida, S. (1991), 'Theoretical prediction of mean field strength for urban mobile radio', *IEEE Transactions on Antennas and Propagation*, 39 (3), 299-302.

International Telecommunication Union, Radiocommunications Sector (1998), 'High Altitude Platform Stations: An Opportunity To Close The Information Gap', *ITU-Q/2, 98* (Genève).

International Telecommunication Union, Radiocommunications Sector (1999), 'Coverage area of a HAPs terrestrial IMT-2000', *ITU-R 39.8* (Document 8-1/381-E).

International Telecommunication Union, Radiocommunications Sector (2000), 'Minimum performance characteristics and operational conditions for high altitude platform stations providing IMT-2000 in the bands 1885-1980 MHz, 2010-2025 MHz, and 2110-2170 MHz in the Regions 1 & 3, and 1885-1980 MHz and 2110-2160 MHz in Reg. 2', *ITU-R M.1456*.

International Telecommunication Union, Radiocommunication Sector (2001-2007), 'Detailed Specifications Of The Radio Interfaces Of International Mobile Telecommunications – 2000 (IMT-2000)', *ITU-R M.1457*

Iskandar, and Rinarso Putro, D. (2008), 'Performance Evaluation of Broadband WiMAX Services over High Altitude Platforms (HAPs) Communication Channel', *The Fourth International Conference on Wireless and Mobile Communications (ICWMC 2008)* (Athens, Greece).

Iskandar, and Shimamoto, Shigueru (2006a), 'On the Performance of IMT-2000 Communication Link based on Stratospheric Platforms', *Makara, Teknologi (Fakultas Teknik Universitas Indonesia),* 10 (1), 1-10.

Iskandar, and Shimamoto, S. (2006b), 'Prediction of Propagation Path Loss for Stratospheric Platforms Mobile Communications in Urban Site LOS/NLOS Environment', *IEEE International Conference on Communications 2006 (ICC'06)* (12; Istanbul, Turkey), 5643-48.

Iskandar, and Shimamoto, Shigeru (2006c), 'On the downlink performance of stratospheric platform mobile communications channel', *The 49th Annual IEEE Global Telecommunications Conference 2006 (GLOBECOM'06)* (San Francisco, CA), 1-5.

ITU (2000), 'Preferred characteristics of systems in the fixed service using high altitude platforms operating in the bands 47.2-47.5 GHz and 47.9-48.2 GHz', *ITU-R M.1456* (International Telecommunication Union, Radiocommunication Sector).

ITU (2005), 'Propagation data and prediction methods for the planning of short-range outdoor radiocommunication systems and radio local area networks in the frequency range 300 MHz to 100 GHz', *ITU-R P.1411-3* (International Telecommunication Union, Radiocommunication Sector).

Jahn, A. (1994), 'Propagation Data and channel model for LMS systems', in ESA (European Space Agency) Final Report (ed.), (DLR (German Aerospace Research Establishment Institute for Communications Technology), Institut Für Nachrichtentechnik).

Jahn, A., Bischl, H., and Heiss, G. (1996), 'Channel Characterisation for Spread Spectrum Satellite Communications', *IEEE 4th International Symposium on Spread Spectrum Techniques and Applications Proceedings, 1996* (3), 1221-26.

Jamison, L., Sommer, G. S., and Porche III, I. R. (2005), 'High-Altitude Airships for the Future Force Army', (Santa Monica, CA, USA: Rand Corp.), 1-74.

Jong-Min, P., Dae-Sub, O., Yang-Su, K., and Do-Seob, A. (2003), 'Evaluation of interference effect into cellular system from high altitude platform station to provide IMT-2000 service', *Global Telecommunications Conference 2003 (GLOBECOM'03)* (1; San Francisco, CA, USA), 420-24.

Kang, Y., Ku, B., and Ahn, D. (2007), 'Introduction to the Performance Evaluation of HAPS-Mobile WiMAX Systems', *25th International Communications Satellite Systems Conference (ICSSC)* (Seoul, South Korea).

Karapantazis, S, and Pavlidou, F. N. (2004), 'Broadband from Heaven [High altitude platforms]', *IEE Communications Engineer*, 18-24.

Karapantazis, Stylianos, and Pavlidou, Fotini-Niovi (2005), 'Broadband communications via high-altitude platforms: A survey', *IEEE Communications Surveys & Tutorials*, 7 (1), 2-31.

Karlsson, P., Börjesson, H., and Maseng, T. (1994), 'A statistical multipath propagation model confirmed by measurements and simulations in indoor environments at 1800 MHz', *5th IEEE PIMRC* (1; Hague, Holland), 149-55.

Katz, Marcos D. and Fitzek, Frank H. P. (2009), *WiMAX evolution : emerging technologies and applications* (Hoboken, N.J.: Wiley; Chichester: John Wiley [distributor]) xxxiv, 468 p.

Ku, B.J., Park, J.M., Kim, Ahn, D.S. (2003), 'Development of receiving APAA using DBF for HAPS to provide IMT-2000 service system', *2003 IEEE 58th Vehicular Technology Conference (VTC 2003-Fall)* (4; Orlando, FL, USA), 2540-43.

Kürner, T., and Meier, A. (2002), 'Prediction of outdoor and outdoor-to-indoor coverage in urban areas at 1.8 GHz', *IEEE Journal on Selected Areas in Communications,* 20 (3), 496-506.

Le Vine, D. M., and Karam, M. A. (1996), 'Dependence of attenuation in a vegetation canopy on frequency and plant water content', *IEEE Transactions on Geoscience Remote Sensing*, 34, 1090-96.

Liikanen, E. (2002-2010), 'The eEurope Broadband Strategy - Broadband for all', The European Telecommunications Network Operators' Association Conference 'Making Broadband Happen in Europe,' Speech & Interview.

Likitthanasate, P.; Grace, D.; Mitchell, P.D. (2005), 'Coexistence performance of high altitude platform and terrestrial systems sharing a common downlink WiMAX frequency band', *Electronics Letters,* 41 (15), 858-60.

Liu, S, Niu, Z., and Wu, Y. (2003), 'A blockage based channel model for high altitude platform communications', *The 57th IEEE Semi-annual Vehicular Technology Conference (VTC-2003 Spring)* (Jeju, Korea), 1051-55.

Loo, C. (1985), 'A statistical model for land mobile satellite link', *IEEE Transactions on Vehicular Technology*, 34 (3), 122-27.

Loo, C., and Butterworth, J. S. (1998), 'Land Mobile Satellite Channel, Measurements and Modeling', *Proceedings of the IEEE*, 86 (7), 1442-63.

Lutz, E., Cygan, D., Dippold, M., and Panke, W. (1991), 'The Land Mobile Satellite Communication Channel-Recording, Statistics, and Channel model', *IEEE Transactions on Vehicular Technology*, 40 (2), 375-93.

Ma, Maode (2009), Current technology developments of WiMAX systems (New York: Springer) xvi, 300 p.

Macedo, A. S., Sousa, E. S. (1997), 'Coded OFDM for broadband indoor wireless systems', 1997 IEEE International Conference on Communications (ICC'97), 'Towards the Knowledge Millennium' (2; Montreal, Quebec), 934-38.

Martijn, E. F. T., and Herben, M. H. A. J. (2003), 'Characterization of radio wave propagation into buildings at 1800 MHz', *IEEE Antennas and Wireless Propagation Letters*, 2, 122-25.

Martin, J. N., and Colella, N. J. (1999), 'High-speed Internet Access via Stratospheric HALO Network'.

Miura, Riu, and Suzuki, Mikio (2003), 'Preliminary Flight Test Program on Telecom and Broadcasting Using High Altitude Platform Stations', *Wireless Personal Communications,* 24 (2), 341-61.

Mohr, W. (1995), 'Modeling of wideband mobile radio channels based on propagation measurements', Sixth IEEE International Symposium on Personal, Indoor and Mobile Radio Communications (PIMRC'95). 'Wireless: Merging onto the Information Superhighway'. (2; Toronto, Ont., Canada), 397-401.

Molina-Garcia-Pardo, J.-M.; Rodrigo-Penarrocha, V.-M.; Juan-Llacer, L. (2004), 'Characterization at 450, 900, 1800, and 2400 MHz of regular and chaflane street corners by measurements', *IEEE Transactions on Antennas and Propagation*, 52 (12), 3390-94.

Mondin, M., Dovis, F., and Mulassano, P. (2001), 'On the use of HALE platforms as GSM base stations', *IEEE Personal Communications*, 8 (2), 37-44.

Morisaki, T. (2005), 'Overview Of Regulatory Issues And Technical Standards On High Altitude Platform Stations', *Proceedings of The International Workshop on High Altitude Platforms Systems (WHAPS'2005)* (Athens, Greece).

Nakadate, M. (2005), 'Flight Test Overview of Low Altitude Stationary Flight Test Vehicle', (Tokyo, Japan: Aircraft Application Technology Center, Japan Aerospace Exploration Agency).

Núñez López, Pablo Andrés, Universidad Autónoma de Madrid. Departamento de Ingeniería Informática, and Universidad Autónoma de Madrid. Escuela Politécnica Superior (2009), *Estudio de propagación de señales electromagnéticas en edificios en bandas de Wi-Fi y WiMAX* 187 p.

Oestges, C., and Paulraj, A. J. (2004), 'Propagation into buildings for broad-band wireless access', *IEEE Transactions on Vehicular Technology*, 53 (2), 521-26.

Ohmori, S., Yamao, Y., and Nakajima, N. (2001), 'The Future Generations of Mobile Communications based on Broadband Access Methods', *Wireless Personal Communications: An International Journal,* 17 (2-3), 175-90.

Oodo, M., Tsuji, H., Miura, R., Maruyama, M., Suzuki, M., Nishi, Y., and Sasamoto, H. (2005), 'Experiments On IMT-2000 Using Unmanned Solar Powered Aircraft At An Altitude Of 20 Km', *IEEE Transactions On Vehicular Technology*, 54 (4).

Palma-Lazgare, I. R., Delgado-Penin, J. A., and Perez-Fontan, F. (2008), 'An Advance in Wireless Broadband Communications based on a WiMAX-HAPS Architecture', *26th International Communications Satellite Systems Conference (ICSSC'2008)* (San Diego, CA), AIAA-2008-5502.

Palma-Lazgare, I. R., Delgado-Penin, J. A. (2008a), 'Efectos de Distorsión Presentes en el Canal de Propagación en un Sistema de Comunicaciones de Banda-Ancha WiMAX basado en HAPS', in Actas del XXIII Simposium Nacional de la Unión Científica Internacional de Radio (URSI 2008) (ed.), *XXIII Simposium Nacional de la Unión Científica Internacional de Radio (URSI 2008) España* (Madrid, España: Actas del XXIII Simposium Nacional de la Unión Científica Internacional de Radio (URSI 2008)), ID Artículo: RP15.

Palma-Lazgare, I. R., and Delgado-Penin, J. A. (2008b), 'Fixed Broadband Wireless Access based on HAPS using COFDM Schemes: Channel Modelling and Performance Evaluation', *Australasian Telecommunication Networks and Applications Conference (ATNAC 2008)* (Adelaide, SA, Australia), 62-66.

Palma-Lázgare, I. R., Delgado-Penín, J. A., Pérez-Fontán, F. (2006), 'HAP-based broadband communications under WiMAX standards – A first approach to physical layer performance assessment', *First COST 297-HAPCOS Workshop* (Document No: COST297-0141-WG10-PRI-P02; York, UK).

Palma-Lázgare, I. R., Delgado-Penín, J. A., and Pérez-Fontán, F. (2010), 'Performance Approach of the State-Oriented Channel Modelling for WiMAX HAPS-based Communications', *URSI-EiC 2010 Asia-Pacific Radio Science Conference (AP-RASC'2010)* (Toyama, Japan), Session F4b-5 'Satellite and terrestrial propagation'.

Palma-Lázgare, I. R., and Delgado-Penín, J. A. (2010a), 'High Altitude Platform Stations in Design Solutions for Emergency Services', *IEEE Buran Magazine*, (25), 52-57.

Palma-Lázgare, Israel R., and Delgado-Penín, Jose A. (2010b), 'WiMAX HAPS-based Downlink Performance Employing Geometrical and Statistical Propagation Channel Characteristics', *Radio Science Bulletin URSI - Special Issue on High-Altitude Platforms*, (332), 50-66.

Palma-Lázgare, Israel R., and Delgado-Penín, José A. (2010c), 'A Performance Evaluation Approach on the Urban Outdoor-Indoor Propagation Model for WiMAX HAPS-based Communications', *URSI-EiC 2010 Asia-Pacific Radio Science Conference (AP-RASC'2010)* (Toyama, Japan), Session FBC-3 'Mobile propagation'.

Palma-Lázgare, Israel R., and Delgado-Penín, José A. (2010d), 'Contributions on Channel Modelling for the Performance Evaluation of WiMAX HAPS-based Communication Systems', in Universitat Politècnica de Catalunya J. L. González & A. Rodríguez (ed.), *2010 Barcelona Forum on Ph.D. Research in Communications, Electronics and Signal Processing* (Campus Nord UPC (Edifici C2), Barcelona, Spain), 61-62.

Parks, M.A.N., Butt, G., Willis, M.J., and Evans, B.G. (1996a), 'Wideband propagation measurements and results at L- and S-bands for personal and mobile satellite communications', *Fifth International Conference on Satellite Systems for Mobile Communications and Navigation 1996* (London, UK), 64-71.

Parks, M. A. N., Saunders, S. R., and Evans, B. G. (1996b), 'A Wideband Channel Model Applicable to Mobile Satellite Systems at L- and S-band', *IEE Colloquium on Propagation Aspects of Future Mobile Systems* (Digest No. 1996/220; London, UK), 12/1-12/6.

Parsons, J. D. (2000), *The Mobile Radio Propagation Channel*, ed. Second Edition (Second Edition edn.: John Wiley & Sons Ltd).

Pätzold, Matthias (2002), *Mobile Fading Channels* (1st edn.; England: John Wiley & Sons, Ltd.).

Pedro-Eira, J. and Rodrigues, A. J. (2009), 'White Paper - Analysis of WiMAX data rate performance', in Technical University of Lisbon Instituto de Telecomunicações/Instituto Superior Técnico (ed.), (Lisboa, Portugal: Instituto de Telecomunicações/Instituto Superior Técnico, Technical University of Lisbon).

Peha, J. M. (2005), 'Regulatory and policy issues protecting public safety with better communications systems', *IEEE Communications Magazine*, 43 (3), 10-11.

Pérez Fontán, Fernando, and Mariño Espiñeira, P. (2008), *Modeling The Wireless Propagation Channel, A Simulation Approach With Matlab®* (First Edition edn.; London, UK: A John Wiley and Sons, Ltd. Publication) 268.

Pérez-Fontán, F., Vázquez-Castro, M. A., Buonomo, S., Poiares-Baptista, J. P., and Arbesser-Rastburg, B. (1998), 'S-Band LMS propagation channel behaviour for different environments, degrees of shadowing and elevation angles', *IEEE Transactions on Broadcasting*, 44 (1), 40-76.

Pérez-Fontán, F., Delgado-Penín, J. A., and Palma-Lázgare, I. R. (2006), 'A case study: WiMAX HAPS system at S-Band', in Action Document for WG1 Meeting (ed.), *COST 297 - HAPCOS Meeting* (Document No: COST297-0088-WG10-PUB-P01 edn.; Oberpfaffenhofen, Germany).

Pérez-Fontán, F., Hovinen, V., Schönhuber, M., Prieto-Cerdeira, R., Delgado-Penín, J. A., Teschl, F., Kyröläinen, J., and Valtr, P. (2008), 'Building entry loss and delay spread measurements on a simulated HAP-to-indoor link at S-band', *EURASIP Journal on Wireless Communications and Networking,* Vol. 2008 (Article ID 427352), 6 pages.

Ryu, S.; Kwon Park, S.; Oh, D.; Sihn, G.; Han, K.; Hwang, S. (2005), 'Research Activities on Next-Generation Mobile Communications and Services in Korea', *IEEE Communications Society*, 43 (9), 122-31.

Saeed, M. A., Ali, B. M., and Habaebi, M. H. (2003), 'Performance Evaluation of OFDM Schemes over Multipath Fading Channels', *The 9th Asia-Pacific Conference on Communications (APCC'2003)* (1; Malaysia), 415-19.

Saleh, A. A. M., Valenzuela, R. A. (1987), 'A statistical model for indoor multipath propagation', *IEEE Journal on Selected Areas in Communications,* SAC-5 (No. 2), 128-37.

Saunders, S. R., and Bonar, F. R. (1994), 'Prediction of Mobile Radio Wave Propagation Over Buildings of Irregular Heights and Spacings', *IEEE Transaction on Antennas and Propagation*, 42 (2), 137-44.

Saunders, S. R., and Evans, B. G. (1997), 'A Physical-Statistical model for Land Mobile Satellite Propagation in Built-up Areas', *10th International Conference on Antennas and Propagation* (IEE), 44-47.

Simeone, O.; Bar-Ness, Y.; and Spagnolini, U. (2004), 'Pilot-Based Channel Estimation for OFDM Systems by Tracking the Delay-Subspace', *IEEE Transactions on Wireless Communications*, 3 (1), 315-25.

Stephen, M., and Makrinos, T. (2005), 'High Altitude Airships for Homeland Security - Commercial and Military Operations', (NJ, USA: CACI Technologies Incorporated).

Stuckmann, P., and Zimmermann, R. (2007), 'Toward Ubiquitous and Unlimited-Capacity Communication Networks: European Research in Framework Programme 7', *IEEE Communications Magazine*, 45 (5), 148-57.

The Space & Advanced Communications Research Institute, SACRI (2006), 'White Paper on Emergency Communications', (Washington, DC, USA: George Washington University).

Thornton, J.; Grace, D.; Spillard, C.; Konefal, T.; Tozer, T.C. (2001), 'Broadband communications from a high-altitude platform: the European HeliNet programme', *Electronics & Communication Engineering Journal,* 13 (3), 138-44.

Tila, F. Shepherd, P. R., and Pennock, S. R. (2001), '2 GHz Propagation & Diversity Evaluation for In-Building Communications up to 4 MHz using High Altitude Platforms (HAP)', *IEEE VTC, 54th Vehicular Technology Conference 2001* (1; Atlantic City, NJ, USA), 121-25.

Tozer, T.C., and Grace, D. (2001), 'High-Altitude Platforms for Wireless Communications', *Electronics & Communication Engineering Journal,* 13 (3), 127-37.

Tozer, T.; Grace, D.; Thompson, J.; Baynham, P.; (2000), 'UAVs and HAPs-potential convergence for military communications', *IEE Colloquium on Military Satellite Communications (Ref. No. 2000/024)*, 10/1-10/6.

Vázquez-Castro, María, Pérez-Fontán, Fernando (2002), 'Channel modeling for satellite and HAPS system design', International Journal on Wireless Communications and Mobile computing, Special Issue: Advances in 3G Wireless Networks, 2 (3), 285-300.

Vázquez-Castro, M. A., Belay-Zeleke, D., and Curieses-Guerrero, A. (2002), 'Availability of systems based on satellites with spatial diversity and HAPS', *IEE Electronics Letters*, 38 (6), 286-88.

Vivier, Emmanuelle (2009), Radio resource management in WiMAX : from theoretical capacity to system simulations (London: ISTE) xiv, 381 p.

Vogel, W. J., and Torrence, G. W. (1993), 'Propagation measurements for satellite radio reception inside buildings', *IEEE Transactions on Antennas and Propagation*, 41 (7), 954-61.

Vucetic, B., and Du, J. (1992), 'Channel modelling and simulation in satellite mobile communication systems', *IEEE Journal on Selected Areas in Communications,* 10 (8), 1209-18.

Wang, H., Belzile, J., Despins, C. L. (2000), '64-QAM OFDM with TCM coding and waveform shaping in a time-selective Rician fading channel', *2000 International Zürich Seminar on Broadband Communications. Proceedings* (Zürich, Switzerland), 257-61.

WHAPS'05, Giorgos Theodoridis 'http://newton.ee.auth.gr/haps, International Workshop on High Altitude Platform Systems - WHAPS'2005'.

Widiawan, A. K., and Tafazolli, R. (2007), 'High Altitude Platform Station (HAPS): A Review of New Infrastructure Development for Future Wireless Communications', *Wireless Personal Communications*, 42 (3), 387-404.

WiMAX, White Paper (2005), 'WiMAX Deployments with Self-Installable Indoor Terminals', (WiMAX Forum), 18.

Yang, Z., Grace, D., Mitchell, P. D. (2005), 'Downlink performance of WiMAX broadband from high altitude platform and terrestrial deployments sharing a common 3.5GHz band', *14th IST Mobile & Wireless Communications Summit 2005* (Dresden, Germany).

Yang, Z, Mohammed, A., and Hult, T. (2008), 'Performance Evaluation of WiMAX Broadband from High Altitude Platform Cellular System and Terrestrial Coexistence Capability', *EURASIP Journal on Wireless Communications and Networking*, 2008 (4).

Yang, Z.; Mohammed, A.; Hult, T.; Grace, D. (2007a), 'Assessment of Coexistence Performance for WiMAX Broadband in HAP Cellular System and Multiple-Operator Terrestrial Deployments', *4th International Symposium on Wireless Communication Systems 2007 (ISWCS'07)* (Trondheim, Norway), 195-99.

Yang, Z.; Mohammed, A.; Hult, T. (2007b), 'Uplink Performance Evaluation of WiMAX Broadband Services via High Altitude Platforms (HAPs)', *The Second European Conference on Antennas and Propagation 2007 (EuCAP'07)* (Edinburgh, UK), 1-5.

Zhang, W.; Ma, X.; Gestner, B.; Anderson, D. V. (2009), 'Designing low-complexity equalizers for wireless systems', *IEEE Communications Magazine*, 47 (1), 56-62.

Published Papers

Journal publications

Palma-Lazgare, Israel R., and Delgado-Penín, Jose A. (March, 2010), 'WiMAX HAPS-based Downlink Performance Employing Geometrical and Statistical Propagation Channel Characteristics', *Radio Science Bulletin URSI - Special Issue on High-Altitude Platforms*, (332), ISSN: 1024-4530, pp. 50-66.

Conference papers and Proceedings

Palma-Lázgare, I. R., Delgado-Penín, J. A., Pérez-Fontán, F. (October 23-27th, 2006), 'HAP-based broadband communications under WiMAX standards – A first approach to physical layer performance assessment', *First COST 297-HAPCOS Workshop* (Document No: COST297-0141-WG10-PRI-P02; York, UK).

Palma-Lazgare, I. R., Delgado-Penin, J. A., and Perez-Fontan, F. (June 10-12th, 2008), 'An Advance in Wireless Broadband Communications based on a WiMAX-HAPS Architecture', *26th International Communications Satellite Systems Conference (ICSSC'2008)* (San Diego, CA), Paper No: AIAA-2008-5502.

Palma-Lazgare, I. R., Delgado-Penin, J. A. (Septiembre 22-24, 2008), 'Efectos de Distorsión Presentes en el Canal de Propagación en un Sistema de Comunicaciones de Banda-Ancha WiMAX basado en HAPS', Actas del XXIII Simposium Nacional de la Unión Científica Internacional de Radio (URSI 2008) (ed.), *XXIII Simposium Nacional de la Unión Científica Internacional de Radio en España* 2008 (Madrid, España: ISBN 978-84-612-6291-5), ID Artículo: RP15.

Palma-Lazgare, I. R., and Delgado-Penin, J. A. (December 7-10th, 2008), 'Fixed Broadband Wireless Access based on HAPS using COFDM Schemes: Channel Modelling and Performance Evaluation', *Australasian Telecommunication Networks and Applications Conference (ATNAC 2008)* (Adelaide, SA, Australia), Print ISBN: 978-1-4244-2602-7,

INSPEC Accession Number: 10473969, DOI: 10.1109/ATNAC.2008.4783296, pp. 62-66.

Palma, I. R., Delgado, J. A., and Perez, F. (September 22-26th, 2010), 'Performance Approach of the State-Oriented Channel Modelling for WiMAX HAPS-based Communications', *URSI-EiC 2010 Asia-Pacific Radio Science Conference (AP-RASC'2010)* (Toyama, Japan), Proceedings ISBN: 978-4-88552-250-5 C3855, Session F4b-5 'Satellite and terrestrial propagation'.

Palma, I. R., and Delgado, J. A. (September 22-26th, 2010), 'A Performance Evaluation Approach on the Urban Outdoor-Indoor Propagation Model for WiMAX HAPS-based Communications', *URSI-EiC 2010 Asia-Pacific Radio Science Conference (AP-RASC'2010)* (Toyama, Japan), Proceedings ISBN: 978-4-88552-250-5 C3855, Session FBC-3 'Mobile propagation'.

Palma-Lázgare, Israel R., and Delgado-Penín, José A. (2010), 'Contributions on Channel Modelling for the Performance Evaluation of WiMAX HAPS-based Communication Systems', in Universitat Politècnica de Catalunya J. L. González & A. Rodríguez (ed.), ISBN: 978-84-7653-495-3, *2010 Barcelona Forum on Ph.D. Research in Communications, Electronics and Signal Processing* (Campus Nord UPC (Edifici C2), Barcelona, Spain), 61-62.

Cooperative papers

Pérez-Fontán, F., Delgado-Penín, J. A., and Palma-Lázgare, I. R. (April, 2006), 'A case study: WiMAX HAPS system at S-Band', in Action Document for WG1 Meeting (ed.), *COST 297 - HAPCOS Meeting* (Document No: COST297-0088-WG10-PUB-P01 edn.; Oberpfaffenhofen, Germany).

Magazine publications

Palma-Lázgare, I. R., and Delgado-Penín, J. A. (March, 2010), 'High Altitude Platform Stations in Design Solutions for Emergency Services', *IEEE Buran Magazine*, Barcelona, IEEE Student Branch, No. 25, Year 17, pp. 52-57.